ABSTRACT

Title of dissertation: REGIONAL ASPECTS OF THE NORTH AMERICAN LAND SURFACE-ATMOSPHERE INTERACTIONS AND THEIR CONTRIBUTIONS TO THE VARIABILITY AND PREDICTABILITY OF THE REGIONAL HYDROLOGIC CYCLE

Yan Luo, Doctor of Philosophy, 2006

Dissertation directed by: Professor Ernesto Hugo Berbery
Department of Atmospheric and Oceanic Science

In this study, we investigate the pathways responsible for soil moisture-precipitation interactions and the mechanisms for soil moisture memory at regional scales through analysis of NCEP's North American Regional Reanalysis dataset, which is derived from a system using the mesoscale Eta model coupled with Noah land surface model. The consideration of the relative availability of water and energy leads to the relative strengths of land–atmosphere interaction and soil moisture memory, which are related to the predictability of the regional hydrologic cycle. The seasonal and geographical variations in estimated interaction and memory may establish the relative predictability among the North American basins. The potential for seasonal predictability of the regional hydrologic cycle is conditioned by the foreknowledge of the land surface soil state, which contributes significantly to summer precipitation: (i) The precipitation variability and predictability by strong land-atmosphere interactions are most important in the monsoon regions of Mexico; (ii) Although strong in interactions, the poor soil moisture memory in the Colorado

basin and the western part of the Mississippi basin lowers the predictability; (iii) The Columbia basin and the eastern part of the Mississippi basin also stand out as low predictability basins, in that they have good soil moisture memory, but weak strength in interactions, limiting their predictabilities. Our analysis has revealed a highly physically and statistically consistent picture, providing solid support to studies of predictability based on model simulations.

REGIONAL ASPECTS OF THE NORTH AMERICAN LAND SURFACE – ATMOSPHERE INTERACTIONS AND THEIR CONTRIBUTIONS TO THE VARIABILITY AND PREDICTABILITY OF THE REGIONAL HYDROLOGIC CYCLE

By

Yan Luo

Dissertation submitted to the Faculty of the Graduate School of the
University of Maryland, College Park, in partial fulfillment
of the requirements for the degree of
Doctor of Philosophy
2006

Advisory Committee:
Professor Ernesto Hugo Berbery, Chairman/Advisor
Professor Kaye L. Brubaker
Professor Eugenia Kalnay
Professor Daniel Kirk-Davidoff
Professor Fedor Mesinger
Professor Ning Zeng

ACKNOWLEDGEMENTS

I am deeply indebted to my advisor Dr. Ernesto H. Berbery, whose scientific knowledge and insight have enriched my scientific pursuits. His selfless, patience, encouragement, and scientific supervision at all levels have fostered my enthusiasm for the research presented here. He has provided me with guidance, motivation and inspiration in all phases of my research: all of the important ingredients for success as a graduate student. A special thank goes to Dr. Eugenia Kalnay for her thoughtful remarks and valuable input leading to significant improvements in the dissertation. I would also like to express my sincere appreciation to Drs. Daniel Kirk-Davidoff, Ning Zeng, Kaye L. Brubaker, and Fedor Mesinger for serving as members of my advisory committee. I am honored to have them as members of my dissertation committee. I wish to thank all the members for their valuable suggestions for improvement.

A good part of this work could not be possible without the NARR data provided by the NARR Science team at EMC of NCEP. It is a pleasure to acknowledge the entire NARR team for their assistance. I am grateful to Dr. Kenneth E. Mitchell, for his tremendous support of this research. He dedicated part of his valuable time for our curiosity and provided constructive comments during the course of the study.

I truly appreciate Drs. Wei Shi and Wayne Higgins for kindly having provided the CPC precipitation datasets. Many thanks go to Drs. Ed Maurer and Dennis Lettenmaier for supplying the data set of land surface fluxes and states based on the VIC model. We shared many discussions with them on the characteristics of the gridded precipitation analyses. Their assistance was essential in the first stage of the research.

Further, I would also like to thank the all faculty and staff of our department. Their excellent management guaranteed a suitable and pleasant environment for study and research. Then, of course, there are my lab mates and other colleagues for sharing their technical wisdom and their research experience; my experience would not have been as rewarding without them. I also want to express my appreciation to Emily Becker for reading the manuscript of this dissertation and providing many suggestions for improvements. Guidance and encouragement from faculty members in our department are gratefully acknowledged.

Finally, I would like to dedicate this dissertation to my family for their infinite love and long-lasting support and encouragement. I would especially like to thank my husband Feng Ding, and our lovely son, Yixuan, for always being the source of energy and joy that keep me going…

TABLE OF CONTENTS

LIST OF TABLES

LIST OF FIGURES

LIST OF ABBREVIATIONS

AGCM – Atmospheric General Circulation Models

CMAP – CPC Merged Analysis of Prediction

CPC – Climate Prediction Center

EDAS – Eta Data Assimilation System

EMC – Environmental Modeling Center

ENSO – El Niño/Southern Oscillation

GAPP – GEWEX Americas Prediction Project

GCIP – GEWEX Continental –Scale International Project

GCM – General Circulation Models

GDAS – Global Data Assimilation System

GEWEX – Global Energy and Water Cycle Experiment

GOES – Geostationary Operational Environmental Satellites

GR – Global Reanalysis

ISLSCP – International Satellite Land Surface Climatology Project

JOSS – Joint Office of Science Support

LCL – Lifting Condensation Level

LDAS – Land Data Assimilation System

LSM – Land Surface Model

NAMS – North American Monsoon System

NARR – North American Regional Reanalysis

NCAR – National Center for Atmospheric Research

NCEP – National Centers for Environmental Prediction

NESDIS – National Environmental Satellite, Data and Information Service

NEXRAD – Next Generation Radar

NLDAS – North American Land Data Assimilation System

NOAA – National Oceanic and Atmospheric Administration

NSIPP – NASA Seasonal to Interannual Prediction Project

OI – Optimal Interpolation

PBL – Planetary Boundary Layer

PRISM – Parameter-elevation Regressions on Independent Slopes Model

RMSE – Root Mean Square Error

SST – Sea Surface Temperature

TOVS-1b – TIROS Operational Vertical Sounder - sensor 1b

VAD – Velocity-Azimuth Display Wind Profile

VIC model – macroscale hydrologic Variable Infiltration Capacity model

3DVAR – 3-D Variational approach

CHAPTER 1: INTRODUCTION

1.1 Background

1.1.1 Surface Water and Energy Budgets

The water cycle is a key component of the Climate System, and the quality of its representation is intimately linked to the adequate simulation of climate variability and predictability. For this reason it can be used to evaluate a model's performance, and thus it is important in climate change studies and scenarios. Additionally, some model parameterizations are based on principles associated with the water cycle. Multiple estimates of the Mississippi water cycle have been presented in the literature as a result of efforts supported by the Global Energy and Water Cycle Experiment (GEWEX) Continental-scale International Project (GCIP). The Water and Energy Budget Synthesis (WEBS) article by Roads et al. (2003) summarized the uncertainties in quantifying the water and energy budgets. That initiative compares the estimates of different regional and global models, together with global reanalyses and a Land Data Assimilation System (LDAS) data set. Collectively, they characterize the seasonal cycle and interannual variability of water and energy budgets and provide a measure of the resulting uncertainties, which has been called the "closure of the budget".

Many of the relevant hydrologic variables at regional to large scales are either not measurable or poorly measured. In some situations, topographic and geographic distributions have important impacts on the water cycle. Firstly, precipitation is measured at irregular and widely spaced stations in gauges, and these gauges may

notably underestimate the precipitation, owing to the under-catch effect of wind on precipitation, especially snowfall (Groisman and Legates 1994; Adam and Lettenmaier 2003). Secondly, in mountainous regions, most of the long-term precipitation stations are located in valleys (see, e.g., Daly et al. 1994 and Roads et al. 1994). Since snowfall increases rapidly with elevation in most mountain areas of the west (Daly et al. 1994), precipitation over complex terrain tends to have systematic biases and needs orographic adjustment. Further, characterization of the surface hydrologic cycle requires adequate long-term records of not only precipitation but also runoff and evaporation, but such records are unfortunately lacking. Given the number of deficiencies that prevent even a qualitative closure of the water and energy budgets from observations alone, we depend on model-based four-dimensional data assimilation procedures and forecasts for data synthesis to quantify the energy and water cycle. Thus, model-generated data is a powerful augmentation to observed data. Regional model simulations over the western United States focusing on hydrologic aspects (e.g., Kim and Lee 2003; Leung et al. 2003) have shown that it is possible to achieve a better depiction of the spatial structure and amplitude of precipitation than with global analyses, although this improvement does not translate necessarily to other variables derived from the model's land surface representation. Moreover, the choice of convective scheme in models has a large influence on surface water terms like runoff, which depends more on individual storm precipitation than on monthly totals (Gochis et al., 2003). Still, a mesoscale model provides comprehensive hydroclimatic output that is a supplement to (but not a replacement for) meager observations.

Understanding the hydrologic cycle is a needed step to improve modeling of seasonal and interannual variability associated with observed soil moisture anomalies. Hydrologic components can also be used to assess the ability of a forecast model to estimate the water balances on river basin scales. Current efforts to better diagnose the hydrologic cycle remain focused on both observations and modeling.

1.1.2 Land Surface Effects

A large number of observational and model studies conducted over the last decades have demonstrated the importance of the interactions or feedbacks between land surface and atmospheric processes. Particularly, numerical simulations have been extensively employed to investigate the sensitivity of precipitation to characteristics of the surface conditions. Land–atmosphere interactions may influence atmospheric variability because the land surface state affects the surface-atmosphere fluxes of water and energy. The regional land surface states include soil moisture, vegetation, snow, albedo, topography and other factors. Among them, soil moisture is an important link between land surface and the atmosphere. Soil moisture may play an important role in increasing the persistence and magnitude of floods and droughts (Shukla et al., 1982; Hong and Kalnay, 2000). Many observational and numerical studies have shown that soil moisture significantly impacts model-simulated climate and atmospheric variability: not only does it act as a strong control on the partition between sensible heat flux and latent heat flux at the surface as indicated by the Bowen ratio, but it also can modulate precipitation over a given basin by the interaction with near-surface fields, namely, land-atmosphere feedback effects that

could result in changes in the precipitation patterns (Eltahir 1998). In turn, soil moisture reflects past precipitation and is regulated by surface temperature and evaporation. Both atmospheric forcings (precipitation and evaporation) exert significant control on the evolution of the soil moisture state and appear explicitly as key terms in the surface water balance equation. Therefore, being able to reliably provide insight into climate assessments, and seasonal-to-interannual description of feedbacks or interactions becomes a main subject of research in climate diagnostic studies.

The study of land-atmosphere interactions relies on not only observations but also model-based research. The dearth of relevant observations, both in time and space, limits the study of such interactions, since this study requires long-term records of variables with high temporal and spatial resolutions, and such observational records usually do not exist. As a result, it is extremely difficult to test hypotheses of predictability and assess the sensitivity of precipitation to land surface states. For example, it is not possible to provide direct and detailed quantification of real-world coupling strength from available observations at the continental scale. Introducing the products derived from a model is a very efficient way to solve this problem. In fact, the land surface-atmosphere interactions have been studied in different opportunities by using observational datasets, numerical simulations, and regional analysis diagnostics. Currently, there are various ongoing land data assimilation efforts, in which land surface models estimate surface flux variables indirectly through their integration of observed precipitation and other forcing data. These efforts can substantially enhance our understanding of the land surface – hydrological cycle

interactions or feedbacks at diurnal, monthly, seasonal or even longer time scales in different regions. Therefore, with more complete data provided by models, there are more capabilities to describe the characteristics of land surface-hydrological cycle interactions or feedbacks.

Many studies highlighted the importance of soil states in land surface-atmosphere interactions. Studies based on numerical models have shown that soil moisture has a clear impact on precipitation (Shukla and Mintz 1982; Koster et al. 2000; Hong and Kalnay 2000). These studies investigated the land-atmosphere feedback from changes in soil moisture affecting both the surface energy and water cycles. One reasonable explanation is that wet soil conditions enhance evaporation and result in increased rainfall. Because soil moisture both reflects past precipitation and influences the state of atmosphere above it, it has been hypothesized that a positive soil moisture-rainfall feedback may exist: above (below) normal rainfall yields high (low) soil moisture, which in turn yields additional (limited) rainfall. Evaporation (which supplies water vapor from the land surface to the atmosphere) from the land surface contributes water vapor and latent energy to the atmosphere. Evaporation as a source for precipitation over land depends on availability of surface moisture, which in turn depends greatly on the surface characteristics and vegetation. Precipitation should be most sensitive to land surface conditions where local feedbacks exist through recycling of moisture via evapotranspiration.

In addition to being reflected in the water cycle, land-atmosphere interactions govern the energy balance at the land-atmosphere boundary layer, and it reflects the nature of the coupling between boundary layer conditions and rainfall processes. The

energy budget of the surface is intimately related to the hydrological cycle, since evaporation from the surface is a key component in the budgets of both energy and water. Nowadays, it is generally believed that soil states play a role in surface energy budgets and in determining the boundary conditions that control weather and climate at different time scales. Soil moisture is a critical state variable in atmospheric hydrology in that it determines the overlying boundary layer variables, like equivalent potential temperature, specific humidity, evaporation, and sensible heat flux that can in turn strongly affect the evolution of the atmospheric boundary layer. For example, Entekhabi (1995) concluded that wet soil conditions force larger equivalent potential temperatures, greater cloudiness and precipitation potential. Betts et al. (1996, 1998) showed that the boundary layer variables, like equivalent potential temperature and specific humidity, depend at least in part on the underlying soil moisture. Eltahir (1998) also acknowledged the complex nature of these interactions, and identified a large number of processes that relate soil moisture with precipitation, recognizing the importance of the Bowen ratio in the feedbacks. These links obviously involve complex nonlinear feedbacks, since precipitation and its infiltration affect the multiple processes that take place in the subsurface (runoff, drainage, etc.), which in turn affect evaporation and consequently the Bowen ratio and the boundary structure (Beljaars et al., 1996; Betts et al., 1996; Eltahir, 1998).

Several mechanisms have been proposed to account for the strength, direction, and seasonal variability of the land-atmosphere interaction from continental to regional scales. Land-atmosphere interactions can be positive or negative feedbacks, and can be strong or weak depending on different local physical mechanisms, as

suggested by various model and diagnostic studies. Overall, land surface processes are believed to be especially important in spring and summer. Entekhabi (1995) showed consistent trends of drier summertime soil moisture, higher summertime temperature, decreased evapotranspiration and precipitation. Many numerical modeling studies, with a few exceptions, conclude that a positive feedback exists between soil moisture and rainfall. Dry soil plus high temperature enhances dry convection through the increase of turbulent mixing that accompanies increased sensible heat flux and decreased latent heat flux. This cycle supports the positive feedback mechanism between dry soil conditions and reduced precipitation. Positive feedbacks between these surface and atmospheric states may lead to persistent wet or dry spells (Betts et al., 1996), while negative feedbacks precisely oppose such persistence. It has been shown that both floods and droughts can be enhanced through a regional positive feedback and land surface memory due to soil moisture storage (Entekhabi et al., 1992). There also is evidence in some cases of negative correlation between soil moisture and rainfall. This negative feedback can be explained by local recycling effects being unimportant in the development of extreme climatic regions compared to a dry soil initial condition period for increased sensible heat flux, which contributes greater buoyancy to the air, enhancing convective systems and producing more precipitation. Pan and Mahrt (1987) and Betts et al. (1996) have proved that on diurnal time scales, a decrease in soil moisture may induce an increase of surface temperature, convective instability and precipitation. This cycle supports the negative feedback mechanism between soil condition and precipitation.

The strength of land-atmosphere feedback in a given region is controlled largely by the relative availability of energy and water. The land-atmosphere feedback is suppressed when the land surface is extremely dry or extremely wet, i.e. where there is little sensitivity of evaporation to fluctuations in soil moisture. Dirmeyer (2003) has shown that during winter the land surface is largely decoupled from the atmosphere due to increased baroclinic activity in the land-dominated Northern Hemisphere, while at the same time tropical ocean anomalies have their strongest influence.

Up to now, most studies of such interactions emphasize that these interactions often differ from region to region. In other words, soil moisture has a very regional effect. Findell and Eltahir (2003) examined the role of land states in the land surface atmospheric boundary layer interactions by developing a classification based on the early morning convective triggering potential and a low-level humidity index to define the relative importance of the feedback between land surface and atmosphere over different regions in the United States. Their results show that feedbacks between rainfall and soil moisture are *positive* toward the east, and *negative* in the semiarid southwest, while strong feedbacks are not present in the rest of the west. However, this land surface effect could be more important over some regions but weak over others, particularly at monthly to seasonal time scales.

The development of high-resolution regional models now provides great possibility for more accurate evaluation of these interactions of the land surface-atmosphere. At the present, two-way coupled atmosphere and land surface models have been used with increasing success. Recently, Berbery et al. (2003) have

advanced the understanding of these interactions through the analysis of the Eta regional model products. They discussed the critical role of soil moisture at monthly time scales in the subbasins of the Mississippi Basin: subbasins that have a relatively high Bowen ratio show stronger relations between soil moisture and the formation of clouds. Consequently, they found that in the western half of the Mississippi basin, feedbacks show better relationships that can be described as follows: increased soil moisture is associated with a slight increase of net radiation at the surface; latent heat flux also increases with soil moisture while sensible heat decreases, resulting in an almost linear increase of the evaporative fraction. Increased soil moisture is also associated with a lower lifting condensation level and an increase of observed precipitation (though not statistically significant). The overall results are consistent with the concept of a positive climatic feedback in which increased soil moisture affects surface fluxes in such a manner that increases precipitation results. However, toward the wetter east (e.g. the Ohio basin), there are no well-defined land surface-atmosphere interactions, suggesting that other effects, like the advection of moisture, may be more relevant for precipitation processes.

Since the strength of land-atmosphere interactions in a given region is controlled largely by the relative availability of energy and water there, the Ohio basin is an "energy limited" (or "water abundant" basin)—not enough net radiation to evaporate the abundant soil moisture, whereas the lower Missouri basin is a "water limited" basin—not enough soil moisture to meet the evaporative demand of the high net radiation. Here, surface evaporation, and thus sensible heat flux and LCL in the Missouri sub-basin are very sensitive to soil moisture anomalies.

1.1.3 Soil Moisture Memory

Another important aspect of in studies of predictability is the persistence or memory of soil moisture anomalies. According to Koster et al. (2001), soil moisture memory is defined as the soil being able to persist in (i.e. remember) wet or dry conditions for a long time, even after these conditions have been forgotten by the atmosphere. Thus, the land acts as a source of long term "memory" of past precipitation events (Entekhabi, 1995). Accordingly, a measure of this persistence or memory effect can be inferred from the autocorrelation of soil moisture. Recent advances in measuring soil moisture memory have come through the autocorrelation equation of soil moisture, which can be expressed on four terms (Koster et al., 2001):

$$\langle w_n, w_{n+1} \rangle = f\{\underbrace{\frac{\sigma_{w_n}}{\sigma_{w_{n=1}}}}_{A}, \underbrace{\frac{R}{C_s}}_{B}, \underbrace{\frac{P}{C_s}}_{C}, \underbrace{\frac{\langle w_n, F_n \rangle}{\sigma^2_{w_n}}}_{D}\} \tag{1.1}$$

Where W_n stands for the average degree of saturation of the soil column, or a measure of the soil moisture; σ_{wn} refers to the square root of the variance of W_n; Cs is the column's water holding capacity, R is the net radiation at the surface, P is the precipitation, and F_n is a forcing term, dependent on the precipitation and net radiation (other model-dependent constants are implicitly included). In other words, the autocorrelation of soil moisture is controlled by: (A) the nonstationary of the atmospheric forcing (seasonality); (B) the variation of evaporation with soil moisture; (C) the variation of runoff with soil moisture; and (D) the correlation between the atmosphere state and antecedent soil moisture (land-atmosphere feedbacks are implied in the formulation of autocorrelation of soil moisture). Hence, the

atmospheric state appears to be connected to the antecedent soil moisture. These terms are particularly useful as they have novel features that can represent soil moisture memory connected to predictability of the hydrologic cycle. It has been concluded by Koster et al. (2000) in recent experiments that soil memory can be a dominant source of long-term weather predictability for some midlatitude continental regions.

1.1.4 Uncertainties and Predictability of the Water Cycle

The coupling of the atmosphere with slowly-evolving surface boundary conditions, like SST and soil moisture, has potential to improve the skill of prediction on long-term time scales (e.g., Shukla et al. 2000 and references therein), since better memory of surface boundary conditions tends to improve the predictability. However, the challenge to produce skillful short-term climate predictions still remains. The lack of skillful predictability is partly due to the dominance of synoptic scale atmospheric variability. Nevertheless, because of the soil moisture reservoir's considerably longer memory than that of most of the atmospheric processes, the land can either strengthen or weaken atmospheric anomalies, depending on soil moisture persistence. The soil moisture may serve to integrate past atmospheric forcing and enhance prediction skill for regional climates.

Predictability of the hydrologic cycle became a component of the GEWEX North Americas Prediction Project (GAPP), which has the aim of improving our ability to predict summer precipitation. SST anomaly typically has a longer time scale memory than soil moisture, and its effects have been an important issue. In an

investigation of the relative role of soil moisture and SST in climatic predictability, Koster et al. (2000) found that the oceans and land have different domains of influence: The Tropics are mostly dependent on the ocean influence, while outside those regions, as another "slow" component of the earth's climate system, the land surface state has an impact on atmospheric properties in summer midlatitudes that appears quite large, and land-atmosphere feedbacks amplify the precipitation variance. In other words, knowledge of soil moisture has a greater impact on the predictability of summertime precipitation over land at midlatitudes than sea surface temperature (SST). With this fact in mind, the emphasis of this research in part will be on the soil moisture memory over continental North America.

In recent years, the role of soil moisture has been extensively studied using modeling approaches. Betts et al. (1996) suggest that improved predictability exists in both short and extended range forecasting, due to the memory of the soil moisture reservoir. In their study, the success of these precipitation forecasts for the extreme flood event of July 1993 emphasized the importance of memory in the land surface boundary condition. Koster and Suarez (2003) and Dirmeyer (2003) have shown land surface initial conditions have an important role in the quality of seasonal forecasts over regions that have large soil moisture anomalies, their evaporation is strongly sensitive to soil moisture, and in turn their precipitation is sensitive to evaporation. These initial conditions will persist in time because of the slowly varying nature of soil moisture, therefore affecting the boundary layer for longer times. This has been confirmed recently by Koster et al. (2000) in experiments where the land surface moisture state contributed significantly to the long-term weather predictability for

some midlatitude continental regions. The memory associated with land surface soil moisture may turn out to be the chief choice source of forecast skill for summer precipitation on middle latitude continents, partially this effort is of special significance in that if the atmosphere there responds in realistic and predictable ways to the soil moisture anomalies, especially when strong interactions exist between soil moisture and precipitation processes (Koster et al. 2000). On a global scale, Koster et al. (2004) have evaluated the land–atmosphere interactions using a dozen climate-modeling groups. Their study allows a multimodel estimation of the region on Earth where precipitation is affected by soil moisture anomalies during Northern Hemisphere summer.

Here, we will investigate the land-atmosphere interactions and soil moisture memory. We will explore the potential advantages of applying land-atmosphere interactions and the roles of soil moisture memory on the hydrologic cycle at regional scales derived from North American Regional Reanalysis (NARR), to assess the variability and predictability of the regional hydrologic system.

1.2 Scientific Objectives and Relevance of this Study

The main goal of this research is to diagnose land surface-atmosphere interactions at regional scales and evaluate the role of soil moisture memory on the hydrologic cycle, and ultimately assess the predictability of the hydrologic system at basin scales. Further, it will provide understanding of which aspects of the coupled land-atmosphere system are most likely to be associated with predictability. Our

research emphasizes improved predictability based on an enhanced understanding of regional land surface processes at monthly and seasonal time scales.

The first part of this study is to diagnostically estimate land surface-atmosphere interactions over basins of North America from monthly to seasonal time scales, applying NCEP's Regional Reanalysis products available over the 24 years. The NCEP North American Regional Reanalysis (NARR) is a long-term, consistent, high-resolution climate data set for the North American domain (Mesinger et al. 2002). One critical question for our study is determining how well the water and energy cycles are represented in the reanalyses. Originating from Eta/EDAS operational forecast suite, NARR benefits from improvement arising from upgrades and changes to the suite over the years. Hence, it is worthy to first include an evaluation of the products of Eta/EDAS operational forecasts. Despite some deficiencies, Regional Reanalysis provides the best estimate of precipitation that has been recorded in the real land-atmosphere coupled system. Without detailed evaluation of the NARR, we cannot be confident about its relation to reality. This is a fundamental and necessary first step towards investigating linkages between the soil states and specific components of the hydrological cycle of North American basins. Once this evaluation is complete, we analyze different components associated with the soil moisture-precipitation interactions mostly using correlation analysis between soil moisture and atmospheric processes. In order to relate the surface–atmosphere interaction characteristics of a given basin to the predictability of its hydrologic cycle, we identify cases in which the feedbacks enhance or weaken atmospheric anomalies. Primarily, these computations identify basins and time scales where land surface-

atmosphere interactions are strongest or weakest.

The second part is to investigate the temporal and spatial distribution of soil moisture memory processes. We characterize such soil moisture memory in terms of its time scales and the spatial, vertical and seasonal variations of one-month-lagged and multi-month-lagged autocorrelations. In this framework, we will show that there is a regional and ground depth dependence of the soil moisture anomaly persistence. The soil moisture memory processes will be analyzed for warm, cold and transitional seasons.

Land surface–atmosphere interactions and soil moisture memory processes provide the scientific basis for the last part, which will focus on the predictability of the hydrologic system at basin scales by utilizing the established interactions between soil states and the hydrologic cycle for each of these basins. In other words, both establish a basis for the predictability analysis and uncertainties. Figure 1.1 illustrates the various components of the study and how they inter-relate. The question as to what extent the regional water cycle is predictable in terms of land processes can be best addressed by examining the relationship in regions of well-defined land surface-hydrologic cycle interactions. In the case of regions where no feedbacks are found, the analysis will focus on how this relates to the degree of uncertainty of the water cycle.

The methodologies and results presented in this dissertation have applications to predictability of the hydrologic cycle on monthly to seasonal time scales. As stated earlier, the rationale for performing short-term climate prediction is based on the assumption that the slowly varying surface boundary conditions can influence some

statistical aspects of the atmosphere. With the ever-improving monitoring of the Earth's surface boundary conditions, particularly by satellite measurements, the challenge is to assess the utility of this information for model simulation and prediction. This study assesses statistically where and when the land is more likely to influence the atmospheric variability. The results then can help in assessing the usefulness of the surface boundary conditions that could lead to improved prediction procedures.

Current studies in regional climate prediction rely on products from sophisticated coupled land-atmosphere models. Any attempt at estimating those interactions should also provide a measure of the dispersion among the difference estimates, (e.g., Berbery et al., 1999). In this research we will address this concern by referring to a number of studies on the same topic to reinforce the conclusions from the Regional Reanalysis products.

1.3 Study Areas

The focus of this research is on North American basins with diverse climate regimes, defined in Figure 1.2. The Mississippi River basin was extensively studied during GCIP. In a detailed review provided by Coughlan and Avissar (1996), a large degree of heterogeneity in distinct climate regimes was revealed among its sub-basins. The Mississippi River Basin is the largest on the North American continent, draining almost 15% of the continental landmass and 41% of the Conterminous United States with a 3.2 million km^2 basin (see website at http://www.mrba.org). The Mississippi River basin was chosen as the study area in part because it is one of the

major river systems of the world and in part because of its data richness from abundant networks for upper and surface observations (Roads et al., 2003).

Next, we wish to investigate western basins with distinct climate features. The Global Energy and Water Cycle Experiment (GEWEX) Americas Prediction Project (GAPP) has chosen the Columbia and Colorado basins as study areas because of the role the hydrologic cycle plays in the scarce water resources of the western United States. The Columbia River is the third largest river system in the United States. It flows from the North American continent into the North Pacific Ocean, and its 668,000 km^2 basin covers portions of seven western states and the Canadian province of British Columbia, draining about 85% of the northwestern part of the country. The Columbia River Basin has orographically forced precipitation that is largest during winter. The hydrology of the Columbia River basin is dominated by winter snow accumulation (Leung and Ghan 1998) as the region receives less than 20% of the precipitation during June-August (Pulwarty and Redmond 1997). Thus, the Columbia River is primarily a snowmelt-driven system; it has relatively high runoff per unit area and low reservoir storage relative to the mean annual inflow (Payne et al. 2004). In view of this seasonal distribution, the Columbia basin places greater emphasis upon the winter and spring seasons when most of the mountain snowpack develops and melts. The fact that the Columbia basin is in a snow-dominated and high topographic area makes it more challenging for any numerical model to predict correctly the winter precipitation in that region. It is now widely acknowledged that the high topography in the northern part of the country imposes a limit of accuracy in precipitation measurement from both models and observations. Simulation of

precipitation over the complex terrain of the western United States with mesoscale models (e.g., MM5) reveals different types of biases so a fairly strong degree of uncertainty can be found in this basin, from overestimation and shift of winter precipitation maxima over the northwest to underestimation of summer precipitation over the southwest (Leung et al., 2003). The Eta model is also known to have regional terrain-related biases over mountains (see, e.g. Berbery and Rasmusson 1999; Berbery et al., 2003). Our current evaluation (Luo, et al., 2005) shows that with changes in the Eta model over the last three years, there have been important reductions in the biases due to orography (still, there may be a question whether the observed precipitation is correctly adjusted to topographical effects, as discussed by Adam and Lettenmaier, 2003). Temporal and spatial scales at which the water cycle components can still be reliably identified, and the consequences for longer-term variability, will be assessed later.

The Colorado River originates in the Rocky Mountains and flows generally west and south, discharging into the Gulf of California. The Colorado basin covers about 637,000 km^2 and spreads over the southwestern United States and a small portion of Mexico. Much of the basin is arid, and runoff derives from the high elevation snowpack over the Rocky Mountains, which contributes about 70 % of the annual runoff (Christensen et al. 2004). The hydrological cycle of the semiarid Colorado River basin is affected by the North American Monsoon regime during the warm season (Gochis et al., 2003) and by snow accumulation during the preceding cold season (Gutzler, 2000). The Colorado River system is also one of the most

heavily regulated, as it provides water supply, irrigation, flood control and hydropower to a large area of the U.S. Southwest (Christensen et al. 2004).

Other monsoon-affected basins are included in this research. Small (2001) found land surface may affect North American Monsoon System (NAMS) variability. Basins of interest are those related to the core monsoon and to the out-of-phase summer precipitation regime (Douglas and Englehart 1996, Higgins et al. 1997, Barlow et al. 1998). The Core Monsoon (Berbery 2001) is not strictly one basin, but the aggregation of several mountain basins draining towards the Gulf of California. However, they are all directly influenced by the monsoon precipitation. The Colorado River is also affected by the fringes of the monsoon precipitation (the southwest monsoon). Basins affected indirectly by the North American monsoon are those that lie in regions where the out-of-phase summer precipitation regime is best defined. Included in this case is the Rio Grande / Rio Bravo basin covering part of the southern Texas, and some portions of the Mississippi basin. Located on the eastern slopes of the Sierra Madre Occidental, the region identified as Central Mexico will also be inspected to ascertain whether it has any role in the North American Monsoon System.

Studying these interesting basins expands our results and conclusions to a wide climate range, including basins with significant cold-season snowfall and with a much larger runoff fraction, as well as those with a strong summer hydrologic cycle associated with the North American Monsoon. In this way, a deeper and wider understanding of the land surface-atmosphere interactions and their relationships to the variability and predictability of water cycle at basin scales can be achieved.

The roadmap of the dissertation with the major goals of this study is as follows. In Chapter 2 we statistically document and assess the development of Eta/EDAS operational forecast system and its performance that led to the generation of Regional Reanalysis. The results give sufficient confidence in the NARR data set for use in the dissertation study. In Chapter 3 we examine the basin-scale features of surface water and energy budgets estimated from NARR as the background for the study in Chapters 4 and 5. In Chapter 4 we investigate the linkages of the land surface and the atmosphere, and describe some characteristics of seasonal variability and basin dependence. In Chapter 5 we evaluate the basin scale features of soil moisture memory. We also assess the implications of the land-atmosphere interactions on the predictability of the hydrological cycle. A separate study on applications of land-atmosphere interactions and soil moisture memory for summer precipitation prediction is covered in Chapter 5, and conclusions including a summary and plans for future work are presented in Chapter 6.

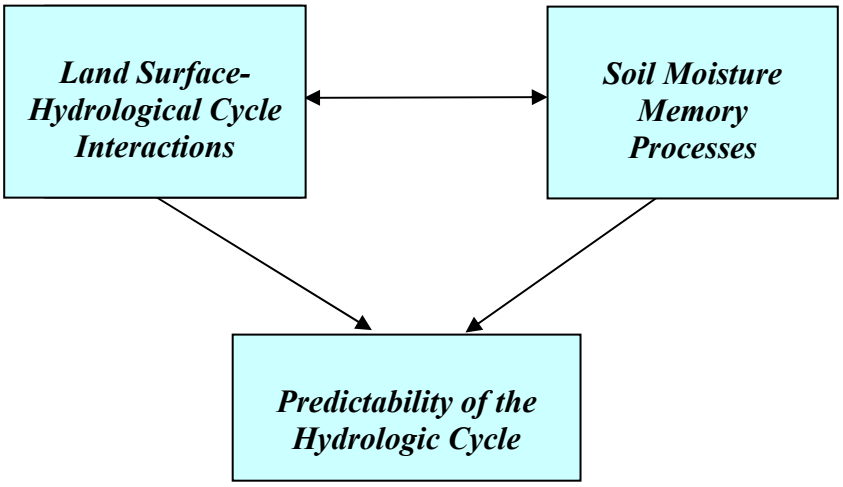

Figure 1.1 Schematic of proposed integrated study framework.

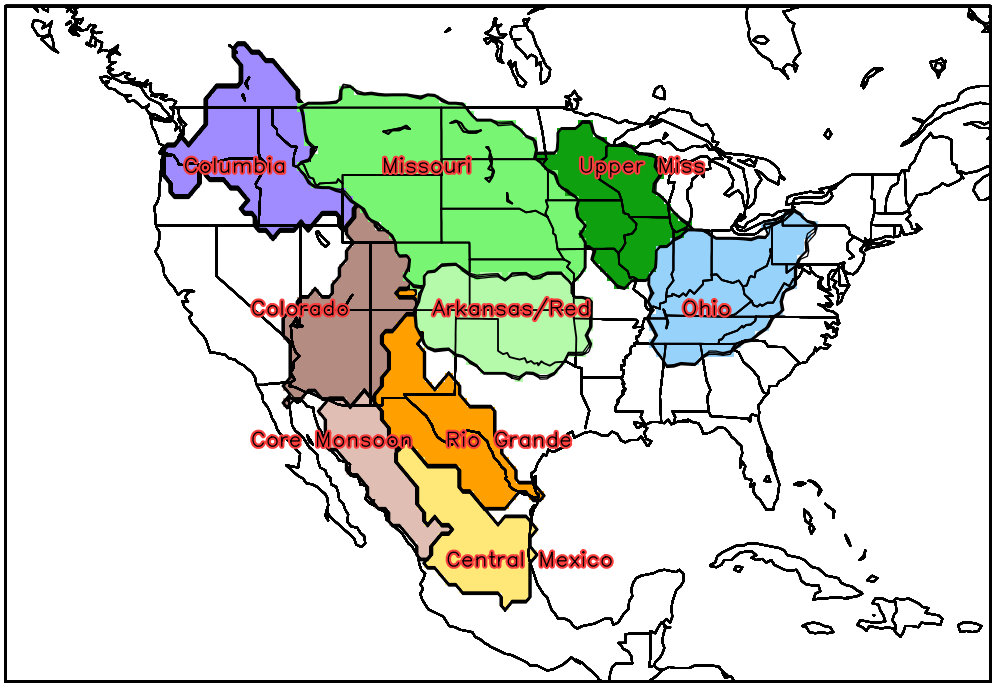

Figure 1.2 Location of the selected North American basins.

CHAPTER 2: NCEP'S ETA/EDAS OPERATIONAL FORECASTS

2.1 Introduction

A recent development with the coupled Eta model and its land surface model, Noah, is NCEP's completion of NARR, which consists of 25 years of Eta model-based assimilation and forecast products. The NARR system is based on the frozen version of the operational Eta model and its companion Eta-model based data assimilation system (EDAS) as of April 2003, although some changes were added to optimize the data assimilation system.

Examination of the Eta model forecasts can reveal characteristic features of the water cycle and point out some of the serious issues that still affect the ability to develop adequate surface water budgets over large-scale river basins. There are several reasons to support this approach. First, such research helps to demonstrate how different changes in the Eta model suite during the late 1990's and early 2000's improved the Eta model hydrologic estimates of mainly the western basins, and thus such research illustrates the improved model and assimilation behavior to be expected from the NARR. Although the study was done for the Mississippi basin as well, here we focus on the west because it is one of the most complex regions to represent. Secondly, the NARR products are not exempt of potential errors or biases, and one way of verifying their quality is by comparison against recent operational products of

the Eta model suite. Also this study will partially and indirectly provide an important indication of the quality of available data products of NARR. Having in hand the present study with operational forecasts as a benchmark, we carry out a follow-on NARR-based study of these same basins (Mississippi, Columbia, Colorado) in Chapter 3.

The primary purpose of this chapter is to assess the performance of NCEP's operational Eta model 12-36 hour forecasts for studies of the surface branch of the hydrologic cycle over the United States, in particular the Columbia and Colorado basins. Although the hydrometeorologic behavior of the Mississippi River basin differs considerably from that of the western basins, some of the model issues are general in nature as addressed later. Others, in particular the errors in the representation of the solid precipitation processes in the model, are much more important for the Columbia basin. We mainly use the western basins to highlight the improvement in the Eta analysis system.

Because this is the operational version of the Eta model, its changes throughout the years may have affected other output variables. As will be shown, despite substantial progress in the development of Eta model there is still much uncertainty. This uncertainty arises in part from the lack of adequate observations to fully characterize all of the processes. For example, soil moisture, evaporation and sensible heating, and various radiative components, are only measured in a few regions, and water and energy transports can only be calculated from radiosondes over large-scale regions. Even a few variables that are inferred from remote sensing, such as surface skin temperature and solar radiation, must use a model tuned to only a

few sites. Atmospheric and hydrologic models that attempt to synthesize this information are imperfect and even analysis output, which attempts to make use of all available data, is biased toward imperfections in the model.

The objective here is to analyze the multi-year water cycle at the surface from NCEP's Eta model products and examine the impacts that model changes and upgrades that positively affect its performance. Results are compared with available gridded precipitation analyses and land surface hydrologic estimates from the Variable infiltration Capacity (VIC) macroscale hydrologic model. The detailed description of surface water and energy budgets will be discussed from NARR in the next chapter (Chapter 3).

The Eta and VIC model data sets and observation-based precipitation analyses used in this study are introduced in section 2.2. The analysis of observed precipitation and the evaluation of model precipitation are presented in sections 2.3. Model evaporation will be discussed in section 2.4. Notably, these sections show that significant improvements in Eta model surface hydrologic products were achieved with the implementation of continuous soil moisture cycling in the Eta Data Assimilation System (EDAS) in early June 1998. With June 1998 in mind, the analysis in Section 2.5 of the basin-average climatology of Eta model surface hydrologic cycle is based on the five years (June 1998 – May 2003) following this milestone. This study will illustrate how much progress in regional scale of surface hydrological cycle has been made in the last 10 years in Eta/EDAS system.

2.2 Data Sources

2.2.1 Eta/EDAS Operational Forecasts

The Eta model is the operational model being executed at NCEP for short-range continental forecasts over North and Central America. It has a concurrent system called Eta Data Assimilation System (EDAS) that generates its initial conditions by ingesting a diverse mix of observations. The Eta forecast model has been executed at NCEP operationally for over 10 years, and the EDAS assimilation suite was implemented operationally in April 1995 (Rogers et al. 1996). The Eta/EDAS operational forecast system is coupled to a land surface model (Ek et al. 2003), named as "Noah", which applies the energy and water balance equations at every grid point and produces surface variables such as evaporation, runoff, soil moisture, and snow water equivalent that are consistent with the surface forcing from the atmospheric component of the Eta model or EDAS.

Since the Eta model is NCEP's operational mesoscale model, both components (model and assimilation system) have undergone significant changes along the years, in particular in its atmospheric physical package, land surface model, and data assimilation system, therefore their products are not uniform. A log with all modifications is provided online at http://www.emc.ncep.noaa.gov/mmb/research/eta.log.html. The more important changes can be found in Table 2.1. As shown in this table, resolution in the Eta model has been increased from an initial 48-km grid spacing in 1995 to 12-km at present. Unevenly distributed vertical levels provide increased high resolution from thirty-eight in 1995 to the current sixty levels. From 1995 to 1997, the Eta model was run at 48 km and 38 levels. On February 1998, September 2000 and November 2001, the model resolution increased, respectively, to 32 km/45 levels,

22km/50 levels, and 12km/60 levels. Each resolution increase implied large increases in the volume of model output.

Probably the most significant changes to the Eta land component physics in the data assimilation system correspond to the change from Optimal Interpolation to a 3-D Variational approach (February 1998), the full and continuous self-cycling of atmospheric and land states including soil moisture and temperature without nudging (June 1998), and the assimilation of observed precipitation that started in July 2001 (Rogers et al., 2001b). Within the fully continuous cycling of land states (Rogers et al., 2001a), the soil moisture is the result of the EDAS atmospheric surface forcing fields and the Eta land model physics. Land and atmosphere states began to be continuously cycled in EDAS in June 1998. However, a fire in the NCEP main computer in September 1999 interrupted the cycling, which was restarted again in December 1999 and since run continuously.

The model physics has also been modified in different opportunities, including major upgrades to the land surface physics. In January 1996 the old bucket model was replaced by a 2-layer soil model (Chen et al., 1996), and in February 1998 the number of soil layers was increased to four. Other upgrades involved parameterizations of surface evaporation, cloud physics, vegetation, and snow. The most recent significant upgrade to the Eta-model land physics occurred on 24 July 2001, with the inclusion of 1) the frozen soil and snowpack physics discussed by Koren et al. (1996) and 2) the upgrades to the soil thermodynamics, bare soil evaporation, and ground heat flux components presented by Ek et al. (2003). With the latter upgrades, the Eta model land component is now referred to at NCEP as the

Table 2.1 Significant Eta model changes during May 1995 – March 2004

1	12 Oct 1995	A 12-h Eta model-based Data Assimilation System (EDAS) is introduced (four 3-h cycles) replacing initialization the atmospheric states of the Eta forecast from the NCEP Global Data Assimilation System (GDAS). The 0-h initial atmospheric states of the 12-h EDAS are taken from the GDAS. An explicit cloud microphysics scheme for precipitation and cloud water/ice was added, to replace the simple super-saturation physics, new treatment of roughness length for heat added in surface layer physics (Chen et al. 1997).
2	31 Jan 1996	Major generational upgrade made to the land surface physics. Old bucket model with temporally invariant initial conditions was replaced with a new 2-layer soil model with explicit vegetation physics (with seasonal cycle) and snowpack physics. Initial conditions for soil moisture and temperature at beginning of the 12-h EDAS taken from GDAS. Substantial upgrades were implemented in the PBL physics.
3	18 Feb 1997	The global ISLSCP I database for monthly green vegetation fraction was replaced with a new monthly green vegetation fraction database from NESDIS. The empirical adjustment of the initial soil moisture taken from the global GDAS at the beginning of the 12-hour EDAS was changed. Improvements were made to the physics of melting snow and the treatment of direct surface evaporation from bare soil. Refinements were implemented in the radiation physics to reduce the high bias in surface solar insolation.
4	09 Feb 1998	Spatial resolution was increased from 48 km to 32 km and from 38 to 45 vertical levels. The number of soil layers was increased from two (10 and 190 cm) to four (10, 30, 60, 100 cm), in both the forecast model and Eta Data Assimilation System (EDAS). The Optimal Interpolation (OI) approach in the EDAS analysis/update step was replaced with a 3-D Variational approach (3DVAR), including the assimilation of GOES satellite-based 3-layer precipitable water estimates for the first time.
5	03 Jun 1998	Fully continuous cycling of all EDAS atmospheric states (including cloud water/ice) and land states (including soil moisture) was implemented, such that the EDAS is no longer restarted every 12-hours from the global data assimilation system (GDAS). The initial snow cover fields in the Eta model started being initialized once daily from the new NESDIS "IMS" daily 23-km N. Hemisphere snow cover analysis.
6	3 Nov 1998	A number of changes were made to the 3DVAR to improve the low-level moisture analysis and to improve the 3DVAR analysis fit to both radiosonde data and surface observations in general (including surface air temperature and surface winds).
7	13 May 1999	Changes to 3DVAR to improve mass-wind balance.
8	28 Sep 1999	The NCEP mainframe CRAY computer caught fire and was destroyed. For the next three months until early January 2000, the operational Eta/EDAS system was executed in a degraded mode of reduced resolution and reduced volume of assimilated observational data, including some breaks in the continuous assimilation system.
9	26 Sept 2000	The model spatial resolution was increased to 22 km and to 50 levels in the vertical. Direct assimilation of GOES and TOVS-1B satellite radiance data was implemented in the EDAS, and further refinements to the 3DVAR analysis fit to radiosonde moisture data were done. Vertical advection of cloud water/ice and minor modifications to the Betts-Miller-Janjic cumulus convection scheme were added. The horizontal diffusion was further reduced.
10	24 Jul 2001	The EDAS began operational assimilation of the hourly, national, 4-km "Stage IV" radar/gage precipitation analyses. Frozen soil physics was introduced into the land physics, as well as a substantially upgraded treatment to the physics of snowpack and ground heat flux. Snowpack density was added as a new state variable. Vegetation canopy resistance treatment was refined and the bare soil evaporation scheme was improved.
11	27 Nov 2001	The horizontal resolution was increased to 12 km and to 60 vertical levels. The cloud and precipitation microphysics were substantially upgraded, including the addition of several new cloud water/ice state variables. The 3DVAR analysis scheme was improved.
12	26 Feb 2002	Changed thermal conductivity for patchy and full snow coverage.
13	21 May 2002	Changes in the precipitation assimilation to correctly pass convective precipitation to radiation.
14	19 Jun 2002	The radiation driver was modified to perform numerically stable computations of shortwave radiative fluxes. The land-surface physics was changed to avoid very dry soil conditions that led to negative soil moisture availability.
15	8 Jul 2003	Modifications to the cloud physics and radiation. Assimilation of GOES cloud top pressure, Stage IV precipitation data and super-observations of NEXRAD radial wind data. [Changes outside the period covered in this study.]
16	16 Mar 2004	Began use of daily gauge data for adjustments to the precipitation bias assimilation. Land-surface model precipitation now based on model microphysics. [Changes outside the period covered in this study.]

"Noah" land surface model. The evolution of the Noah land model physics over the past 5 years is provided by the following references: Chen et al. (1996, Section 1.1), Chen et al. (1997), Betts et al. (1998), Koren et al. (1999), and Ek et al. (2003).

Of the more recent period, the comprehensive changes to the land surface model (July 2001) and cloud microphysics (November 2001) can be considered major; changes after 2001 include modifications to the sub-surface thermal conductivity over patchy and full snow cover (February 2002), and modifications to the land surface physics to avoid slightly negative soil moisture availability under very dry soil conditions (June 2002). Later changes, although listed in Table 2.1, do not cover the period employed in this study. The operational EDAS began precipitation assimilation (hourly) in late July 2001, using radar-based, non-orographically corrected precipitation estimates. Given that radar-based precipitation estimates cannot reliably infer frozen precipitation, the operational EDAS omits precipitation assimilation at any grid point where the model simulation indicates frozen precipitation. (Aside: The NARR assimilates gauge-based orographically corrected precipitation and does not apply any exclusion for frozen precipitation.)

One should notice that model changes at NCEP are grouped; that is, a "bundled" set of changes is put into operations simultaneously on a given date. Thus, it is difficult to ascertain what the impact of an individual change in the bundle is on the forecasts.

We employ Eta products for the period June 1995- May 2003. In this study the monthly averages from short-term 12-36 h Eta forecasts are employed to produce an 8-yr climatology of the model precipitation and evaporation, and a 5-yr

climatology of the surface water cycles. In reconstructing such a time series, we document a series of changes between 1995 and 2004. Figure 2.1 presents a time line that associates the model modifications as described in Table 2.1 with the time series of the Mississippi basin-averaged 12-36 h forecast precipitation, which will be discussed in section 2.3.

2.2.2 VIC Hydrologic Model Products

Since the observations available to evaluate the Eta model products are rather limited, this assessment is complemented with data from the variable infiltration capacity hydrological model (VIC) products (Maurer et al., 2002) available at University of Washington. The VIC model is a macroscale hydrologic model described in detail by Liang et al. (1994; 1996). It was designed to balance energy and water at each grid point at each 3-hourly time step. It was employed by Maurer et al. (2001, 2002) to develop a 50-yr (January 1950 – July 2000) dataset of surface variables covering the United States and nearby regions with 0.125^{o} grid spacing. The Datasets comprise the initial observed data (forcing e.g., precipitation, surface temperature) and derived data (e.g. downward solar radiation). The VIC model thereby provides surface variables such as evaporation, runoff, soil moisture, and snow water equivalent, that are consistent with the external forcing and the model surface energy and water balance equations.

The dataset (Maurer et al., 2002) has been validated by direct comparison to runoff collected. According to Maurer et al. (2002), the computed runoff matches well the observed runoff mean seasonal cycle for the Mississippi basin. The observed

precipitation employed as a forcing by VIC has corrections to reduce biases due to orographic effects (Maurer et al. 2002) by using the statistical topographic-precipitation relationship developed by Daly et al. (1994). It is important for capturing the mesoscale orographic precipitation pattern that is a prominent feature of the western United States.

This VIC-derived dataset of land surface states and fluxes has served as a reference for a wide variety of studies, especially where many observations are missing and in particular to assess model-predicted land-atmosphere exchanges of moisture and energy. Applications of the VIC model for water and energy budget studies are described in Maurer et al. (2001, 2002). Though the VIC dataset ends in July 2000, hence having some difference between its averaging period (about 5 years) and that of the Eta forecasts here (8 years), this difference does not affect the chief results presented here.

2.2.3 CPC Rain-gauge Based Precipitation Datasets

Table 2.2 lists the characteristics of three precipitation analyses, which are all daily analyses based on gauge observations. The methodological differences described below in the production of these precipitation analyses result in noticeable differences among the corresponding precipitation fields, an important aspect to consider when evaluating the Eta model products. As noted in Table 2.2, none of the three precipitation analyses employ corrections for snow undercatch by gauges. As will be discussed later, this is a notable caveat for both the Columbia and Colorado River basins, which experience significant snowfall in winter.

The first analysis, designated $\boldsymbol{P}_{CPC}$, is a Continental U.S. (CONUS)-only analysis prepared on a 0.25° × 0.25° grid by NCEP's Climate Prediction Center (CPC) using a Cressman analysis scheme to interpolate the gauge observations to the grid (Higgins et al., 2000). This analysis scheme utilizes a radius of influence, which is a function of the average separation-distance between reporting stations and with an upper bound of 200 km that is sufficiently large to ensure that no landmass grid points are left undefined. The $\boldsymbol{P}_{CPC}$ analysis is the only one of the three that omits orographic adjustments. This is of particular concern for the mountainous Columbia and Colorado River basins.

Table 2.2 Characteristics of the precipitation datasets.

	Origin	**Gauge-based analysis (A) or Forecast (F)**	**Orographic correction**	**Includes Canada portion of Columbia basin**	**Snow undercatch correction**	**Grid spacing**	**Interpolation method and radius of influence**
$\boldsymbol{P}_{CPC}$	CPC	A	No	No	No	0.25°	Cressman/ 200 km radius
P_{CPC}^{ORO}	CPC	A	Yes	No	No	0.125° (14 km)	Inverse of square distance/ 50 km
$\boldsymbol{P}_{UW}$	UW	A	Yes	Yes	No	0.125° (14 km)	Inverse of square distance/ dynamic radius[1]
$\boldsymbol{P}_{ETA}$	Eta	F	No	Yes	Not applicable	See Table 1	Not Applicable

[1]Function of the number of reporting stations within a search radius that increases until attaining four reporting stations.

The second analysis, designated P_{CPC}^{ORO} **,** is also a CONUS-only analysis prepared by CPC, but on a higher resolution 0.125° × 0.125° grid (about 14-km), utilizing a different analysis scheme and including an orographic correction procedure that employs the Parameter-elevation Regressions on Independent Slopes Model (PRISM). PRISM is set of monthly precipitation data for the period 1961-1990. The

analysis scheme is an inverse square-distance interpolation algorithm applied with a short influence radius of 50 km. The methodology of PRISM and a general discussion of precipitation gradients with respect to topography can be found in Daly et al. (1994). The PRISM is important for developing more reliable estimates of precipitation in the mountainous western United States. This precipitation analysis was employed for the assimilation of precipitation in the NARR 0-3h forecasts.

The third set of precipitation analyses, designated $\boldsymbol{P}_{UW}$, was developed and produced by the University of Washington (on the same 0.125° × 0.125° grid as P_{CPC}^{ORO}) by applying, as described in Maurer et al. (2002), a PRISM orographic correction and the analysis scheme of Shepard (1984); the $\boldsymbol{P}_{UW}$ long term average is set up to match the PRISM climatology. This analysis scheme utilizes an inverse square-distance weighting algorithm with a dynamic radius of influence that increases until four reporting stations are attained. The dynamic treatment of influence radius in $\boldsymbol{P}_{UW}$ is sufficient to ensure that no landmass grid points are left undefined. The rainfall Co-op dataset was employed for the United States, while a sparser distribution of raingauges was employed for Canada (which could lead to a lower quality analysis over that region). The $\boldsymbol{P}_{UW}$ analyses were used as the precipitation forcing for the offline, uncoupled executions of the VIC model described next.

2.3 Precipitation Evaluation

A primary indication of the performance of the overall Eta/EDAS system is the realistic estimation of model precipitation. In this section, we show how the model precipitation changed with time, how it related to the model forecast system

development, and to the initial input data source. We chose the Mississippi River basin and two western basins including the Columbia and Colorado River basins as study areas, but with an emphasis on the western basins where there is more convincing evidence in the model improvements.

2.3.1 The Mississippi River Basin

The 1995–2002 time series of the Mississippi basin area-averaged Eta model 12–36 h forecast precipitation and observed precipitation $\boldsymbol{P}_{CPC}$ (based on the daily analyses of Higgins et al. (2000) are presented in Figure 2.1, along with a sequence of numbers that represent the major changes in the model as described in section 2.2 and Table 2.1. In general, the fit to precipitation observations has improved with time. The two curves depict close similarity in magnitudes and the year-to-year variability, but some changes are noticed over the years. Differences are larger before 1998, as the forecast precipitation (dash line) tended to have higher month-to-month variability and discrepancies in magnitude. From mid–1998 onward, when atmospheric and land states (including soil moisture) began to be cycled without a dependence from NCEP's global model (indicated by 5 in Figure 2.1), the observed and forecast precipitation tend to show a closer agreement. The last part of the record (marked with number 10) shows even closer correspondence. This was the time when the EDAS began to assimilate observed precipitation.

The distribution shift between the early and late periods are shown in the scatterplots of monthly observed vs. forecast precipitation averaged for the Mississippi basin (Figure 2.2). During 1995–1997 (Figure 2.2a) the Eta model had a

distinct dry bias during both the cold and warm seasons, particularly in the range 1–3.25 mm day^{-1}. On the other hand, during 1998–2002 (Figure 2.2b) a more even distribution of points along the symmetric axis is noticed. There appears to be a slight wet bias, particularly for large precipitation during winter, but the magnitude is smaller than the dry bias of previous years. The dry bias during the first years was observed in all subbasins except the Ohio basin (not shown), but it was removed beginning in mid-1998. The slight wet bias during the 1998–2002 winters affects the Missouri and Upper Mississippi basins.

2.3.2 The Western United States Basins

Evaluation of the Eta model 12-36 h precipitation forecasts over the western United States was done by means of comparison with the observation-based precipitation analyses as discussed in section 2.2.

a. Time-mean basin-scale precipitation

Table 2.3 shows the precipitation estimates for the two western basins (Figure 2.3). Unlike $\boldsymbol{P}_{UW}$ and $\boldsymbol{P}_{ETA}$, the $\boldsymbol{P}_{CPC}$ and P_{CPC}^{ORO} estimates do not include the Canadian portion of the Columbia basin. Therefore, for comparison purposes, Table 2.3 presents $\boldsymbol{P}_{UW}$ and $\boldsymbol{P}_{ETA}$ with and without the Canadian portion. The area averages without Canada's precipitation can be directly compared to the CPC estimates, while those that include the whole basin (last two rows of Table 2.3) are consistent with the other surface water terms to be discussed in section 2.5. The Columbia-averaged precipitation $\boldsymbol{P}_{UW}$ is significantly larger than $\boldsymbol{P}_{CPC}$ and P_{CPC}^{ORO} for the period June 1995

- May 2000. The mean difference between the two is larger over the Columbia basin than over the Colorado, reflecting that topography effects are larger in the former than the latter. The June 1995-May 2000 average of P_{CPC}^{ORO} for the Columbia basin is larger than $\boldsymbol{P}_{CPC}$, but the relation is inverted in the last three years (June 2000 – May 2003). This contradicts what would be expected of the orography correction. Moreover, a decreasing trend was noted in P_{CPC}^{ORO}. Fewer raingauges were included after 2002 in both CPC precipitation analyses. In turn, due to the short radius of influence in the analysis scheme of P_{CPC}^{ORO}, its interpolation technique may have resulted in an increased number of missing values, however, this does not seem to be the cause of the trend. A preliminary analysis of the NARR (will be discussed in next chapter) reveals that the decreasing trend for P_{CPC}^{ORO} was translated to NARR, which can only be noticed in the Columbia and Missouri basins (both have important topographic effects).

Table 2.3 Annual mean precipitation for western US basins.

BASIN	***Columbia***		***Colorado***	
Period	**5-yr June 1995 May 2000**	**3-yr June 2000 May 2003**	**5-yr June 1995 May 2000**	**3-yr June 2000 May 2003**
P_{CPC} (1)	***1.80***	***1.56***	***0.77***	***0.74***
P_{CPC}^{ORO} (1)	***2.11***	***1.54***	***0.81***	***0.71***
P_{UW} (1)	***2.29***	***--***	***0.88***	***--***
P_{ETA} (1)	***2.29***	***1.85***	***0.52***	***0.89***
P_{UW} (2)	***2.45***	***--***		
P_{ETA} (2)	***2.33***	***1.93***		

(1) Estimate does not include Canadian portion of basin; (2) Estimate includes Canadian portion of basin. Units are mm day^{-1}.

In contrast, over the Colorado basin, during June 1995 – May 2000, the mean $\boldsymbol{P}_{ETA}$ was smaller than $\boldsymbol{P}_{CPC}$ (-32%) and $\boldsymbol{P}_{UW}$ (-41%). In general, there was a dry bias of the model over the southwest U.S., which would suggest that in this case the convective parameterization scheme -or its triggering function- are the ones that do not respond adequately. Note that when considering the last 3 years, the differences are reduced, and actually $\boldsymbol{P}_{ETA}$ becomes larger than $\boldsymbol{P}_{CPC}$ or P_{CPC}^{ORO}. These results highlight the model improvement in precipitation physics.

All these estimates were done for the area average of the U. S. portion of the Columbia basin. However, the water budget requires having an estimate for the whole basin. The last two rows in Table 2.3 show that significant precipitation occurs over Canada's portion of the basin, which is reflected in larger averages for both $\boldsymbol{P}_{ETA}$ and $\boldsymbol{P}_{UW}$.

b. Observed precipitation

Figure 2.4 depicts the June 1995-May 2000 5-year annual mean CPC precipitation analysis ($\boldsymbol{P}_{CPC}$ and P_{CPC}^{ORO}) and the University of Washington precipitation analysis ($\boldsymbol{P}_{UW}$), as well as their differences, over the western United States (recall that $\boldsymbol{P}_{UW}$ was not available after mid 2000). The three precipitation analyses (Figures 2.4a-c) are characterized by large values over the central Columbia basin, along the coastlines (including the Olympic Mountains), over the western slopes of the Cascades and the Sierra Nevada. Referring to the Figure 2.3 which shows the western United States topography, it is not hard to notice the differences between the analyses (Figures 2.4d-f) are small over flat areas, but the orography correction in P_{CPC}^{ORO} and

$\boldsymbol{P}_{UW}$ is evident over the slopes of the Cascades, the Rockies and the Sierra Nevada. In general, if the orography-corrected precipitation analyses are taken to be closer to reality, then $\boldsymbol{P}_{CPC}$ underestimates the real precipitation over most of the western United States due to its prevalent complex terrain. In addition, the differences between P_{CPC}^{ORO} and $\boldsymbol{P}_{UW}$ (Figure 2.4f) show that there are important uncertainties still in gauge-based precipitation analyses, despite the correction for orography effects. Uncertainties in the observations lead to uncertainty in the long-term trends of model precipitation and some uncertainty in the model interannual variability. These differences are of special significance to illustrate the large sensitivity of the monthly precipitation to the topography and northern cold weather conditions, and they reflect the difficulties of estimating reliably the precipitation over the Columbia basin.

c. Eta model forecast precipitation

The model forecast precipitation is assessed for two different periods to show its progress in recent years. Figure 2.5 presents the June 1995-May 2000 averages (as Figure 2.4), while Figure 2.6 shows the averages for June 2000-May 2003 (no $\boldsymbol{P}_{UW}$ was available, though). The model forecast precipitation for the first period (Figure 2.5) captures all the regional features depicted by the precipitation analyses over the northwestern United States, and the intensity over mountains lies between the gridded analyses. In general, the Eta model has a wet bias in the northern sector (particularly near valleys) and a dry bias toward the south. The larger differences (Figure 2.5b-d) are noted in the mountainous west including most of California and the Columbia River basin, where the snowfall is more prevalent. $\boldsymbol{P}_{ETA}$ is closer to $\boldsymbol{P}_{CPC}$ than either

to P_{CPC}^{ORO} or $\boldsymbol{P}_{UW}$, possible due to the fact that after late July 2001 the EDAS assimilation system for the Eta model began ingesting non-orographically corrected precipitation (except, as stated earlier, in situations when and where the Eta simulation infers temperature conditions sufficient for snowfall). According to Figure 2.5c, the biases increase slightly with the orographic correction to the CPC analyses (P_{CPC}^{ORO}) and become even larger in the case of using $\boldsymbol{P}_{UW}$ (Figure 2.5d). In other words, during June 1995-May 2000 the Eta model tended to produce excessive precipitation when compared to the two CPC analyses, while the differences with $\boldsymbol{P}_{UW}$ show that the positive bias is only found in the western sector of the basin. On the other hand, the difference with respect to all three precipitation analyses reveals a dry bias over the Colorado basin. Similarly, a dry bias is observed over California, with the exception of the Central Valley.

According to Figures 2.5b-d, the Eta model forecast precipitation tends to differ more from all the precipitation analyses ($\boldsymbol{P}_{CPC}$, P_{CPC}^{ORO} and $\boldsymbol{P}_{UW}$) over the Columbia basin than over the Colorado basin. As it happened with the precipitation analyses, away from the northern region and coastal areas, the differences are less pronounced bringing closer all estimates.

We recall from Section 2.2 that the horizontal resolution of the Eta model increased from 48-km to 32-km in February 1998, then to 22-km in late September 2000, and finally to its present resolution of 12-km in late November 2001. Also at the latter time, the explicit microphysics in the Eta model was substantially upgraded. Figure 2.6 presents the results for the period June 2000-May 2003 as a counterpart of Figure 2.5. At first sight the mean field for June 2000 – May 2003 (Figure 2.6a)

resembles the mean of the previous years (Figure 2.5a). However, when computing the biases with respect to $\boldsymbol{P}_{CPC}$ and P_{CPC}^{ORO} (Figures 2.6b-c), the reduction in bias magnitude becomes evident. There is a slight wet bias in general, but in most areas it is small, with largest values are about 1 mm day^{-1} (but recall that these precipitation analyses are lower than $\boldsymbol{P}_{UW}$).

d. Basin-scale precipitation variability

The Columbia basin area-averaged time series of precipitation are shown in Figure 2.7a (P_{CPC}^{ORO} is not included because it shows variability similar to the other analyses; also, $\boldsymbol{P}_{UW}$ ended in July 2000). Note that CPC analyses do not cover Canada; therefore a portion of the Columbia basin is not taken into account in the $\boldsymbol{P}_{CPC}$ average. Given that precipitation over Canada is not small, this may be another reason for the lower magnitude of the area average $\boldsymbol{P}_{CPC}$ and P_{CPC}^{ORO} when compared to $\boldsymbol{P}_{UW}$. To some degree, the biases noted in the spatial fields tend to compensate each other in the area averages.

The time series of $\boldsymbol{P}_{ETA}$, $\boldsymbol{P}_{CPC}$, and $\boldsymbol{P}_{UW}$ have a consistently similar evolution, with all showing a larger amplitude of the annual cycle during the first half of the period. $\boldsymbol{P}_{ETA}$, although larger than the precipitation analyses (consistently so in the cold season, and less so in the warm season), seems to reproduce consistently the month-to-month variability. Before mid-1999, according to Figures 2.7b and 2.7c, the model biases have large month-to-month variability and discrepancies in magnitude. The large positive differences and large root mean square error (RMSE) mainly occur in the wintertime over the Columbia basin. In contrast, from mid-1999 onwards, the

analysis and forecast precipitation show notably closer agreement. From near March 1999 to early 2000 there is a remarkable reduction in the RMSE of the model forecast with respect to the CPC precipitation analysis.

Because of relatively lower summer season $\boldsymbol{P}_{ETA}$ biases, it is unclear at what precise moment after mid-1999 the model started performing better. Additionally, the fact that model upgrades are done in "bundles" further complicates determining a unique reason for the improvement. Nevertheless, the changes that may have been relevant appear to be circumscribed by the period spring 1999-autumn 2000.

The drier nature of the Colorado basin is evident in Figure 2.7d. Compared to the Columbia basin, the Colorado basin has a much weaker seasonal cycle and a smaller magnitude of precipitation. Also, the analyses of precipitation (from CPC and UW) and the forecast precipitation ($\boldsymbol{P}_{ETA}$) tend to be much closer over the Colorado basin, again reflecting the fact that despite complex terrain being a factor in precipitation estimation, it is less relevant than over the Columbia. Although the model has a tendency to overestimate the Columbia basin area-averaged precipitation, it underestimates the Colorado basin area averages. According to Figures 2.7e and f, there is better agreement since late 1999, but unlike in the Columbia basin, where large biases were found during winter, the major discrepancies over the Colorado basin occur mostly during the summer months.

e. Model improvements in the annual cycle

From the previous analysis, it is clear that the model precipitation biases have well defined annual cycles, which are different for the two basins and the pre- and

post-1999/2000 periods. In order to further illustrate the model performance in different periods, we averaged the mean annual cycle for the two periods. The 4-year climatology from June 1995 to May 1999 is compared to the 4-year climatology from June 1999 to May 2003, for the Columbia basin in Figure 2.8 and the Colorado basin in Figure 2.9. The shaded bands in Figures 2.8 and 2.9 depict the envelope of spread among the three analyses of precipitation ($\boldsymbol{P}_{CPC}$, P_{CPC}^{ORO} and $\boldsymbol{P}_{UW}$).

- *The Columbia basin*

The mean annual cycles for the Columbia basin are presented in Figure 2.8a. $\boldsymbol{P}_{ETA}$ shows a maximum in December-January and a minimum in August during the two periods, which are consistent in form, if not in magnitude, with observations. The peak near December-January is associated with the large fraction of winter snowfall. For the first four-year average, $\boldsymbol{P}_{ETA}$ is larger than any of the analyses during the cold and wet season. It also has a slight deficit during the summer months. Nevertheless, in sharp contrast, the second period has a remarkable improvement in the quality of the Eta forecasts, as $\boldsymbol{P}_{ETA}$ falls within the range of the analyses with the exception of two months in springtime. Although the summer negative bias seems reduced as well, the major improvement occurs mostly in the winter, with $\boldsymbol{P}_{ETA}$ being reduced by about 2 mm day^{-1}.

In order to better understand the change in model performance before and after 1999, Figure 2.8b presents the mean annual cycle of the convective and large-scale components of the model precipitation during these two periods. Examination of the model's partitioning of precipitation into large-scale and convective contributions reveals that on an annual basis, their ratio is about 5, which is typical of cold climate

and orographically affected basins. During the cold season, the most relevant precipitation is due to large scale processes, which account for much of the total precipitation. The convective precipitation, on the other hand, is close to zero during winter and achieves a maximum during spring. Although it is not as large during summer, it surpasses the large scale component during July-August. Given that the convective precipitation is negligible in the winter, the deficiencies in estimating the Columbia precipitation appear to be associated with the large-scale (explicitly resolved) precipitation component.

- *The Colorado basin*

The Colorado basin has a two-peak mean annual cycle of precipitation (Figure 2.9a), the first one during late winter and probably due to snow storms over the mountains, and the second in mid to late summer associated with the onset of the monsoon season. The annual range of precipitation is quite small. Regardless of the origin, the June 1995-May 1999 average shows that the model had a significant deficit of precipitation throughout most of the year (although larger during the summer months). As in the case of the Columbia basin, the second period (June 1999-May 2003) presents a notable improvement, especially in the warm season, with values well within the range of the precipitation analyses.

Decomposition of precipitation into large scale and convective components (Figure 2.9b) shows that summer precipitation is strongly influenced by convective processes. Therefore, it is likely that the large dry bias is associated with the convective component rather than the large-scale component, which is almost negligible. The changes in the convective parameterization scheme after 1999 were

aimed at enhancing the convective precipitation component in summer and led to model precipitation estimates that were much closer to observations. Given the Eta model's well-known dry bias over semiarid regions traditionally apparent before and during 1999 (Berbery and Rasmusson 1999), the results suggest an improvement in the forecasts quality after 1999. They also agree with Gochis et al. (2002) who find the region's precipitation highly sensitive to the convective scheme employed by mesoscale models in general.

In summary, the dominance of convective processes over large-scale processes in the Colorado basin is in contrast to the dominance of large-scale processes over convective ones in the Columbia basin, affecting the improvement of Eta model performance in different ways. Although the model precipitation in both basins has topography-related problems, they can be traced to the different scales of the precipitation processes in the Eta model (explicitly resolved precipitation microphysics versus convective parameterization) acting under significantly different climate regimes.

The quality of the land-surface water budgets depends on the reliable estimate of basin-averaged precipitation. In both basins, but more importantly for the Columbia basin, the real magnitude of the model bias cannot be ascertained because of the disparity between the observational estimates. Which precipitation estimates can provide more realistic precipitation depictions for model validation continues to be a subject of debate.

2.4 Evaporation Evaluation

Figure 2.10 depicts the June 1995 – May 2000 mean annual fields of the Eta and the VIC model evaporation over the western United States where major differences exists. The VIC model evaporation (Figure 2.10b) shows greater detail and sharper gradients due to the smaller 1/8-th degree grid spacing in the VIC executions (and the coarse 40-48 km Eta output fields utilized in this study). The Eta model 12-36 h evaporation forecast (Figure 2.10a) has values ranging between 0.5 and 3 mm day^{-1} with the largest values toward the southeast, and reveals a clear bias that is more evident in the southwest. The Eta model tends to have a slightly larger evaporation toward Oklahoma/Kansas and smaller evaporation near Oregon and the coastal areas of Washington State. Over the Columbia basin, evaporation is about 1.5 mm day^{-1} in the central part and decreasing toward the higher elevations. However, the Eta model 12-36 h evaporation forecast for the period June 2000 – May 2003 (Figure 2.10c), after performing significant upgrades to the model, reveals a much closer resemblance to the VIC estimate.

2.5 The Surface Water Balance Terms

Table 2.4 summarizes the components of the surface hydrology (except precipitation that was discussed earlier with the support of Table 2.3). According to Table 2.4, the Columbia basin mean annual evaporation from the Eta and VIC models agree to within ~14% for the 5-yr average covering June 1995 – May 2000, but the Eta model value is reduced for the last three years (no VIC data are available to verify it, but this value is closer to the average of the previous period). Over the Colorado

basin, the Eta model evaporation is larger than VIC's by 50% for the first five years of the analysis, but the E_{ETA} values are reduced significantly for the latter 3-yr period.

Table 2.4 Annual mean surface water balance for western US basins.

BASIN	**Columbia**		**Colorado**	
Period	**5-yr June 1995 May 2000**	**3-yr June 2000 May 2003**	**5-yr June 1995 May 2000**	**3-yr June 2000 May 2003**
E_{VIC}	***1.25***	**--**	***0.84***	**--**
E_{ETA}	***1.43***	***1.27***	***1.27***	***0.96***
R_{VIC}	***1.20***	**--**	***0.11***	**--**
R_{ETA}	**--**	***0.92***	**--**	***0.17***
SWE_{VIC}	***67.9***	**--**	***4.4***	**--**
SWE_{ETA}	**--**	***24.6***	**--**	***6.3***

All units in mm day^{-1} except SWE that is in mm.

While in both cases, and for the respective basins, the values are of the same order of magnitude, still the differences are considerable. This is more noticeable in the Colorado basin, where both values are small. The snow water equivalent depth estimated from the Eta model in the Columbia basin is 43.3 mm smaller than the VIC model, while for the Colorado basin they differ by 1.9 mm. However, both models produce deep snow accumulation and rather wet conditions over the Columbia basin and thinner snow accumulation and drier conditions over the Colorado basin.

The water budget equation for the land surface is

$$Residual = \frac{dW}{dt} - (P - E - N) \tag{2.1}$$

Where W is the soil water storage, P is precipitation, E is evaporation and N is the runoff. Therefore, the sources of soil water include precipitation, snowmelt, and condensation of atmospheric water vapor onto the ground. Sinks included surface evaporation and runoff. Ideally, the water storage W should not change over a long time period such as several years, so the precipitation should be balanced by evaporation and runoff. In reality, this rarely happens because the inaccuracies in the atmospheric data assimilation system and other possible reasons.

The progress illustrated thus far in estimating the surface hydrologic cycle is substantiated further in Figure 2.11, which presents the residual of the water balance equation. First, most flat areas including almost the entire Mississippi River basin (outlined by yellow) are close to balance (no colors) with a residual that is less than 0.5 mm day^{-1} in magnitude. A questionable feature is the imbalances with a positive residual found over regions with high orography, and a negative residual found along the northwest coast, likely due to the model's orographic effects. As a percentage with respect to precipitation (not shown) the residual is less than 20% in magnitude over flat areas, increasing to between 20 and 80% over mountains.

The area averaged residual for the Columbia basin (Figure 2.11b) shows a well defined annual cycle with mostly positive values during spring and slightly negative values the rest of the year. When the effect of the annual cycle is removed (by performing a running mean; heavy line) it is noticed that the residual term was at times almost as large as 2 mm day^{-1} before the year 2000, but it has since become smaller along the years. While not zero, since mid-2001 the values have remained of the order of 0.5 mm day^{-1} or less. Given the slow decreasing trend in the residuals, it

is possible that there is no unique reason for these improvements, but it can be speculated that the continuous cycling of land and atmospheric states implemented in 1998 which slowly modified variables like soil moisture may have had a significant impact.

The residual term is also reduced for the Colorado basin (Figure 2.11c) from a maximum of about 1.3 mm day^{-1} before the year 2000 to slightly positive values in the more recent years. Unlike in the Columbia basin, there is no well-defined annual cycle, although relatively smaller values are found in autumn. The residual term for the Mississippi River basin (Figure 2.11d) is rather small when compared to the two western basins. Similarly, it has no well-defined annual cycle and relative larger residual with a peak of around 0.9 mm day^{-1} before the year 2000, but significantly reduced and shown much closer to zero (exact balance condition) in the more recent period.

In conclusion, our results indicate improved Eta forecast system performance in the quality of model's precipitation forecast and in the reduction of the residual term of the surface water balance. Both effects are most evident in the last three to four years, suggesting that at least similar (or better) quality is found in studies based on NCEP's recently completed Eta model-based North American Regional Reanalysis**.** A more systematic analysis of the regional surface hydrologic and energy cycles using NARR will be provided in next chapter.

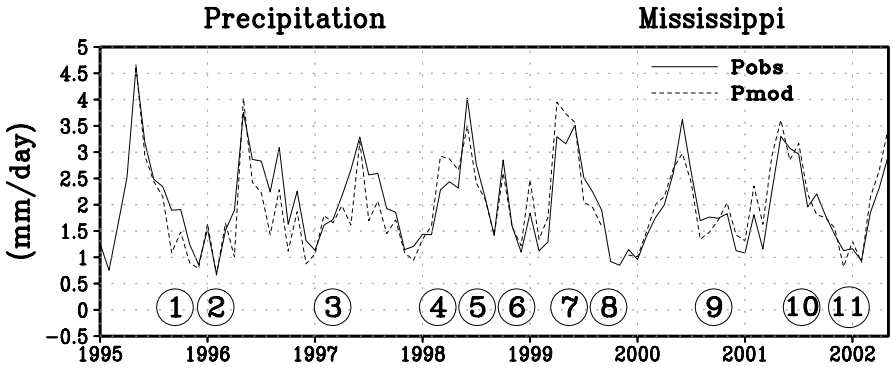

Figure 2.1 Time series of Mississippi basin area-averaged observed precipitation and Eta model 12-36 h forecast precipitation. The circled numbers refer to model changes listed in Table 2.1.

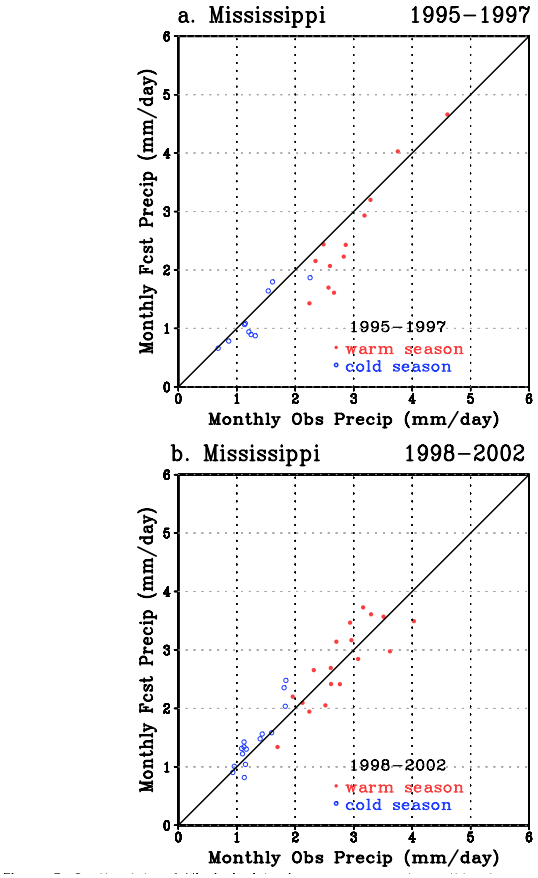

Figure 2.2 Scatterplots of Mississippi basin area-averaged observed precipitation vs. Eta model 12 – 36 h forecast precipitation for (a) 1995-1997, and (b) 1998-2002. Warm season is defined as May - August, and cold season as November - February.

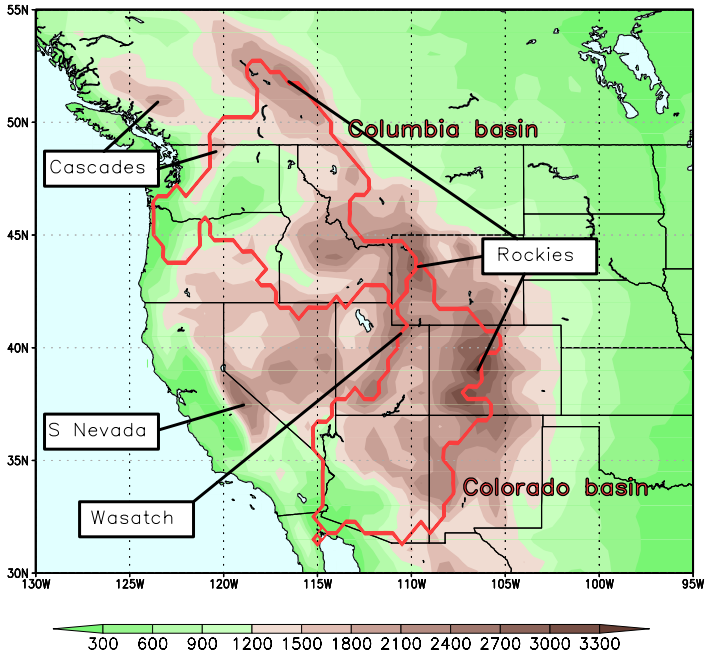

Figure 2.3 The topography of the western United States and the boundaries of the Columbia and Colorado basins.

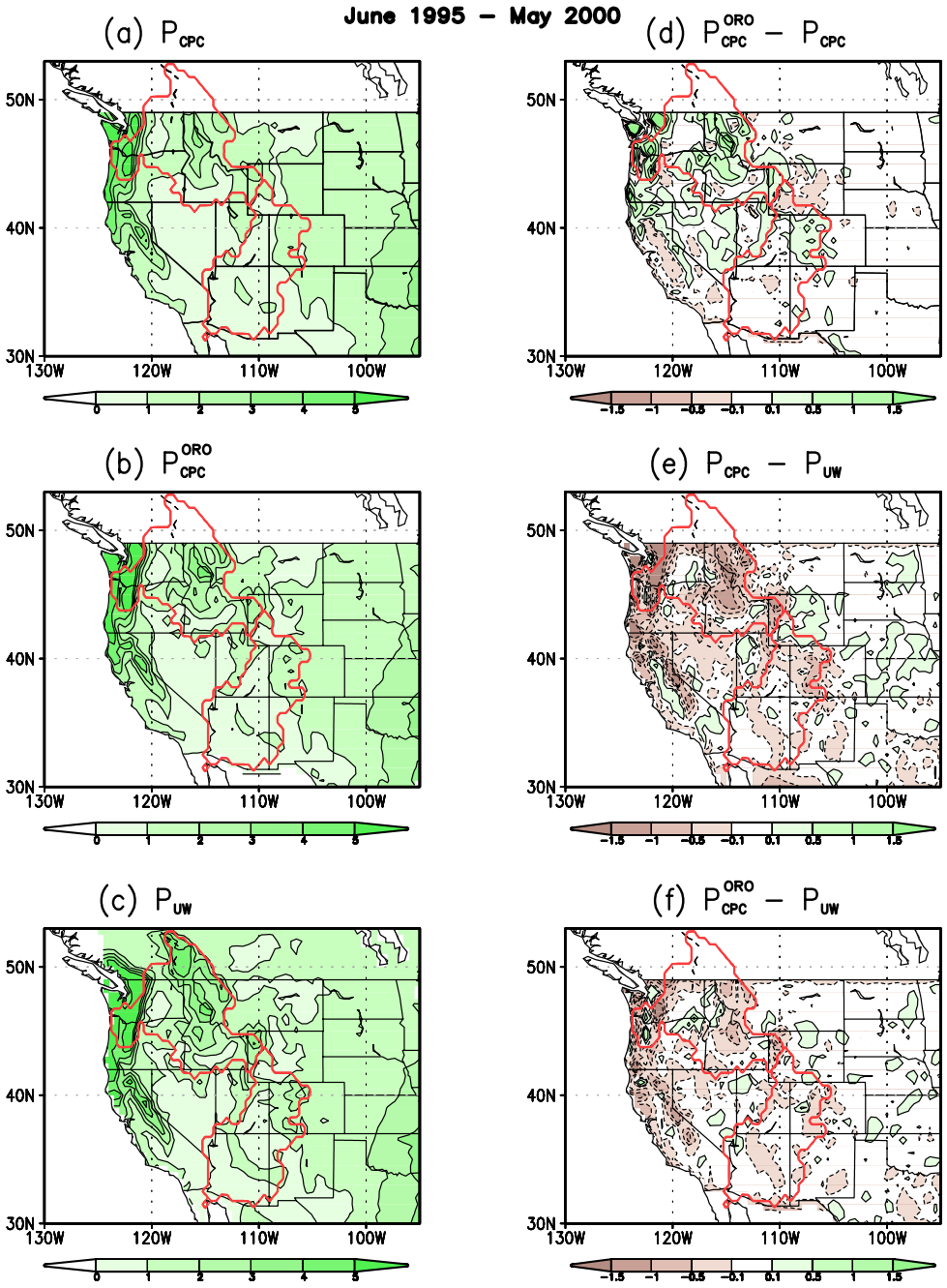

Figure 2.4 June 1995-May 2000 annual mean fields of observed precipitation gridded analyses: (a) CPC precipitation analysis without orographic correction ($\boldsymbol{P}_{CPC}$); (b) CPC precipitation analysis with orographic correction (P_{CPC}^{ORO}); (c) University of Washington precipitation analysis with orographic correction ($\boldsymbol{P}_{UW}$); (d) Difference between the two CPC analyses, P_{CPC}^{ORO} - $\boldsymbol{P}_{CPC}$; (e) Difference $\boldsymbol{P}_{CPC}$ - $\boldsymbol{P}_{UW}$; (f) Difference P_{CPC}^{ORO} - $\boldsymbol{P}_{UW}$. Units are mm day^{-1} and the contour intervals are indicated in the bar below each panel.

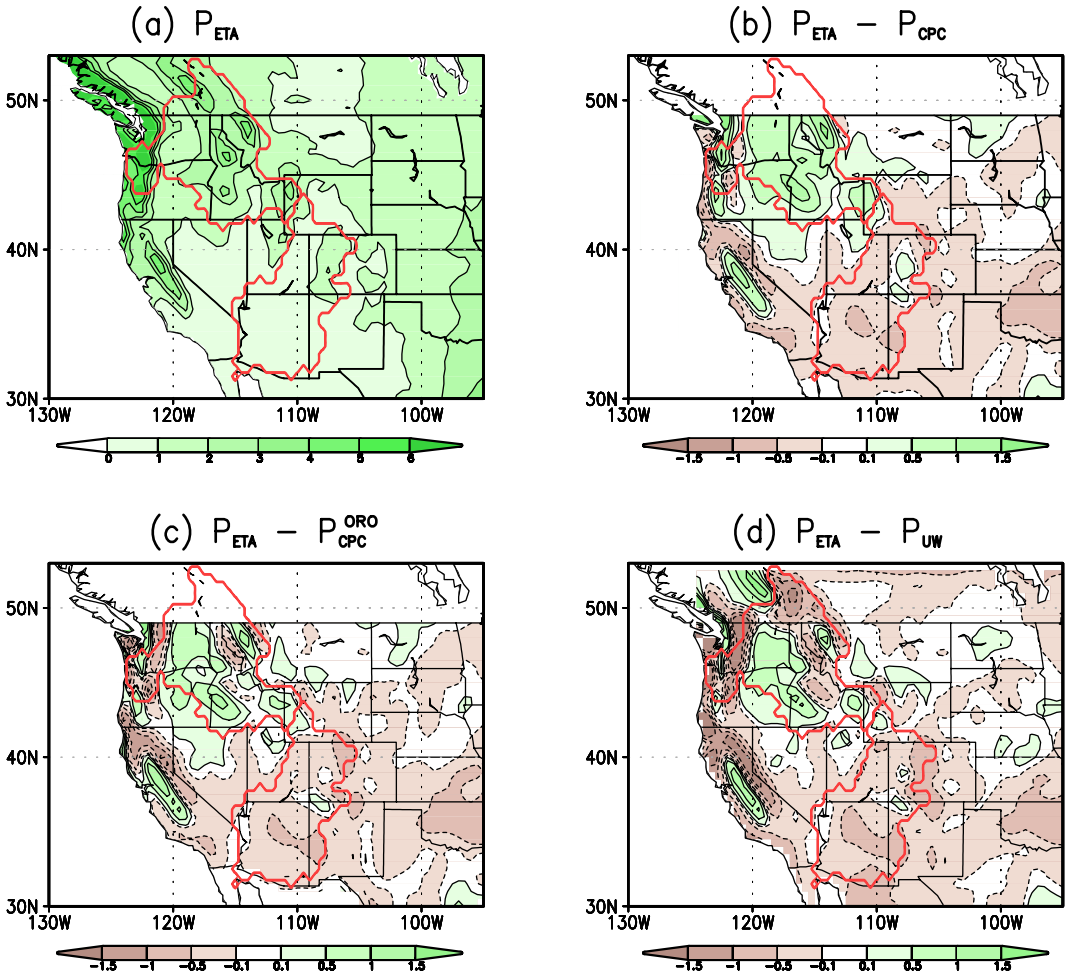

Figure 2.5 June 1995 – May 2000 mean of (a) the Eta model 12-36 h forecast precipitation ($\boldsymbol{P}_{ETA}$), and its difference with the three gridded analyses: (b) $\boldsymbol{P}_{ETA}$ - $\boldsymbol{P}_{CPC}$; (c) $\boldsymbol{P}_{ETA}$ - P_{CPC}^{ORO}; and (d) $\boldsymbol{P}_{ETA}$ – $\boldsymbol{P}_{UW}$. Units are mm day^{-1}, and the contour intervals are indicated in the bar below each panel.

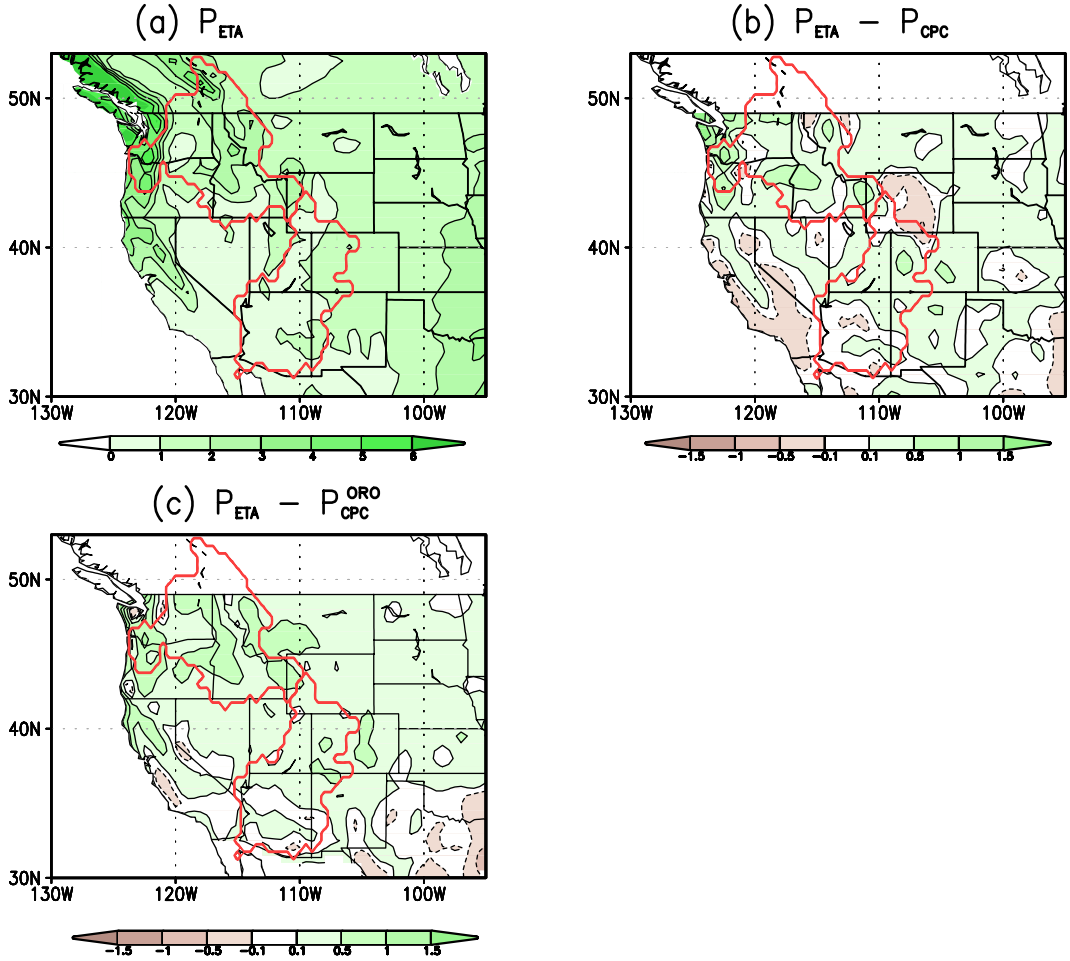

Figure 2.6 June 2000-May 2003 mean of (a) $\boldsymbol{P}_{ETA}$, and its difference with the CPC analyses: (b) $\boldsymbol{P}_{ETA}$ - $\boldsymbol{P}_{CPC}$ and (c) $\boldsymbol{P}_{ETA}$ - P_{CPC}^{ORO} **.** Units are mm day^{-1}, and the contour intervals are indicated in the bar below each panel.

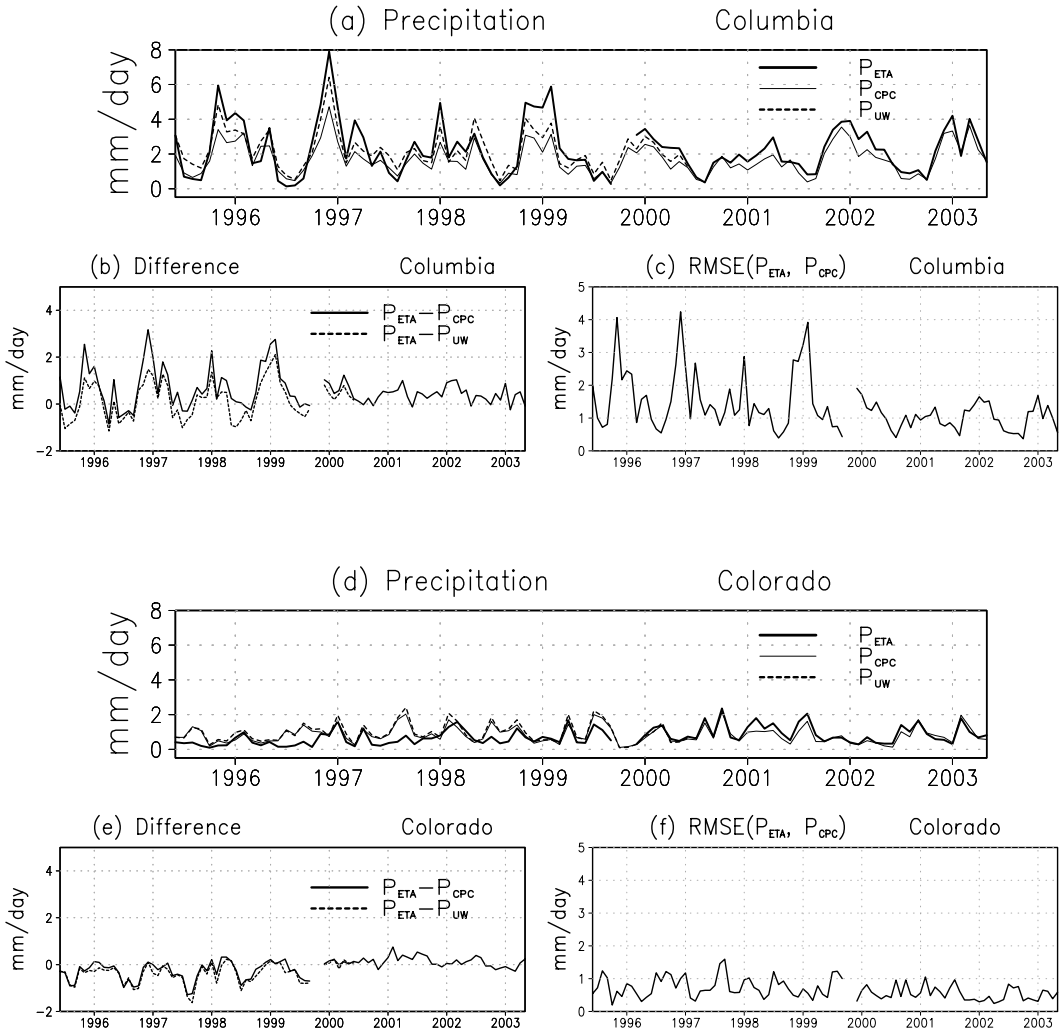

Figure 2.7 June 1995-May 2003 Columbia basin area-averaged time series of (a) Eta model forecast precipitation, University of Washington, and CPC not-orographically corrected analysis; (b) their difference; and (c) the model's precipitation RMSE. (d)-(f) same as (a)-(c) but for the Colorado basin. Units are mm day^{-1}.

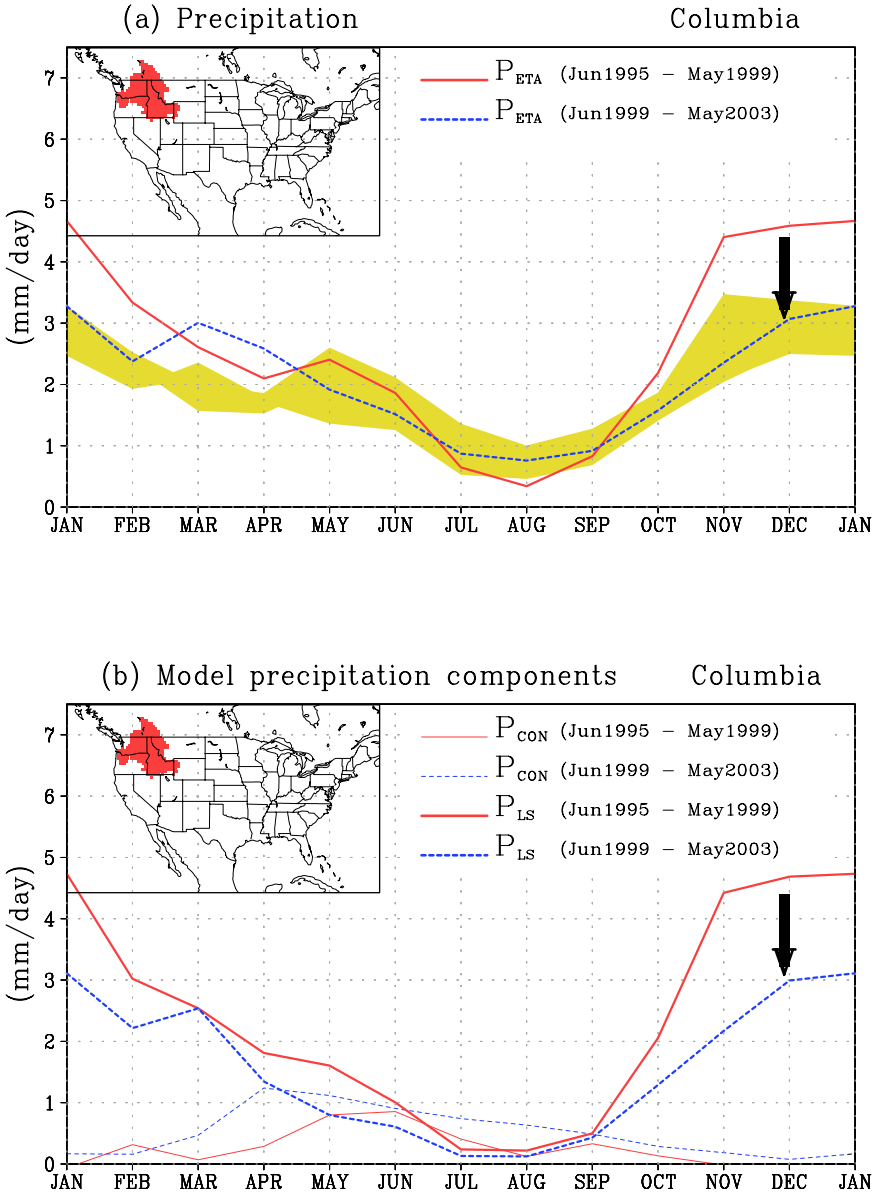

Figure 2.8 (a) Mean annual cycle of the Columbia basin area-averaged Eta forecasts of total precipitation during June 1995 - May 1999 (solid line) and June 1999-May 2003 (dashed line). The yellow band represents the envelope of the mean annual cycle of the three gridded analyses computed for the two periods separately. (b) Mean annual cycle of the Columbia basin-averaged Eta model precipitation components: large-scale (P_{LS}) and convective (P_{CON}) for the same two periods as in (a). Units are mm day^{-1}.

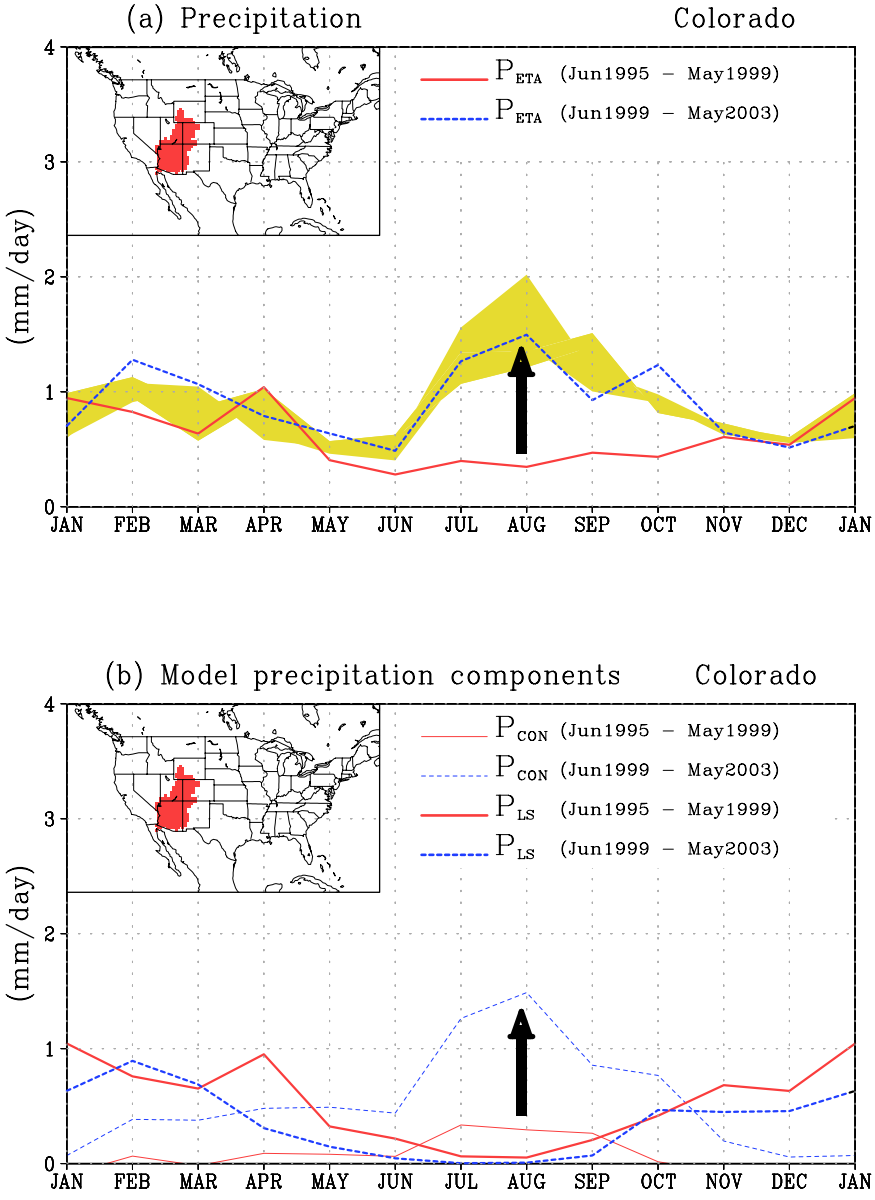

Figure 2.9 Same as Figure 2.8 but for the Colorado basin.

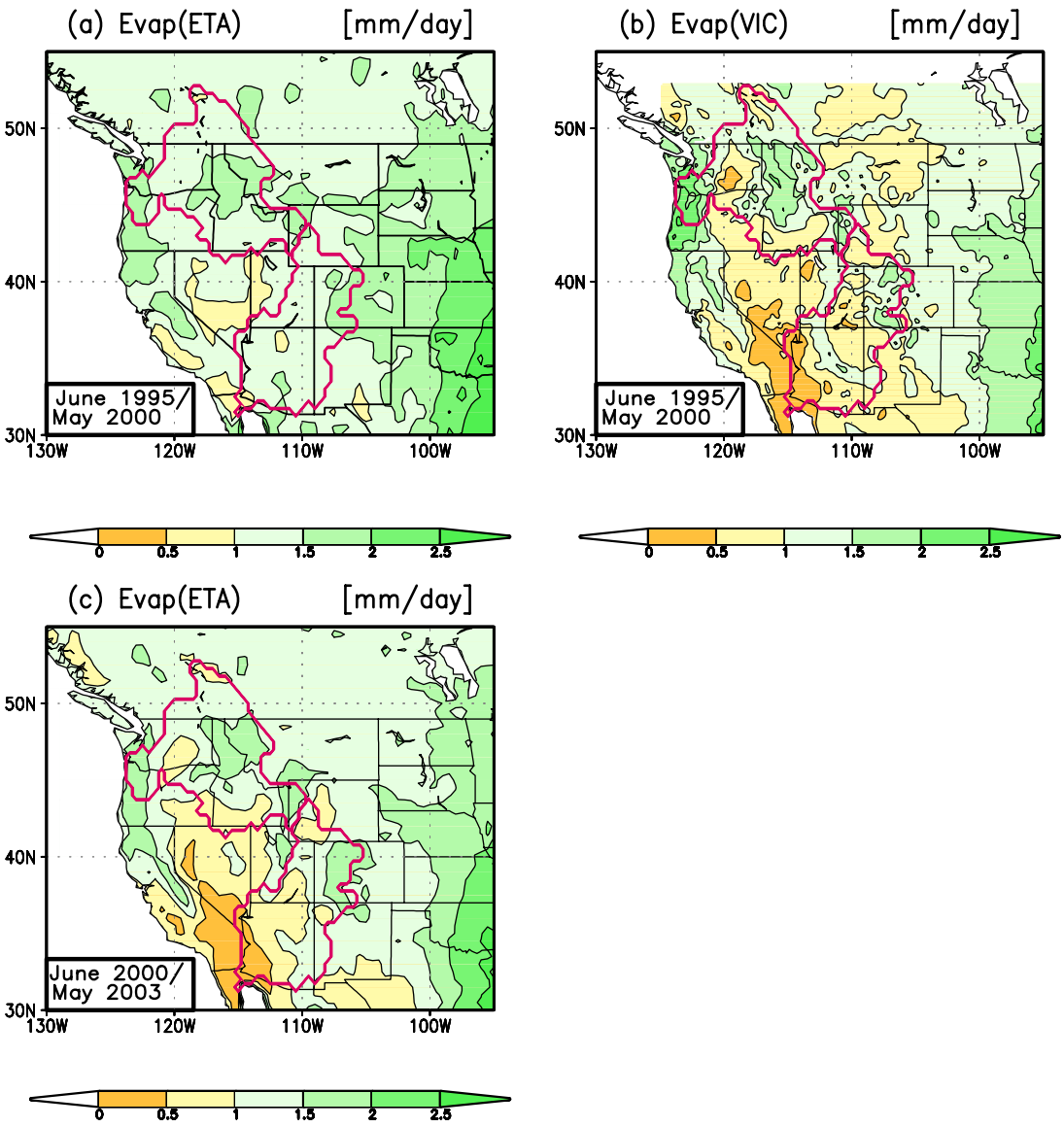

Figure 2.10 Annual mean fields over 5 years (June 1995 – May 2000) of (a) coupled Eta model evaporation and (b) uncoupled VIC model evaporation. (c) the same as (a), but for the 3 year period June 2000 – May 2003. Units are mm day^{-1}.

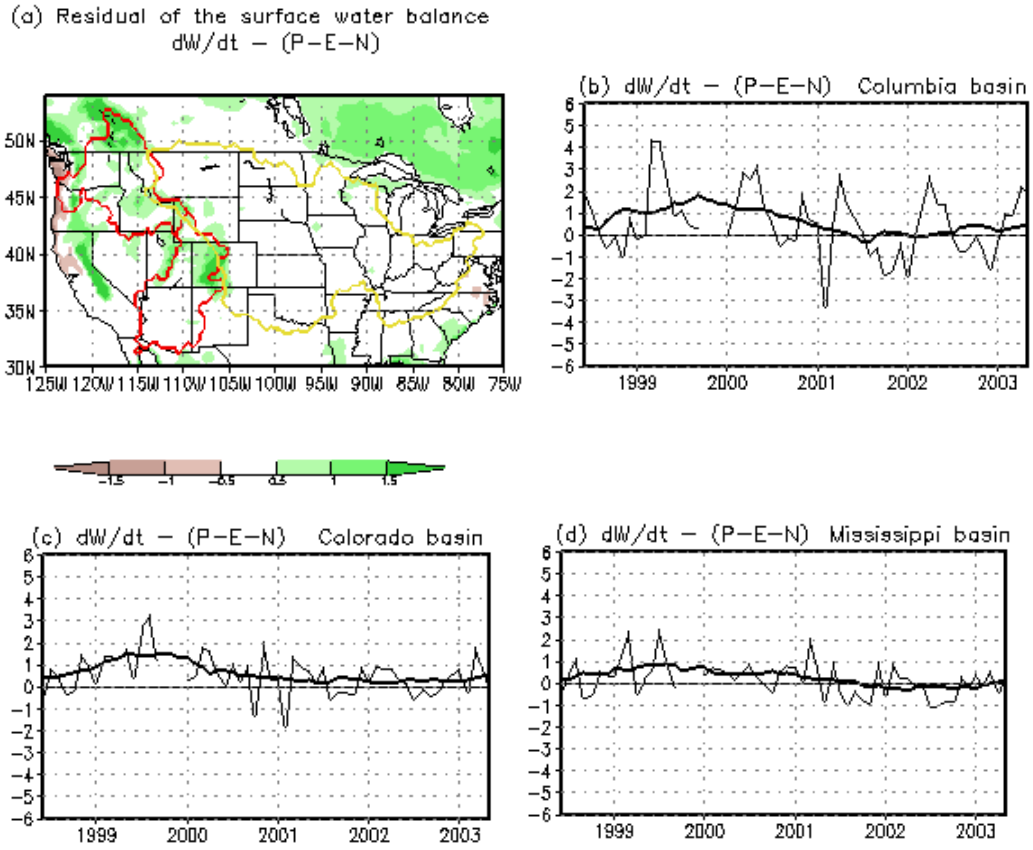

Figure 2.11 The residual term of the water balance equation estimated from the Eta model: (a) the mean field for June 1998 – May 2003, (b) the area average for the Columbia basin, (c) the area average for the Colorado basin, and (d) the area average for the Mississippi basin. The heavy line in (b), (c) and (d) represents a running mean to remove the annual cycle. dW/dt is the local change of surface water (soil moisture and snow water equivalent), P is the precipitation, E the evaporation and N is the runoff plus the baseflow. Units are mm day^{-1}.

CHAPTER 3: REGIONAL REANALYSIS ESTIMATED SURFACE WATER AND ENERGY BUDGETS

3.1 Introduction

Continuing the work in Chapter 2, we use the Regional Reanalysis data to quantify many physical processes which determine the land surface energy and water balance. Therefore, this chapter aims to produce a 'long term' regional climatology of the water and energy cycles over the North American basins. We believe that understanding of the surface water and energy cycles and their variations can provide clues for future prediction. In Chapters 4 and 5, we analyze the NARR data and relate them to land surface-atmosphere interaction processes and soil moisture memory processes respectively, and discuss the differences that exist among those basins.

3.2 The Generation of Regional Reanalysis

3.2.1 Configuration of Regional Reanalysis

The NCEP/EMC Regional Reanalysis project is designed to create a long-term set of consistent regional data for the North America domain (Mesinger et al., 2002). The NARR system uses the frozen version of the Eta Model and 3D-Var Data Assimilation System (EDAS), operational in April 2003. Another aspect of NARR superior to operational Eta/EDAS products is that it can avoid climate jumps introduced by various changes in the model forecast and data assimilation system,

such as improving numerical or data assimilation and physical parameterizations, along with increases in resolution. The system is fully cycled, with a 3-hr forecast from the previous cycle serving as the first guess for the next cycle. Since the reanalysis model is run only in short-term forecast mode, it does not 'drift' with time in the sense of a free-running climate model.

The domain size shown in Figure 3.1 is that of the current operational Eta model, covering North America and extensive parts of the Atlantic and Pacific oceans. The computational grid has a horizontal resolution of 32 Km and there are 45 levels in the vertical, which is the same as that of the operational Eta model prior to September 2000. NCEP/NCAR Global Reanalysis (GR) was used to supply lateral boundary conditions to the NARR. NARR uses a large number of variables including observed precipitation over North America and CMAP (Xie and Arkin, 1997) outside the continent, TOVS-1b radiances, wind profilers, VAD winds, GOES radiance and other land surface variables in the data assimilation system (Mesinger et al., 2002).

The assimilation of observed precipitation with the use of PRISM (Mountain Mapper) is by far the most important data addition to the NARR, because this ensures that model precipitation during the assimilation was close to observations, and therefore is the key to ensuring that the hydrologic cycle is more realistic than it would be otherwise. In particular, we are encouraged by the fact that the water cycle can be presented well by the assimilation of observed precipitation (Luo et al. 2005). Furthermore, the NARR system explicitly accounts for land-atmosphere interactions, enabling us to study the influence of soil moisture on summer precipitation in Chapter 4.

3.2.2 Regional Reanalysis Products in Our Study

NARR datasets available for our study span the 24 years from 1979 through 2002. Additional documentation on this product can be found under http://www.ncep.noaa.gov/mmb/rrean/. Long-term high temporal and spatial resolution data accumulated with a 0-3h short-term forecast is a unique aspect of the NARR, and leads to additional efforts on diurnal cycle studies. This NARR project offers an improved, high-resolution description of land surface conditions that are ideal to accomplish the objectives of our proposed research. Under its retrospective setting, NARR creates opportunities not only for energy and water budget studies, but also is very attractive for the atmosphere-land surface interaction analyses. Undoubtedly, the study of the surface water and energy cycles in this chapter and the analysis in the following chapters can be better quantified thanks to the longer time series of NARR adopted in the study

In this study 3-hr analyses have been averaged to monthly values and then used to produce a 24-year (1979-2002) climatology of the water and energy cycles, including estimates of precipitation, evaporation, runoff, soil moisture, snow, and surface radiation and heat fluxes.

3.3 Updated Comparison of NARR Precipitation with Observations

First we make a comprehensive precipitation evaluation for North America by analyzing multiple time scale aspects of the precipitation.

We have analyzed how precipitation in North America differs among the

Regional Reanalysis, VIC model estimate, and observations. As expected, precipitation is quite well captured temporally and spatially by NARR. On the annual basis, precipitation estimated from Regional Reanalysis was typically slightly less than observed, but higher in the northern part of the western United States. Slightly positive biases were found in the western complex terrain, which is related partially to the cold season precipitation estimation.

For multiple basins, the basin-averaged monthly time series of Regional Reanalysis 0-3h forecast precipitation (Figure 3.2) show a closer agreement with observation than previous studies, with differences within 0.2 mm day^{-1} over most Mississippi basins, except the Ohio which shows a relatively larger bias. The agreement is best for the Mississippi River subbasins, where the data quality and coverage are reasonable. The magnitude of the precipitation over the Core Monsoon region is slightly smaller than that of observations. The Columbia basin and Southwest basins show large differences. This is the result of the difficulties of accurate precipitation measurement in winter over the mountainous regions. The bias has been significantly reduced compared to our previous studies in Chapter 2 by using PRISM corrections.

In summary, the precipitation biases in the Mississippi basin and its subbasins are significantly reduced (even negligible). The Columbia basin has the largest biases, suggesting that there is higher uncertainty of estimates from NARR, and the uncertainty may be mainly caused by uncertainty in the observations themselves over the complex terrain. In general, the similarity in precipitation estimates is perhaps not surprising, since observed precipitation was assimilated in NARR, and thereby

supporting the possibility of better estimating other components in the water and energy cycles. Thus, precipitation estimation has been significantly improved by the configuration of NARR, especially by appropriately applying direct assimilation of observed precipitation with PRISM corrections.

We are also interested in the reliability of NARR for estimating the diurnal cycle of summer precipitation at basin scales. This is because capturing the structure and diurnal march of summer precipitation over North America reflects whether physical processes that conduct to precipitation are properly reproduced in NARR.

The NARR has a reasonable diurnal cycle of precipitation in summer (Figure 3.3-3.4). It has an evening and nocturnal rainfall maximum in most of the Mississippi basin, and does show a near-noon precipitation maximum in monsoon-affected regions, the south coast of Florida and along the Gulf of Mexico, and a quite weak diurnal cycle over the rest of the United States western basins. The diurnal cycle of precipitation exhibits marked regional variations, usually related to the low-level jet in the Great Plains, and geographically-tied summer monsoon circulations (Douglas and Englehart 1996; Higgins et al. 1997). The similarity with observations is encouraging, as broad aspects of the observed diurnal cycle of precipitation were reproduced in the Regional Reanalysis.

3.4 Land Surface Water Budget

Due to the nonexistence of observations of many surface hydrological variables, the spatial and temporal structures of the surface hydrologic cycle from the Regional Reanalysis are firstly assessed using VIC's products, which respond to the

surface water balance equation driven by observed meteorological conditions. Secondly, in this and the next sections we present a detailed description of the basin-scale features of the surface water and energy cycles as estimated from NARR. This will provide background for understanding following study in Chapters 4 and 5.

3.4.1 Mean Annual Fields

Figure 3.5 presents the mean annual fields of precipitation and evaporation as produced by the NARR and VIC model parameterizations. Because VIC data are available only until July 2000, the mean fields in Figures 3.5-3.9 are based on the 21-year period of 1979 – 1999. As in the case of the precipitation and evaporation fields in the Eta model, NARR has most regional-to-large scale aspects of the surface hydrologic components in common with the VIC model, like the location of the maxima and their relation to the mountains. With respect to the VIC model, the tendency that NARR underestimates precipitation mainly in the western US and overestimates evaporation mainly in the eastern part still can be observed, but in a reduced degree as compared to the Eta operational forecast products. Particularly, the dark yellow band along the US-Mexico border in NARR evaporation is observed in Figure 3.5c (but not in Figure 3.5d). This is likely due to either discontinuities in assimilated precipitation over United States and Mexico, or differences in soil characteristics in data sets, and thus further clarification of this disparity is required in the future study.

Figure 3.6 presents the mean annual fields of the other surface hydrologic variables as produced by the NARR and VIC model parameterizations. The NARR

snow water equivalent (SWE) depth has large values exceeding 25-50 mm over mountainous regions corresponding to the Cascades, the Rockies, the Wasatch and the Sierra Nevada mountains. Consequently, deep snow accumulation is dominant in most of the Columbia basin and northern part of the Colorado basin (Figures 3.6a,b). The corresponding magnitude of the SWE depth in the VIC model is larger over the mountain ranges and more localized (Figure 3.6b).

Soil water storage depends on the model's structure and parameter values, and therefore it is highly model dependent (Koster and Milly, 1997; Schaake et al., 2004). This common problem occurs as models use different soil layers, soil types, and values for field capacity and wilting point. Consequently models will have different values for "dry" or "wet" conditions. For this reason, absolute values cannot be compared, but the normalized fields should reflect common behavior in temporal changes of soil moisture (Schlosser et al. 2000; Robock et al. 2003). This is the case of the soil moisture derived from the Eta model's land surface model (Noah) and the VIC land surface model, which cannot be compared directly due to the unmatched scale problem. Therefore, the soil moisture fields of the two models were normalized by their respective minimum-maximum ranges.

The relative content of Eta model-produced NARR soil moisture is presented in Figure 3.6c. Soils are dry in the mid-US and southwestern region which is the driest, affecting the southern portion of the Colorado basin, while wet toward the South East and Columbia basin, the one with the highest soil moisture. The NARR soil moisture field reproduces many of VIC's large scale soil moisture maxima, including those within the Columbia and Ohio basins, despite some discrepancies

with respect to extent and magnitude. For example, large values are found in VIC's results over Texas, Oklahoma, and more relevant for this study over Arizona. Also, some other small-scale maxima noticed in the VIC model are not well captured in the NARR estimates (Fig. 3.6e), which here are based on 32 km coarse resolution model output. Recall that VIC has a grid spacing of $0.125^{o} \times 0.125^{o}$ (about 14 km). For our evaluation, it is not necessary to determine which result is correct since both NARR and VIC's estimates are model products. Their differences should be able to highlight the uncertainties that lie in the computations.

The NARR forecast runoff (Figure 3.6e) is largest near the Sierra Nevada slopes toward the Central Valley in California, the Cascades, the Wasatch Mountains, the Rockies, and the eastern part of the US. It can also be seen that runoff in the Columbia basin originates over the northern Rockies and Cascade Mountains, while that of the Colorado basin originates over the southern Rockies, but also the Wasatch Mountains. As with the other variables, the differences between NARR and VIC are mostly in the magnitude and extent of the maxima. The resemblance to the VIC estimates is encouraging: the large runoff over the high mountainous areas is clearly seen in both fields (Figures 3.6c,f), although the VIC model tends to produce patchy-like patterns with a smaller extent of maximum values in the west. VIC's larger (but more localized) values were also noted by Lohmann et al. (2004), who also found large intermodel differences in runoff among the four land surface models in North American Land Data Assimilation System (NLDAS).

The fields of precipitation, snow accumulation, runoff, and even soil moisture share common locations of their respective maximum centers, implying their close

connections. In other words, where there is strong precipitation (heavier snowfall) over the northern high mountainous regions, the later melting of the deep snow accumulation results in large runoff and increased soil moisture in these same regions. Much of the precipitation excess is often lost to either runoff or streamflow in summer or retained in the snowpack in winter and melted or sublimated later. Generally higher runoff is expected from the greater precipitation.

3.4.2 Basin Scale Estimates

The multi-year monthly time series and mean annual cycle of the monthly and basin-averaged surface water cycle terms are presented in Figures 3.7–3.9 for the Mississippi, Columbia and Colorado basins respectively.

The Mississippi basin-averaged mean annual cycle of surface water variables is presented in Figure 3.7. Compared to VIC, the NARR snow water equivalent (Figure 3.7a) has smaller values during winter, and decays faster during spring. It has nonzero values starting in November, achieves a maximum of about 10 mm in January and later decays (snowmelt) until April-May. Normalized soil moisture (Figure 3.7c) achieves a maximum in spring, about 3 months after the maximum in snow. Then it decays monotonically until September, linked to the increasing evaporation (see Figure 3.7d), and reduced precipitation during summer (Figure 3.2a). The reasons for the excessive evaporation during spring and subsequent reformulation of the bare soil evaporation are discussed by Mitchell et al. (2002) and Ek et al. (2003). NARR runoff (Figure 3.7b) also achieves a maximum during late winter and spring, while snow is melting, after which it also decays until the following winter.

The annual cycle of NARR runoff is weaker than the same term (1979-1999) mean annual cycle of VIC runoff.

Time series in Figures 3.7e-h show broadly close interannual variability of NARR and VIC's estimates. Among the more relevant aspects, the maximum values of snow accumulation in wet years (e.g. 1979, 1982 and1997) always are associated with large peaks in spring runoff and soil moisture, and vice versa with the minimum values (e.g. 1988). The time shifts between NARR and VIC estimates also can be seen in the time series. Along the years, the magnitudes of NARR snow depth and runoff are constantly smaller than VIC model estimates mostly occurring in the cold season, but the NARR evaporation remains larger than that of VIC, particularly during warm season.

The NARR's water equivalent of accumulated snow (Fig. 3.8a) for the Columbia basin has non-zero values starting in October, achieves a maximum of about 25 mm in February, and then depletes rapidly through April. The VIC model estimate achieves a substantially larger and later winter accumulation of snowpack than the NARR, reaching a maximum of about 150 mm in March, and then it decays slowly and extends even into early summer. The VIC model non-zero values during the warm season indicate the presence of not fully-melted snow. VIC has sub-grid elevation bands and vegetation tiles that enable it to retain mountain elevation snow pack in summer (see Sheffield et al., 2003; and section 3.4 of Mitchell et al., 2004). Compared to VIC, the NARR snow water equivalent depth has smaller values, particularly during late winter and spring. The results are consistent with the uncoupled tests of the Noah land model and its comparison with VIC in the NLDAS

project: Pan et al. (2003), as summarized also in Mitchell et al. (2004), found that compared to high elevation SNOTEL measurements, Noah had the smallest values, particularly in late winter and early spring snow water equivalent, among the four NLDAS models. In the uncoupled setting of NLDAS, Noah also manifested an early snow depletion bias due to large snowmelt and snow sublimation in late winter and early spring, while VIC had its largest snowpack depletion in late spring, as is evident also in our analysis of Fig. 3.6. Recently, following the evaluation in the study of Luo et al. (2005) and in the cited NLDAS studies, the early snowpack depletion bias has been eliminated in the Noah land surface component of the Eta model by 1) identifying and solving a low bias in the formulation for snowpack albedo and 2) introducing a subgrid treatment for patchy snowpack in the calculation of snow sublimation.

As the NARR snow accumulates (Fig. 3.8a) in the northwest and western mountains, runoff (Fig. 3.8b) starts increasing slowly and peaks in spring (March) when snow melt is largest. The NARR runoff then decays to low values in July, and remains low until the following winter. As a consequence, the timing of the NARR runoff annual cycle is closely associated with that of snowmelt. The NARR runoff peaks two months before VIC's runoff (June), and its maximum is about 1 mm day^{-1} smaller than that in the VIC maximum. This may be due to the substantially underestimated NARR snow accumulation. Therefore, the two differ considerably: runoff remains very low in NARR. In contrast, the NARR runoff peaks earlier in March when snow melts in the model. The NARR runoff peak occurs when snowmelt runs off "instantaneously" over the surface. In nature, as water penetrates the

snowpack and ground and refreezes, it may delay spring runoff. Snow melts too fast in the model and improvements in describing snow processes are needed.

The annual cycle and amplitude of VIC's runoff is similar to the observed runoff (as derived from streamflow) presented in Fig. 11a of Leung et al. (2003). Additionally, the NARR early peak in runoff seems to be common to other mesoscale models. For example, Leung et al. (2003) (also in their Fig. 12a), show that simulations with the Regional Spectral Model (RSM) and the Pennsylvania State University/National Center for Atmospheric Research (PSU/NCAR) mesoscale model, known as MM5, have maximum runoff in March, and in fact they precede the NARR by one month, therefore having a slightly wider gap with either VIC's runoff or observations. As we will see in next subsection, interestingly, the runoff lags precipitation by about a couple of months.

We next examine soil moisture of both models (Fig. 3.8c), normalized here for comparison purposes. The normalization is done by taking the range between the minimum and maximum values in the basin-averaged time series corresponding to each model. The two models show a well-defined mean annual cycle of soil moisture, also achieving a maximum in spring, about two months after the maximum in snow, and simultaneous with the maximum runoff. Then, soil moisture decays monotonically until October, due to the increasing evaporation (see Fig. 3.8d), and reduced precipitation during summer. The VIC model soil moisture, as its runoff, tends to have a later peak (in June) because its snow melt processes last longer.

In summer, most basins have slightly higher evaporation in NARR. Figure 3.8d shows that not only the order of magnitude of the NARR basin-averaged

evaporation is slightly larger than VIC's, but the discrepancies are also found in the phasing of its seasonal cycle. The NARR estimate is too high (compared to VIC's) during spring but too low during autumn (except for winter, when the two are at a minimum). This difference manifests itself in the NARR calculations by shifting the peak two months earlier with respect to VIC model estimates. Notice, however, that in the comparison of four NLDAS models, VIC tended to have somewhat lower evaporation and peak later than the three other models (Figs. 5 and 9 of Mitchell et al. 2004), suggesting that the correct values will be somewhere in between the two estimates. Again, a similar year-to-year evolution can be noticed in Figures 3.8 e-h, although there are some time shifts with NARR ahead of VIC by 2-3 months, and disparities in magnitudes. For instance, NARR snow and runoff are significantly smaller than those of VIC, while NARR evaporation is noticeably larger than that of VIC.

In comparison with the Columbia basin, the Colorado basin exhibits a fairly weak mean annual cycle of all variables (Fig. 3.9a-d). As in the Columbia basin, the area-averaged mean annual cycles of the surface variables have a consistent evolution. There is a very close relationship among precipitation, snow accumulation, and runoff. Once again in the Colorado Basin, there is a marked 1-2 month shift in the phase between the NARR and VIC model components of the surface hydrologic cycle. Although the NARR captures the basic pattern of variability, it tends to slightly overestimate the magnitude in the surface hydrological variables, particularly evaporation and runoff. It should be noted that in addition to the snow accumulation (Figure 3.9a), this basin has a second peak of precipitation due to monsoonal effects

during the warm months (Figure 3.2f). Therefore, unlike in the Columbia basin, the annual cycles of runoff and soil moisture (Figs. 3.9b,c) also reflect this second source of water. This is particularly evident for soil moisture. The soil moisture normalization may give the wrong impression that values are "high" during most of the year, but the actual magnitude of the soil moisture in both models is smaller than in the Columbia basin. In the case of interannual variability in the Colorado basin, with significant smaller magnitudes of the basin-averaged variables than those of the Columbia basin, the interannual evolutions of the NARR and VIC model estimates show some similar features on time shifts (Figures 3.9e-h). Disparities in magnitude are remarkable. NARR snow depth is significantly smaller than that of VIC until 1998, but close afterwards. NARR runoff (Figures 3.9f) presents fairly large values in the peak years of two periods 1979-1980 and 1996-99. In the case of the small evaporation over the Colorado basin, NARR evaporation is much closer to VIC's evaporation, as opposed to the case of larger estimates as in the Mississippi and the Columbia basins (Figure 3.9h).

3.4.3 The Water Balance Terms

Table 3.1 and Table 3.2 summarize the components of the 24-year (1979-2002) surface hydrology for the North American basins from NARR and the VIC model, respectively. Remember that VIC model products are only available for US basins. NARR has larger mean annual evaporation, but less mean annual precipitation, runoff and snow water equivalent than VIC. When focused on the differences in precipitation estimates among these basins, these values of NARR

show closer correspondence to VIC's in the Mississippi basins (Table 3.2). The difference is less than 0.1 mm day^{-1}. However, a difference as large as 0.5 mm day^{-1} is observed in the Columbia basin.

Table 3.1 NARR estimated annual mean (1979-1999) water budget for all basins

Basin	Arkansas/ Red	Missouri	Upper Miss.	Ohio	Columbia	Colorado	Core Monsoon	Rio Grande	Central Mexico
P, mm d^{-1}	1.931	1.365	2.292	3.114	1.881	0.934	1.335	0.880	1.606
E, mm d^{-1}	1.870	1.451	2.167	2.711	1.570	1.122	1.555	0.890	1.511
N, mmd^{-1}	0.124	0.145	0.323	0.497	0.697	0.212	0.052	0.045	0.080
Snow, mm	0.530	3.460	5.009	1.160	6.344	2.190	0.007	0.224	0.002

Table 3.2 VIC estimated annual mean (1979-1999) water budget for all basins

Basin	Arkansas/ Red	Missouri	Upper Miss.	Ohio	Columbia	Colorado	Core Monsoon	Rio Grande	Central Mexico
P, mm d^{-1}	1.975	1.416	2.321	3.280	2.313	1.044	---	---	---
E, mm d^{-1}	1.540	1.214	1.709	1.924	1.216	0.902	---	---	---
N, mmd^{-1}	0.433	0.207	0.622	1.367	1.096	0.158	---	---	---
Snow, mm	1.074	8.478	7.389	2.089	68.146	13.106	---	---	---

NARR and VIC model evaporation, runoff and snow water equivalent can be compared directly because they do have a large period in common. For the respective basins, most values are of the same order of magnitude, but still the differences may be considerable. The differences in evaporation are small when compared to the other two terms. The NARR runoff is about one half of the VIC runoff in the Missouri, Upper Mississippi, and Columbia basins, or even less than one half in other basins. However, there are more noticeable differences in the Columbia and Colorado basins, where both values of snow accumulation are the largest. The snow water equivalent depth estimated from the NARR in the Columbia basin is 62 mm smaller than the

VIC model, while for the Colorado basin they differ by 11 mm. The rather low runoff is correspondent to low snow accumulation as is estimated from NARR.

Figure 3.10 presents the residual of the water balance equation. When compared to Figure 2.11 which resulted from operational Eta model products, it shows more flat areas are close to balance (no colors) with a residual that is less than 0.5 mm day^{-1} in magnitude. The domain and magnitude of imbalances with a positive residual over regions with high orography are moderately reduced in comparison to the operational analysis results (Figure 2.11). A negative residual along the northwest coast is removed as well.

In Figure 3.10 c, d we consider the basins' different behaviors. When the effect of the annual cycle is removed (by performing a running mean; heavy line), it is noticed that the residual term for the Mississippi basin is smaller along the years compared to Figure 2.11. While not zero, the values have residuals of the order of 0.1 mm day^{-1} or less along the years. The Columbia basin has a similar behavior as the Mississippi basin in the earlier period, but the residual term jumped from 0.2 mm day^{-1} in 1995 to 1.5 mm day^{-1} in 1998 and then dropped slowly remaining with values of less than 1 mm day^{-1}. It can be speculated that the temporal inhomogeneities identified before and after 1999 in the observed precipitation analysis data as model initial conditions may have had a significant impact on the NARR products even though the model is frozen. We have discussed this case in Section 2.2.3 of Chapter 2.

Overall, the mean fields of the hydrological variables in the NARR are in qualitative agreement with those from the Variable Infiltration Capacity (VIC)

macroscale hydrologic model at regional-to-large scales. As expected, the largest differences are found near mountains and the western coastline. While the mean fields of precipitation, evaporation, runoff and normalized soil moisture are in general agreement, important differences arise in their mean annual cycle over individual basins: snow melt in the NARR precedes that of VIC by two months, and this phase shift is also reflected in the other variables. That is, an earlier peak of NARR snow accumulation than VIC estimate is translated into an earlier peak of NARR runoff, as well as an earlier peak of NARR soil moisture and evaporation.

3.4.4. Seasonal Changes of the Surface Water Cycle

Figure 3.11 presents the mean annual cycle of key components of surface water budgets, since the hydrologic cycles of these basins possess unique features which are relevant to their climate and geographic location.

- The Mississippi basin

Following the diurnal cycle and annual variations of the Low Level Jet (LLJ), most Mississippi subbasins have a nighttime precipitation maximum during the rainy period of April to September as shown in Figures 2.3-2.4, and in accordance, they have relatively large precipitation and runoff in summer. The Arkansas/Red monthly mean precipitation (red line in Figure 3.11a) shows a maximum of 3 mm day^{-1} in May and a decrease to minimum values in January. Plentiful precipitation all year around shows a weak seasonal cycle in the Ohio basin (Figure 3.11b), with the maximum amounts up to 4 mm day^{-1} occurring during the late spring (May).

Generally, the magnitude of the annual range in the evaporation is much larger than the range in precipitation. Evaporation (green line) has a similar annual cycle to net radiation, reaching maximum during summer. Evaporation reaches its maximum in June-July with very different values depending on the basins' dry or wet climate. It usually surpasses precipitation during April-September with a peak of about 4-5 mm day^{-1}. Mean evaporation values drop to a minimum of less than 1 mm day^{-1} in the winter months.

In the surface water balance equation, runoff (dark blue line) is a minor term when compared to precipitation and evaporation. The smaller annual cycle of runoff in all basins shows a maximum in spring.

The non-zero residual term (black line) illustrates the difficulties in achieving balance in the water budget. This is because the analysis increment is not included here. The residuals in different regions have somewhat different seasonal behaviors. Most regions have seasonal variations ranging from positive values during the first half year and negative values during the second half. Again, the relatively large negative values during the summer in all basins reflect the deficiencies due to excessive evaporation.

- The Columbia basin

The Columbia basin (Figure 3.11c) has large orographically forced precipitation occurring in winter, which mainly falls as snow over the mountainous areas. The hydrology of the Columbia basin is dominated by winter snow accumulation and spring melt, thus resulting in a large fraction of spring runoff.

Residuals are rather large in the Columbia basin during the winter, indicating the potential errors in the excessive solid precipitation.

- The Colorado basin

With obvious smaller amplitude than the Columbia basin, the semi-arid Colorado basin has two maxima of precipitation during winter and summer with different climate origin: the winter peak has a similar origin as the Columbia basin forced by orographic effect, and the summer peak is mainly tied to the North American monsoon. Compared to other basins, the weakest surface hydrologic cycle with almost the smallest components during the summer is indicative of the semiarid climate in this basin.

- The Core Monsoon region

A hydrologic cycle that is very strong in summer but rather weak in the rest of seasons is observed in monsoon-affected regions: characterized by wet summers and dry winters (Figure 3.11e), much of the precipitation in the Core Monsoon region occurs between July and September. The North American Monsoon System is the source of much of this precipitation, with largest precipitation of about 4.5 mm day^{-1}. It is clear that the summer precipitation maximum favors large evaporation, wet soil and runoff. Again, this well-defined annual cycle can be contrasted with that in the Colorado basin, which is more irregular due to the two maxima in precipitation.

In contrast, precipitation exceeds evaporation during the June-September period in the monsoon region. This runoff term has a rather weak and well-defined

cycle. The Core Monsoon region exhibits the opposite behavior of change in soil water storage, and thus in the residuals compared to the other basins. The positive values of change in soil water storage (light blue line) indicate that precipitation exceeds evaporation from June to September so that the Core Monsoon region is a moisture sink from summer through the fall.

3.5 Land Surface Energy Budget

3.5.1 The Summer Mean Energy Budget Terms

The surface energy balance is closely related to the water cycle and is an integral part of the interactions between the atmosphere and the land surface (soil, vegetation, snowpack). Surface energy budgets can help explain the physical processes by which the atmosphere gains energy (Betts et al., 1996).

The magnitude of the surface energy cycle is fairly large during summer and soil moisture is closely related to this cycle during that time. The terms of the warm season (JJAS) 1979-2002 mean surface energy balance are presented in Figure 3.12. Net radiation (Figure 3.12b) shows the largest gain (~160Wm^{-2}) in the eastern part of the country, with a weak gradient and minimum values (~100/120 Wm^{-2}) toward the western U.S. Loss of energy at the surface is mostly partitioned between sensible heat and latent heat fluxes, with a minor contribution of the ground heat flux. The loss of energy by sensible heat (Figure 3.12c) is largest in the western semiarid regions and other areas with reduced clouds. Minimum values between -40Wm^{-2} and -80 Wm^{-2} are observed to the east, including the eastern part of the Mississippi basin. In general, the latent heat flux (Figure 3.12d) has its largest values toward the east, where there is

more moisture availability, and smallest towards the west. As a result of the opposing gradients, the Bowen ratio (Figure 3.12f), is less than one over the eastern half of the Mississippi, reflecting the dominance of latent heat. It then increases toward the semiarid regions of the southwestern United States and northern Mexico. Over desert regions it exceeds 10, highlighting the very different climate regimes. Once again, as we discussed in the previous section 3.4.1, the narrow band of discontinuities along the US-Mexico and US-Canada borders are also noticed in the fields of latent heat flux and Bowen ratio. This problem may stem from assimilated precipitation blending different observed precipitation data sources discriminated by the borders (Mesinger, 2002). Clearly, the latent heat flux carries the discontinuity into the Bowen ratio field. The ground heat flux (Figure 3.12e) is typically one order of magnitude less than the other terms, and therefore is a small part of the surface balance.

Interestingly, the southwestern US regions including the Colorado basin are wet according to the total soil moisture (Figure 3.12a) due to the winter snow accumulation, spring snow melting and later time storage in the whole soil layer. We define this wet feature as “hydrologic wet”. However, it is dry according to the Bowen ratio, and thus defined as “meteorological dry”.

3.5.2 Seasonal Changes of the Surface Energy Cycle

Figure 3.13 has five pairs of panels for the five corresponding representative basins, each showing the mean annual cycle of key components in surface energy budgets and soil moisture.

- The Mississippi basin

The energy cycle is mainly driven by the energy absorbed at the surface in the form of net radiation (NetRad, red line), showing a minimum in December and a maximum in July. The net radiation at the surface is predominantly balanced by sensible heat and latent heat. The Mississippi subbasins have the largest variation in the solar radiation with a maximum about 180 Wm^{-2} in June. Latent heat flux (LHF, green line) displays an annual cycle that closely follows that of net radiation. The annual range of LHF is usually large during the early summer, but it falls in autumn, which has a similar phase as NetRad. It is a dominant term in the Mississippi basin and its subbasins. In the wet Ohio subbasin, latent heat significantly exceeds the magnitude of sensible heat at all times, and during summer it is extremely large. Unlike LHF, the annual range of sensible heat flux (SHF, dark blue line) is small in the Ohio subbasin, but becomes important in all the western basins.

Ground heat flux (light blue line) and the residual term (black line) have quite small values for each basin. The energy residuals are primarily negative with typical values of around 5–15 Wm^{-2} and larger energy deficiency in the warm seasons. These results may be related to the overestimated downward shortwave radiation at the surface as discussed by Berbery et al. (2003).

- The Columbia and Colorado basins

The minimum winter amount of the NetRad in the Columbia Basin is due to the low incident angles of the sun in the northern regions. Especially the sensible heat flux reaches negative values in the Columbia basin, which means the heat flux is transferred from the surface to the atmosphere. On the other hand, latent heat flux has

the smallest values in the semiarid Colorado basin in all seasons owing to its year-round dry climate.

- The Core Monsoon region

The Core Monsoon region has opposite cycles of LHF and SHF to the Arkansas/Red basin, showing a dry period during spring and wet during the summer rainy season. Sensible heat flux reaches the largest values during the early summer in the Core monsoon region.

Here, soil moisture (pink line) was defined as water contained in the top 2 m of soil, expressed in millimeters. It shows a reasonable response to surface hydrologic processes as shown in these figures. The North American basins fall into three categories in terms of soil moisture: the eastern part of the Mississippi basin (Ohio and Upper Mississippi) and the Columbia basin have soil moisture values ranging between 500 to 700 mm, indicating the higher wetness of these basins. The western part of the Mississippi basin (Missouri and Arkansas/Red) and the Colorado basins are in the middle, somewhat drier with total soil moisture ranging between 450 and 550 mm, while the rest of the three monsoon-affected regions are notably the driest, with values ranging between 350-450 mm. We see that during the summer (JJAS) soil moisture is closely related to the LHF and SHF, and follows a decreasing LHF but an increasing SHF with decreased soil moisture over most basins, or vice versa. The soil moisture increases during spring due to the decrease of sensible heat. However, with the progress of the warm season and dying vegetation, there is a reduction of latent heat that goes along with the drying soil.

As discussed in the last subsection, the Colorado basin is an interesting basin because it is a hydrological wet and meteorological dry basin, whereas the rest of the basins are consistently “dry” or “wet” under both hydrological and meteorological definitions. The meteorological definition plays an important role in determining the different behaviors of those basins in land-atmosphere interactions and soil moisture memory processes, as we will emphasize later.

In summary, it is clear that the Regional Reanalysis gives quite realistic interbasin and seasonal variability of precipitation and summer rainfall. The interbasin differences of precipitation appeared realistically linked to their diverse climate regimes. The intensity and structure of summer precipitation can be adequately resolved by the NARR eight daily output. The bias in regions of steep orography is also reflected in NARR, although it was reduced, but not fully solved by applying assimilation of observed precipitation with PRISM. Our validation work has shown that using estimates derived from NARR datasets can largely reduce the pronounced wet biases in regions of steep orography. The residual terms derived from surface water and energy balance equation have quite small values for each basin (Figure 3.11 and Figure 3.13). This study suggests that both the diurnal cycle and small spatial scale feature of the surface water and energy budgets has a great possibility to be resolved adequately using Regional Reanalysis. All these features suggest that NARR is good enough to be applied to study the interactions between the land surface-atmosphere regionally on diurnal to seasonal scales. NARR will significantly enhance the capability to quantify the relative strength of mechanisms in two-way land-atmosphere interactions.

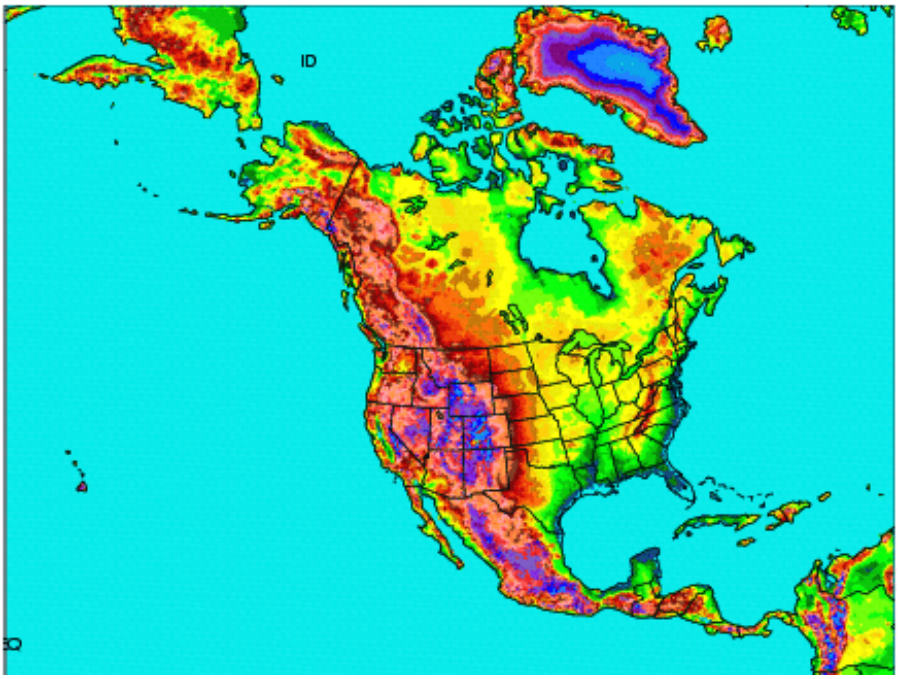

Figure 3.1 The NCEP North American Regional Reanalysis domain and its 32km/45 layer topography. Adapted from Mesinger et al. (2002).

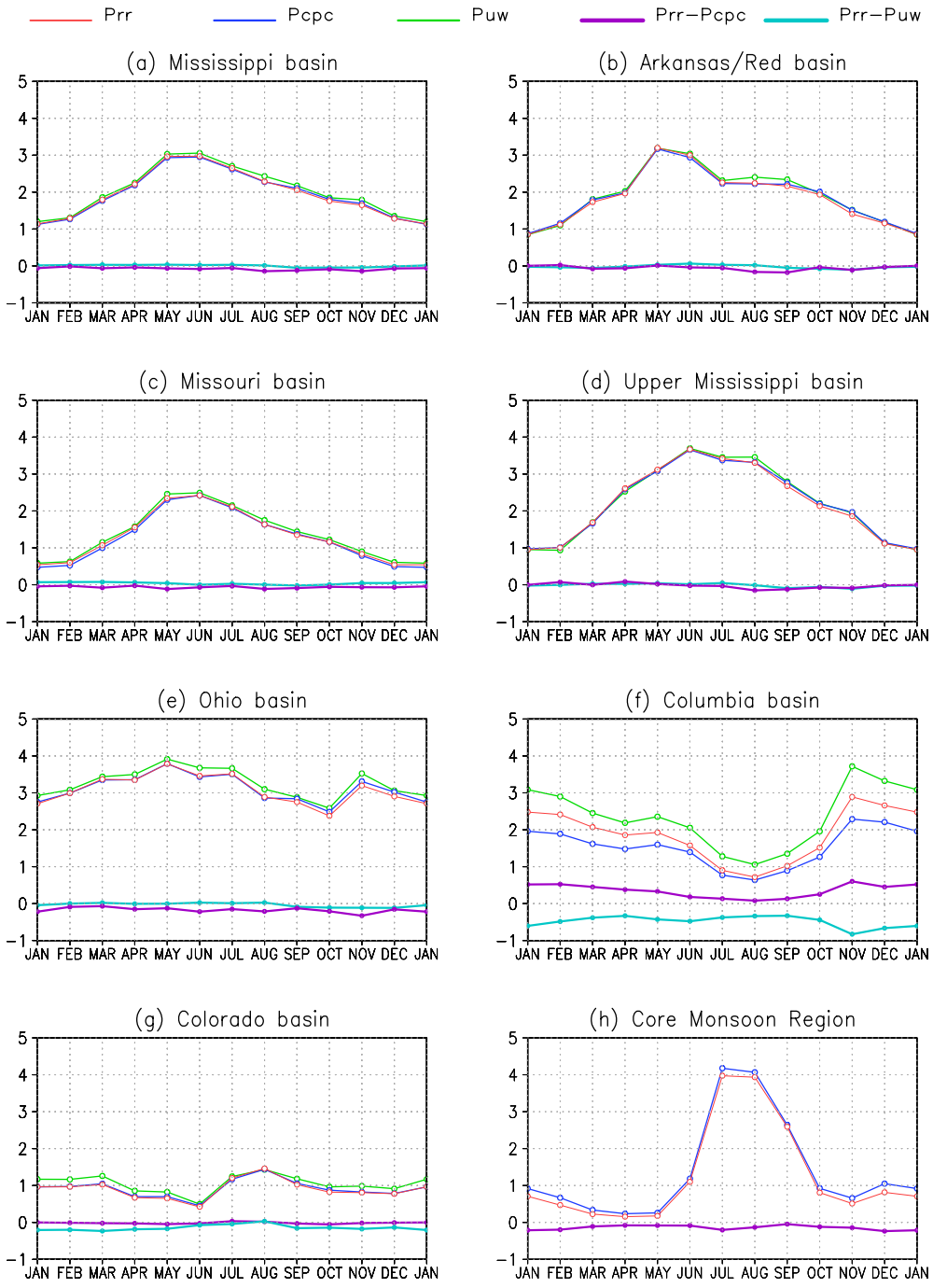

Figure 3.2 Mean seasonal cycle of area-averaged NARR 0-3h forecast precipitation during 1979-2002 and its difference from the two gridded analyses for (a)-(e) Mississippi basin and its subbasins, (f) Columbia basin, (g) Colorado basin, and (h) Core Monsoon regions.

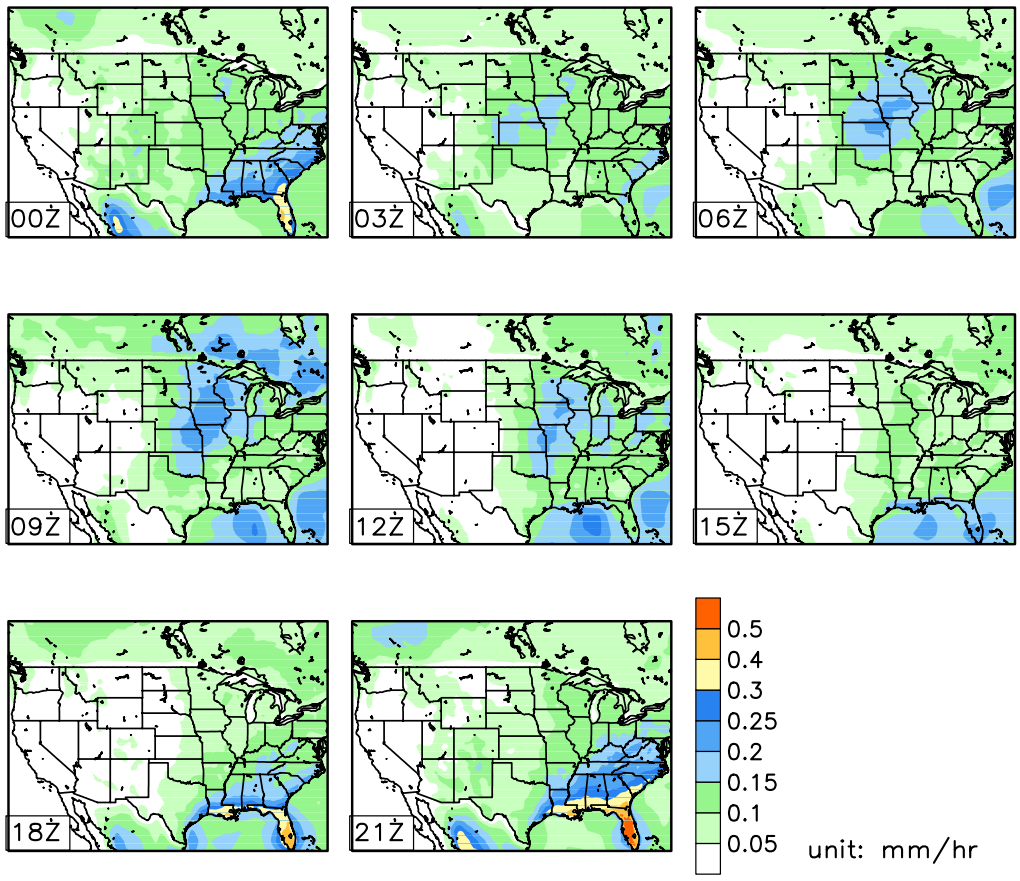

Figure 3.3 The mean summer diurnal cycle of precipitation at 3-h intervals for June-September 1979-2002 in the Regional Reanalysis.

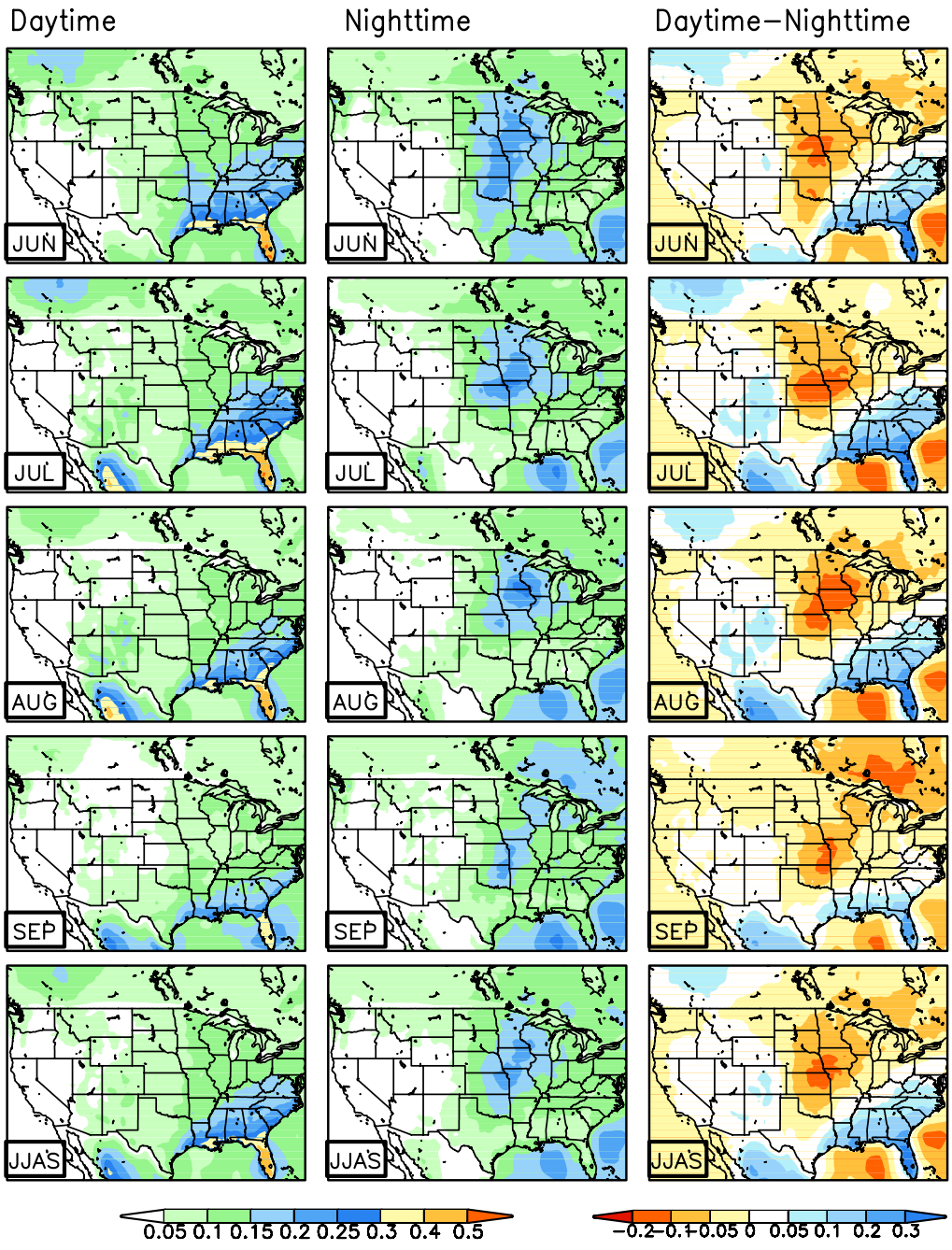

Figure 3.4 Month-by-month summertime daytime (1800-2400UTC) and nighttime (0600-1200UTC) precipitation and their difference, estimated from Regional Reanalysis 0-3h forecasts. Units are mm/hr.

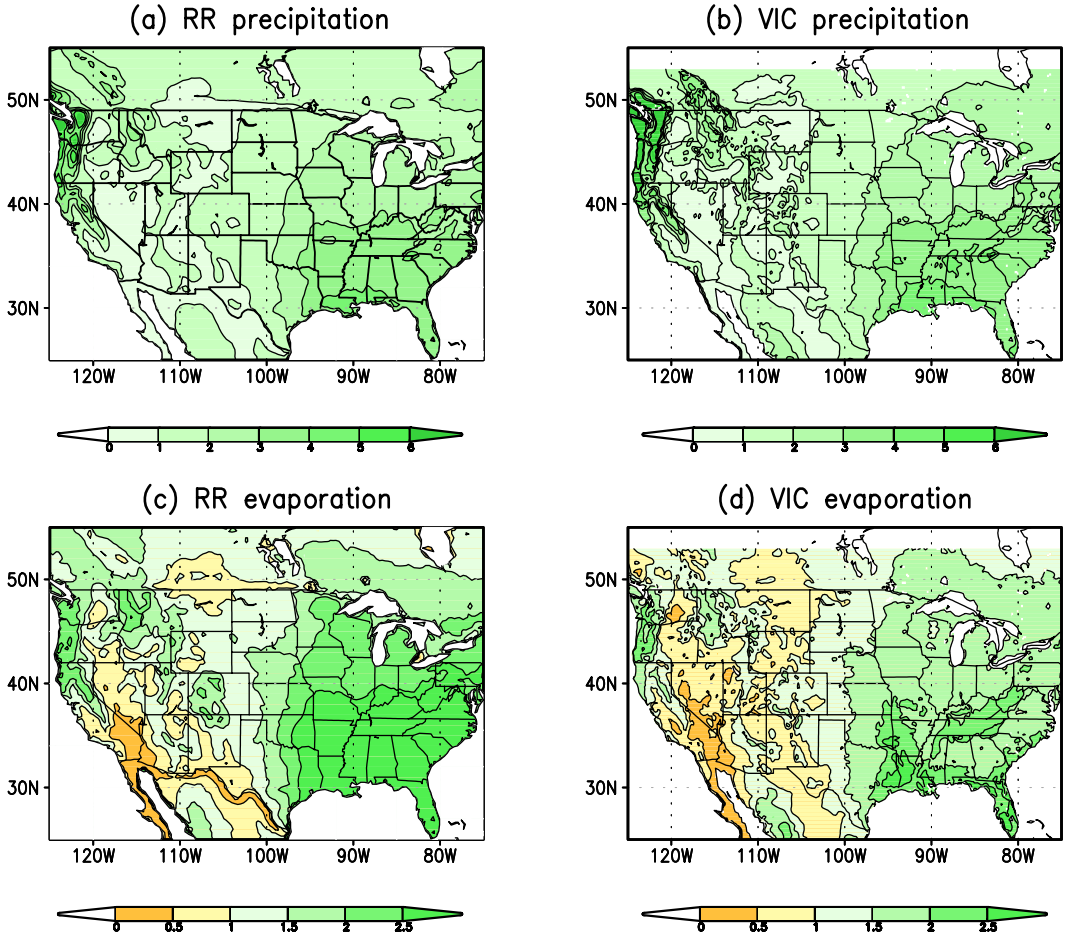

Figure 3.5 The 21-year annual mean fields for the period 1979 – 1999 of the Regional Reanalysis 3-h forecasts of (a) precipitation, and (c) evaporation; (b, d) same as (a, c), but for the VIC model. Units are mm day^{-1}.

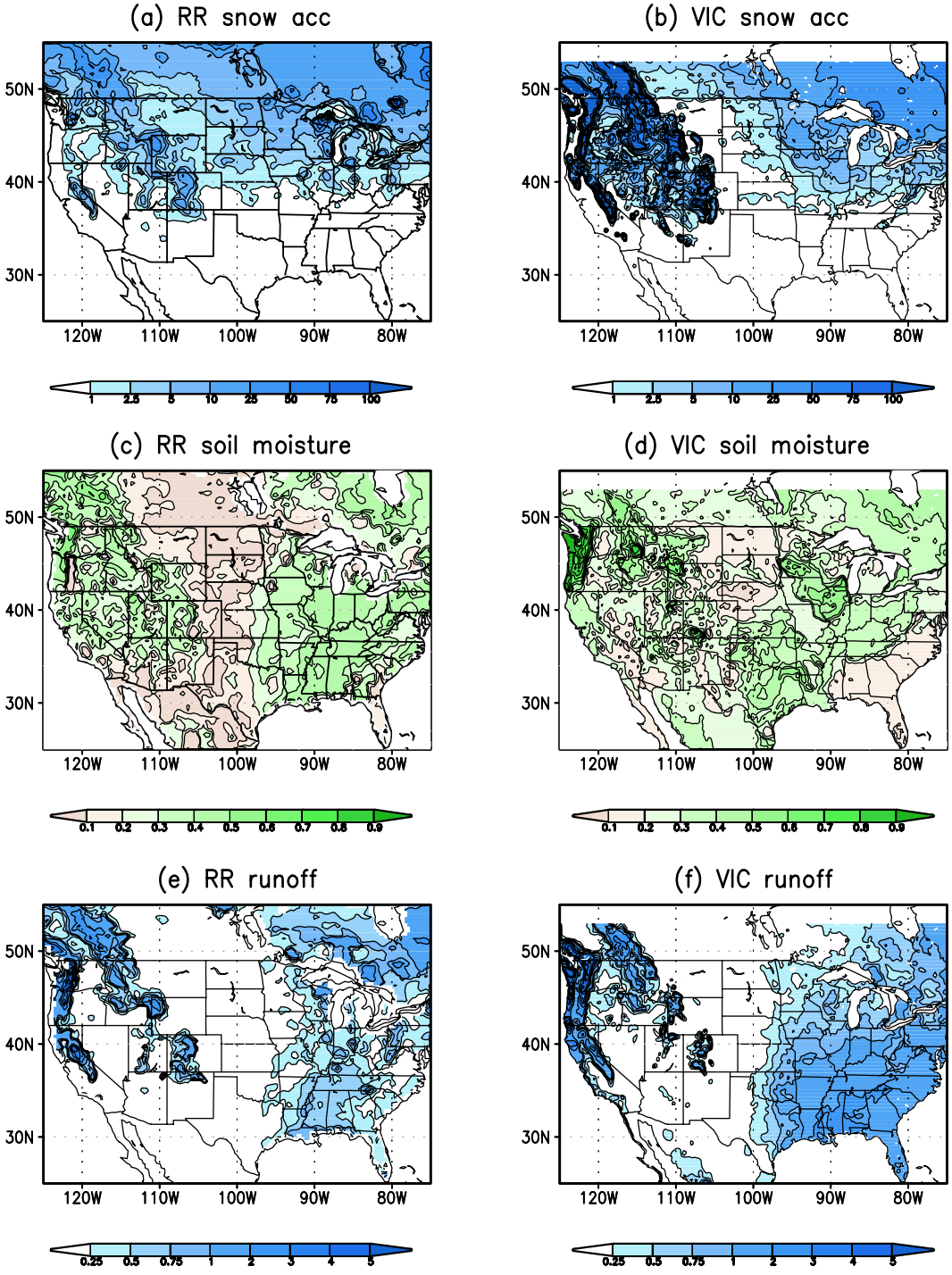

Figure 3.6 The 21-year annual mean fields for the period 1979 – 1999 of the Regional Reanalysis 3-h forecasts of (a) water equivalent of accumulated snow depth, (c) normalized soil moisture for the 0-200cm layer, and (e) total runoff; (b, d, f) same as (a, c, e), but for the VIC model. Normalization of soil moisture was done by taking into account the respective minimum-maximum ranges of the NARR and VIC model soil moisture (see text). Units are mm day^{-1} for runoff and mm for snow depth.

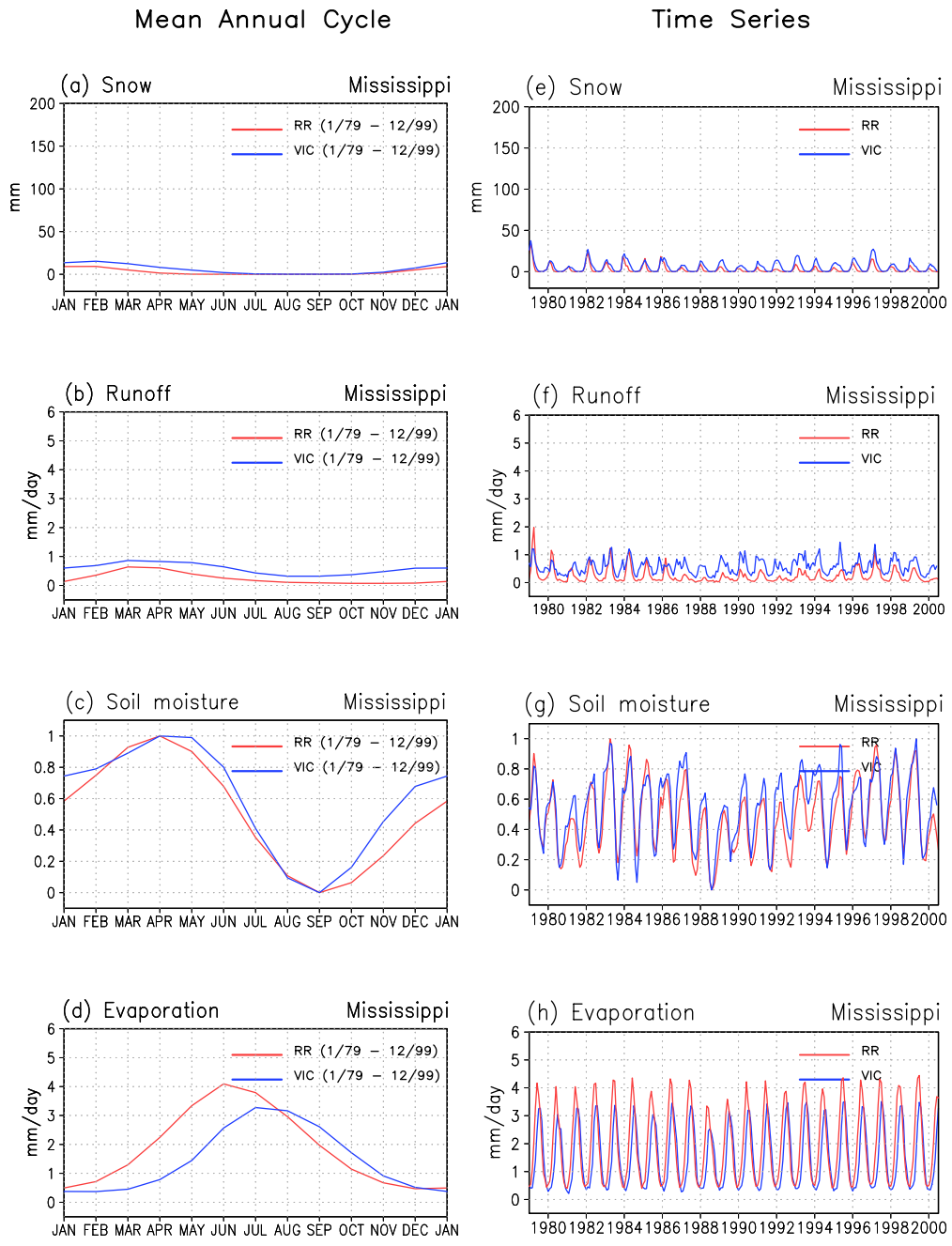

Figure 3.7 Mississippi basin area-averaged mean-annual cycle and time series of the surface water budget components of the Eta model: (a, e) water-equivalent snow depth, (b, f) runoff plus baseflow, (c, g) normalized soil moisture, and (d, h) evaporation. Units are mm day^{-1}.

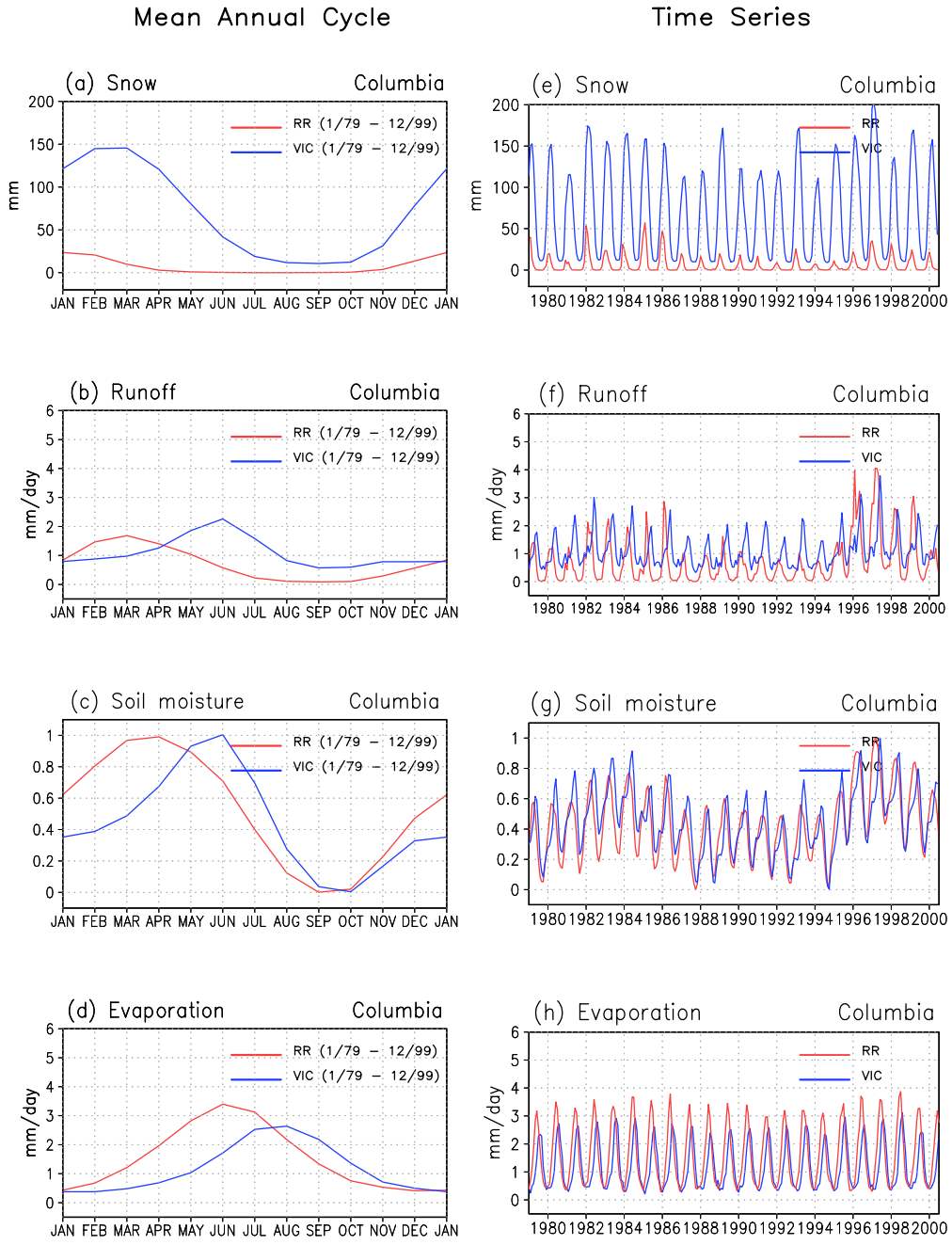

Figure 3.8 The same as Figure 3.7 but for the Columbia basin.

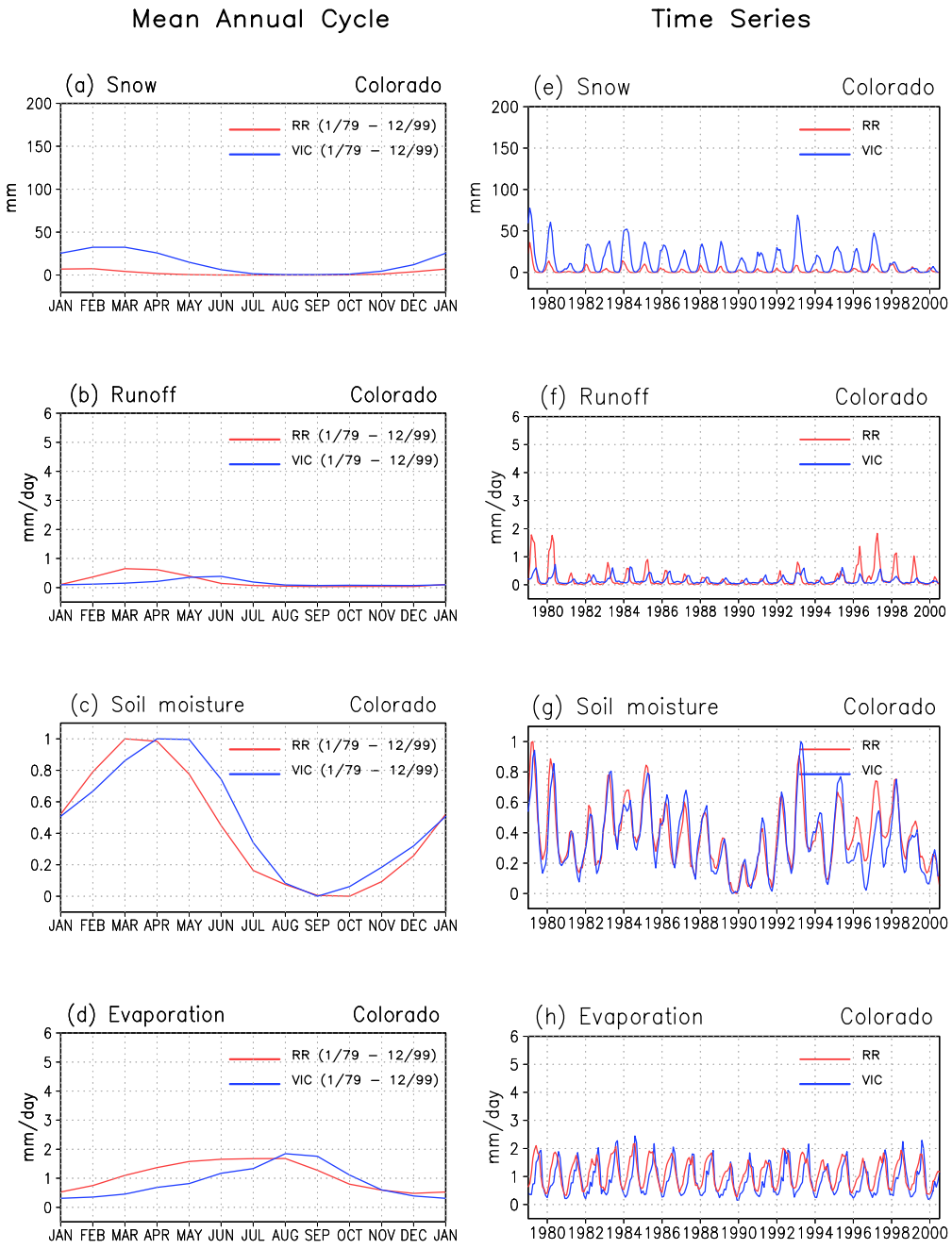

Figure 3.9 The same as Figure 3.7 but for the Colorado basin.

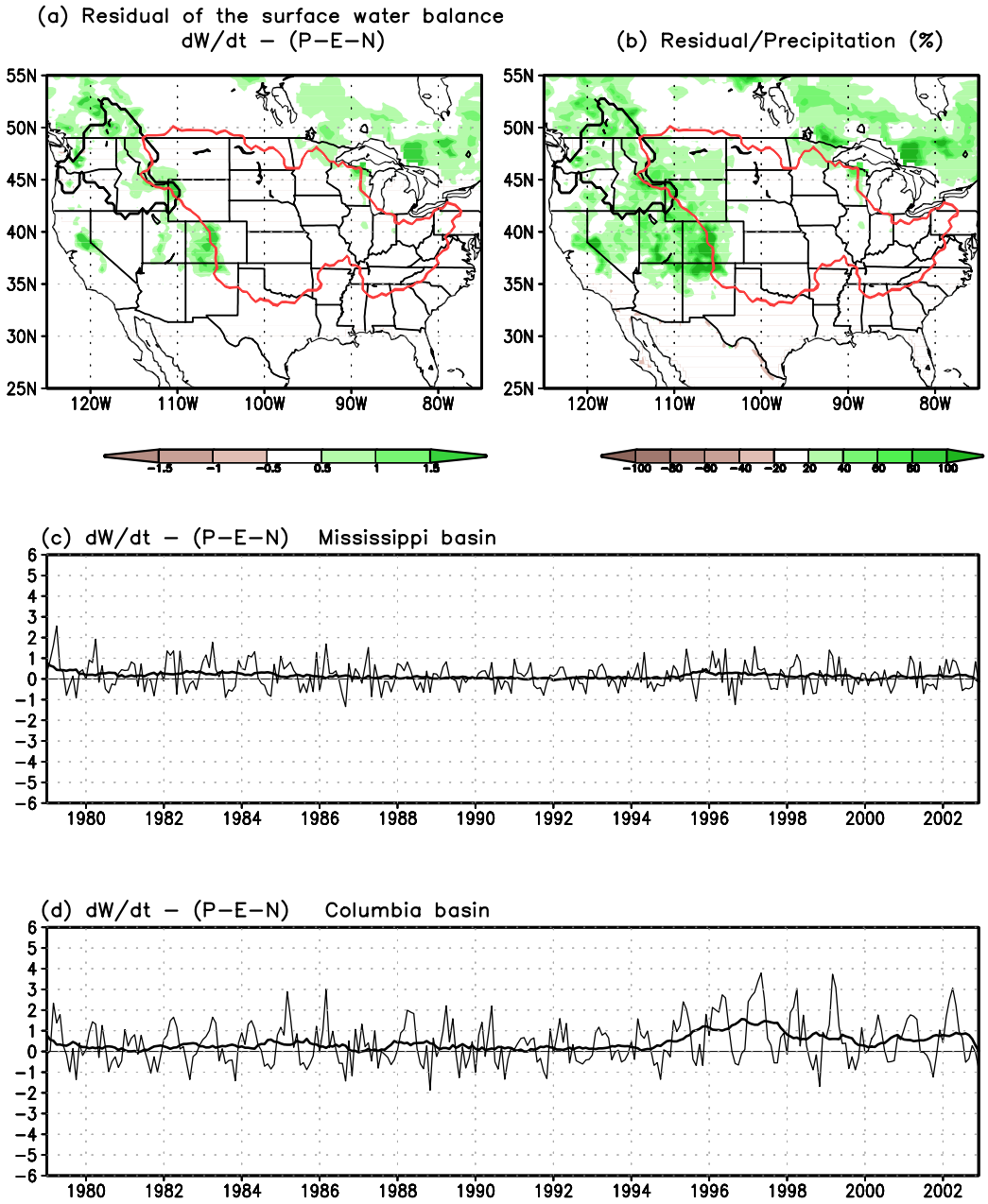

Figure 3.10 The residual term of the water balance equation estimated from the Regional Reanalysis: (a) the mean field for 1979 – 2002, (b) the same residual as a percentage of the precipitation, (c) the time series of the area average for the Mississippi basin, and (d) as (c) for the Columbia basin. The heavy line in (c) and (d) represents a running mean to remove the annual cycle. dW/dt is the local change of surface water (soil moisture and snow water equivalent), P is the precipitation, E is the evaporation and N is the runoff plus the baseflow. Units are mm day^{-1}.

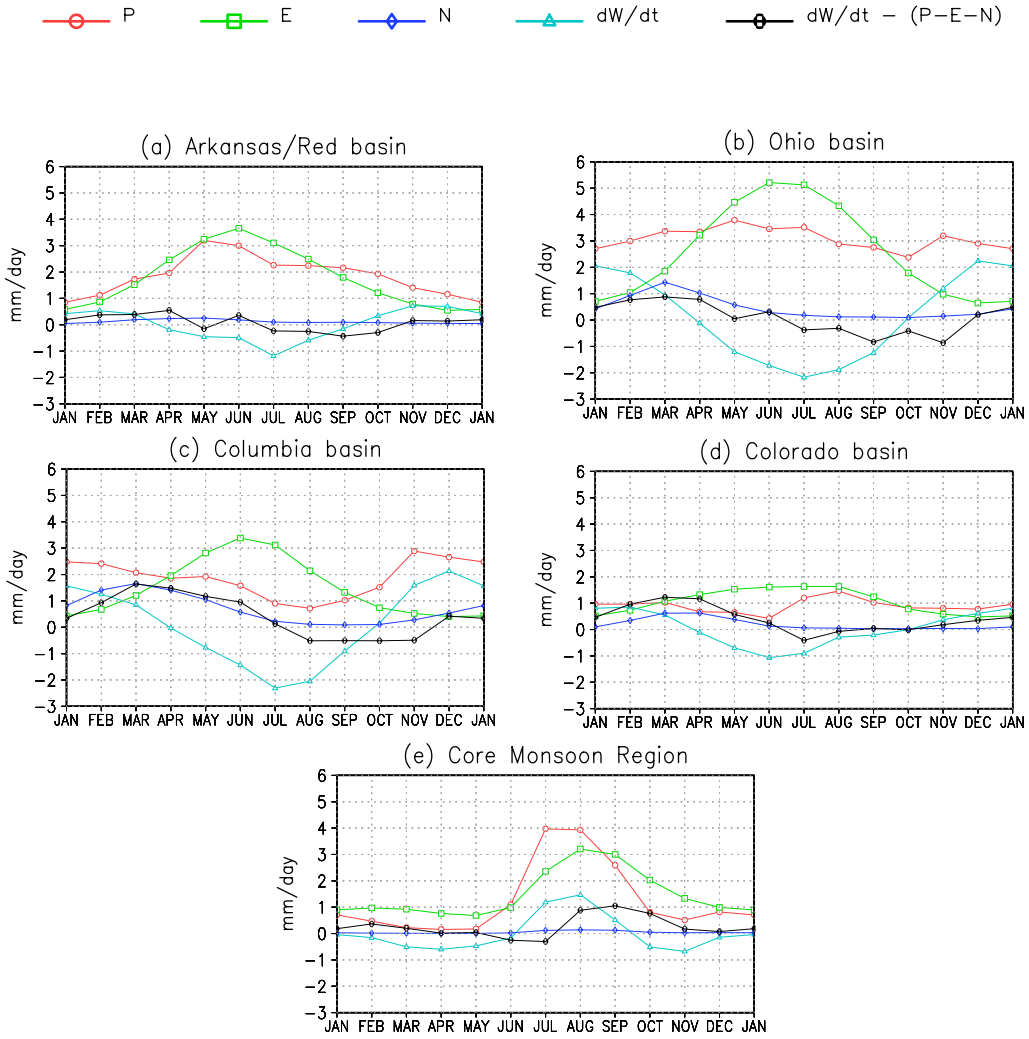

Figure 3.11 Mean annual cycle of surface water budgets estimated from NARR. Each plot shows mean monthly precipitation (P), evaporation (E), runoff (N), change in water storage (dW/dt), and the residual term in mm day^{-1}.

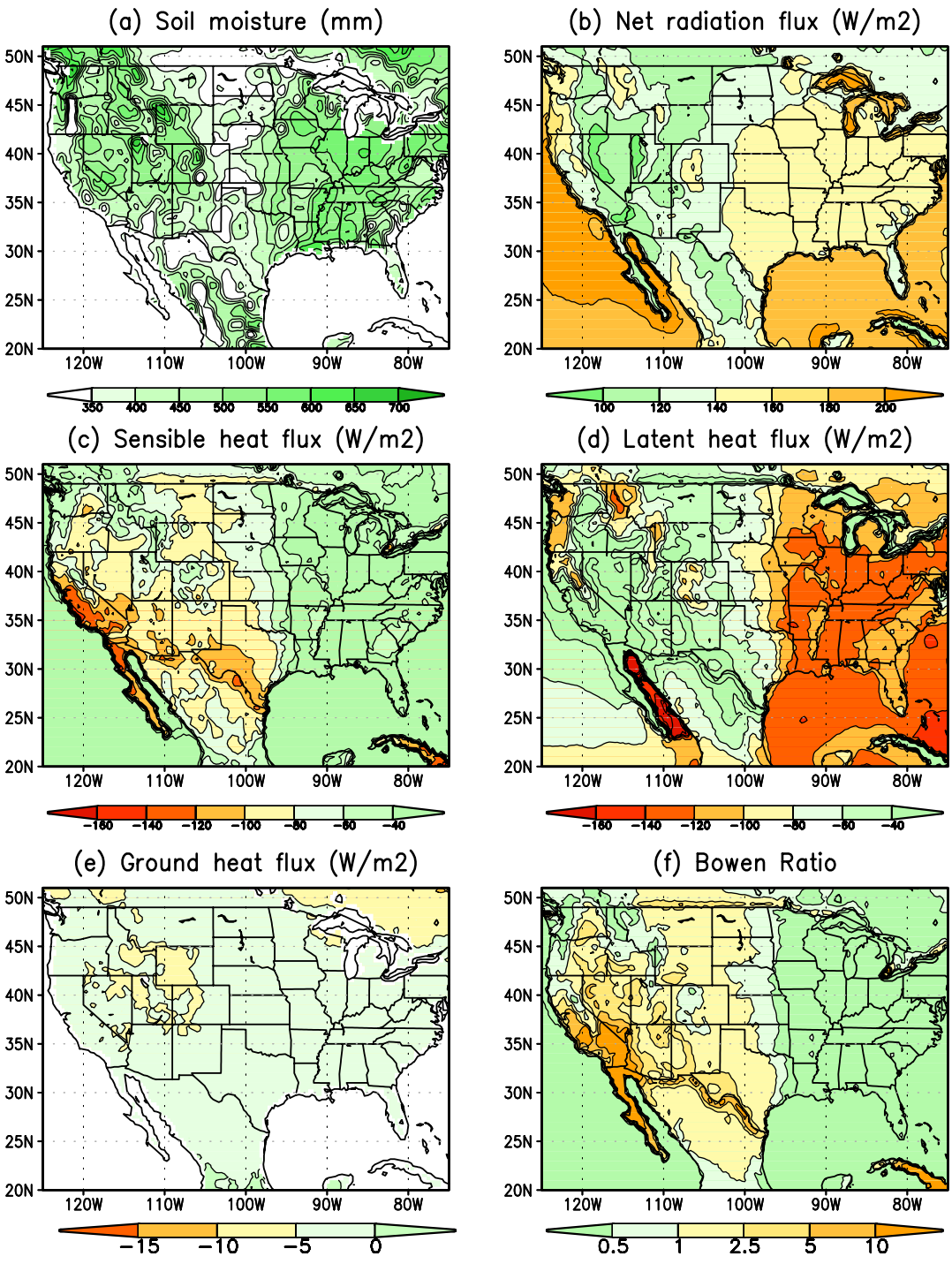

Figure 3.12 1979-2002 summer mean (JJAS) field of (a) soil moisture for the 0-200 cm layer, (b) net radiation flux, (c) sensible heat flux, (d) latent heat flux, (e) ground heat flux and (f) Bowen ratio.

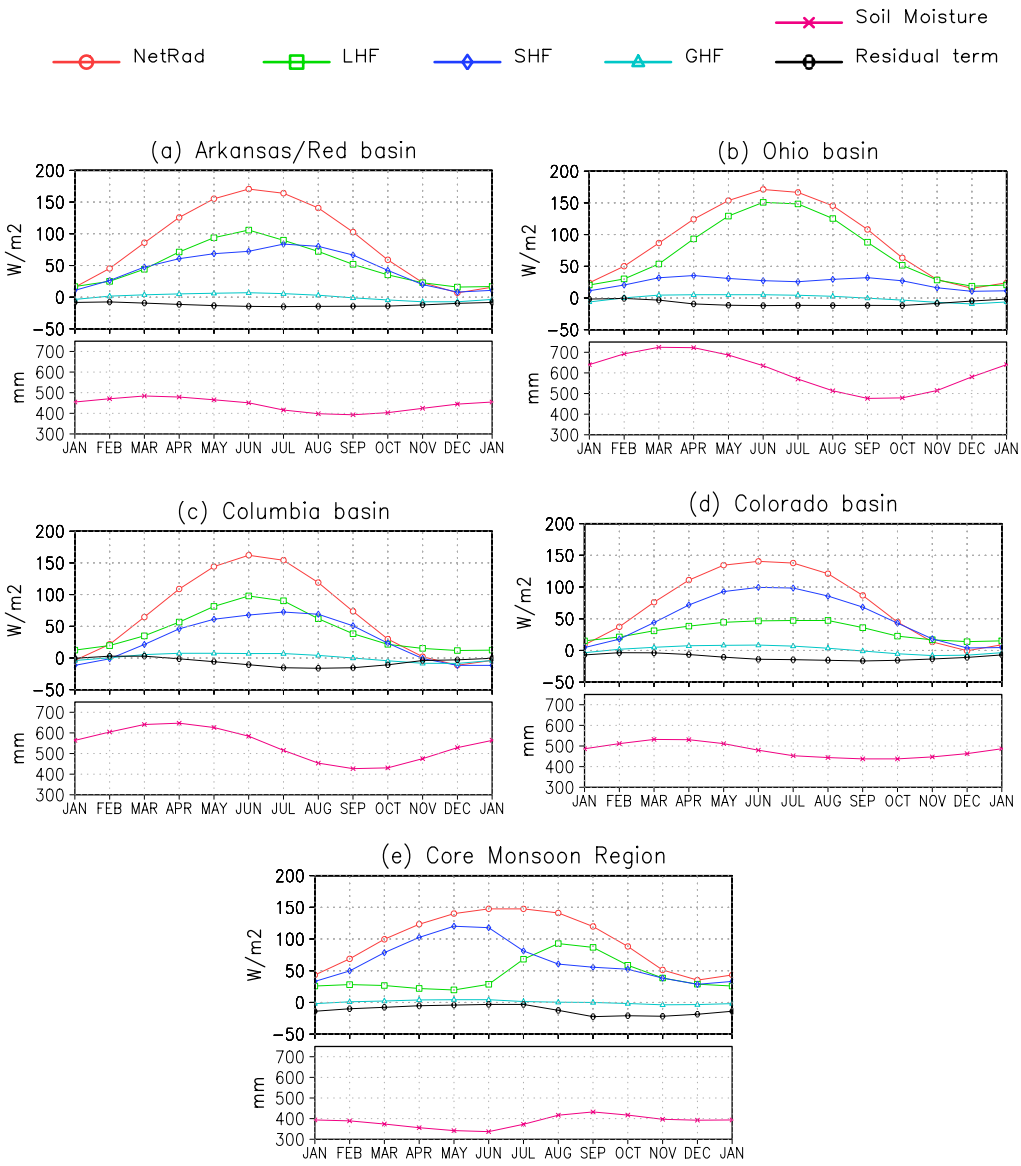

Figure 3.13 Mean annual cycle of surface energy budgets and soil moisture estimated from NARR. Each plot shows mean monthly net radiation (NetRad), latent heat flux (LHF), sensible heat flux (SHF), ground heat flux (GHF), and the residual term, all in Wm^{-2}, and soil moisture in mm over the basins.

CHAPTER 4: REGIONAL ASPECTS OF LAND SURFACE-ATMOSPHERE INTERACTIONS

4.1 Introduction

To date, studying land surface effect has followed typically one of two investigation paths. The first is primarily using climate statistics to diagnose the key mechanisms of the interactions. For this kind of study, although it is desirable to isolate land surface effects from the other effects, there is no straightforward way to carry this out. The second path of study primarily relies on model simulations. In particular, model sensitivity studies are commonly used in an attempt to understand land surface effects by isolating them from other possible impacts on precipitation processes. These may be important for helping to identify cause and effect in the analysis of the role of soil moisture. However, results depend heavily on the model parameterizations, and the realism of the results can be questionable.

Although soil moisture can modulate precipitation at the land-atmosphere boundary, it is by no means the only factor that can affect precipitation. Precipitation variability mainly arises from atmospheric, oceanic and land surface processes. A part of the dynamical forcings, over land the precipitation is determined by surface evaporation, moisture convergence, and convective activity which themselves are tied together by soil moisture in a complex manner. Therefore, a major obstacle in

determining the land surface effects is the difficulty of directly isolating the effects of soil moisture on precipitation, because ocean influence and atmospheric internal forcing itself also can change precipitation patterns. The presence of land-atmosphere interactions, and associated enhancement of variability, is supported by model experiments such as in Hong and Kalnay (2002). These idealized experiments have contributed significantly toward a better understanding of soil moisture's impact on climate and atmospheric variability. However, these experiments cannot be reproduced in the "real world" as it is impossible to control all factors that influence precipitation, because most modeling studies rely on extreme or artificially idealized land surface conditions. For example, in studies using coupled land-atmosphere models, the imposed soil moisture anomalies are typically drastic and applied over extensive regions, and therefore may not provide useful estimates of the strength of this interaction. Hence, the existence of such extreme states in nature has not been addressed properly due to their high dependence on their parameterizations, leaving room for further research on the applicability of these studies to real situations.

Although difficult to isolate the land surface contributions to the variability of continental precipitation, the current statistical analysis allows us to detect the impact of surface processes. Given long-term climatologies, we can deduct the land surface-atmosphere interactions (although not cause and effect), because it is possible to correlate soil moisture with precipitation, and it is also possible to identify relationships between soil moisture and surface fluxes or the state of the atmospheric boundary layer (BL).

In this chapter, a systematic comparison of seasonal land surface-atmosphere interaction analysis is performed first for all seasons. There would not be a priori reasons to discount or exclude any season from the assessment of interactions likely varying among seasons. The objective of the study in this chapter is therefore to quantify the linkages between soil moisture and several variables associated with land surface processes, atmospheric boundary layer conditions, and finally potentially interacting with atmospheric precipitation processes employing the long term set of NARR. The variables we choose are primarily examined based on monthly mean data. The correlation analysis serves to establish the significance of seasonal variations of land surface-atmosphere interactions and identify the geographical regions where they are most relevant to the water cycle. Since land surface effects are local phenomena, such identification has profound implications for predictability of the regional hydrologic cycle.

NARR has been compared over land on monthly time-scales with standard meteorological data, such as precipitation, in Chapter 3; since the biases are relatively small, the coupling processes between land surface and atmosphere could reflect more realistically the corresponding processes.

4.2 Soil Moisture in Four Layers

In NARR, the soil is divided into four layers, 0-10 cm (layer 1), 10-40 cm (layer 2), 40-100 cm (layer 3), and 100-200 cm (layer 4) below ground surface. To investigate how precipitation is related to the depth of the soil moisture layer, we directly evaluated their correlations using monthly anomaly data from June to

September 1979-2002. These results are summarized in Table 4.1. In general, for each basin, the correlations systematically decrease with the thickness of topsoil, suggesting a weaker interaction between soil moisture in deeper soils and precipitation. The largest correlation is found in the surface layer (layer 1) which is very close to the surface. The reason is straightforward—direct interaction usually occurs where the soil layer is close to the overlying atmosphere. Therefore, we choose soil moisture content in the layer 0-10 cm for further evaluations.

Table 4.1. Correlations between monthly anomaly area-averaged precipitation and soil moisture during summer months JJAS 1979-2002 in different thickness of topmost soil.

Basin	Topmost soil thickness			
	0-10 cm	0-40 cm	0-100 cm	0-200 cm
Core Monsoon	**0.86**	**0.79**	**0.68**	**0.60**
Rio Grande	**0.85**	**0.68**	**0.54**	**0.54**
Central Mexico	**0.84**	**0.77**	**0.66**	**0.61**
Colorado	**0.73**	**0.43**	**0.22**	0.14
Arkansas-Red	**0.78**	**0.66**	**0.48**	**0.40**
Missouri	**0.75**	**0.64**	**0.49**	**0.32**
Upper Mississippi	**0.62**	**0.56**	**0.45**	**0.39**
Ohio	**0.50**	**0.46**	**0.37**	**0.30**
Columbia	**0.58**	**0.41**	**0.29**	0.18

4.3 Proposed Pathways Linking Soil Moisture to Precipitation

Figure 4.1 presents a schematic diagram to show some chains of soil moisture related processes including the surface layer, hydrology, cloud fields, radiation fields, boundary layer, and precipitation. We distinguish positive correlations (red line) and negative correlations (blue line) showing how each component is related to the other adjacent one, thus resulting in final links between land surface and atmosphere. This framework is useful for understanding such interactions, and especially helps identify the effect of soil moisture variability on atmospheric variability. This is certainly an

attractive view of a complex system and has links when different surface variables respond to the surface forcing through changes in the soil water conditions.

The effect of precipitation on soil moisture is straightforward and self-evident, because a rainfall event simply wets soil instantly. In contrast, the soil moisture influences on precipitation is a complex process and not easy to understand. Soil moisture not only impacts the water budget of the surface, but it also impacts the energy budget and the planetary boundary layer (PBL). Here, we identify two physical pathways linking soil moisture with precipitation through evapotranspiration (ET). ET is a critical element through which soil moisture feeds back to the atmosphere. The first one (Path1 as a water recycling process) is a direct path indicating that increased soil moisture enhances evaporation, so that more water vapor is available in the air (moistening the PBL, Brubaker et al., 1993; Eltahir and Bras, 1998) and more possibility to form cloud and precipitation. In other words, generally the more evaporation or latent heat arising from the underlying wet soil, the more low cloud cover, which will yield more precipitation. This is a quite intuitive way to understand the path both through this precipitation recycling process and the water balance equation. Another indirect path (as the radiative processes) is going through surface energy processes (Betts and Ball, 1998; Eltahir, 1998). Soil moisture can affect precipitation through the surface energy balance. Starting with the radiation processes, as evaporation increases with soil moisture in summer, generally results in increases in humidity and cloudiness, leading to a decrease of net incoming short wave radiation (the corresponding “SW” feedback).

On the other hand, as soil moisture increases, skin temperature decreases (reducing the outgoing surface longwave radiation due to the Stefan-Boltzmann Law), plus more clouds prevent more long-wave radiation energy going out, resulting in the decrease as net outgoing long wave radiation (the "LW" feedback associated with increasing soil moisture, thus increase downward longwave radiation due to the greenhouse effect of the atmospheric water vapor). Net long and short wave radiation cancel each other so that the net radiation increases or decreases mainly depending on which factor dominates. Hence, the cloud fields modify the SW and LW radiative fluxes at the surface. Clouds can produce a complex picture of feedbacks that differ not only in magnitude but also in sign. The strength of the cloud feedback is an important factor in determining the strength of the response of net surface radiation to change in soil moisture. However, the "SW" and "LW" cloud radiative feedbacks (impact of the cloud field on the radiation budget) have been recognized as the major source of uncertainty in numerical models (Betts and Viterbo, 2005). Thus, the cloud feedbacks complicate and may even weaken the impact of soil moisture conditions on net radiation. Since our results depend on the physical parameterizations in the model, this kind of uncertainty is also reflected in our results as we will show later. The results highlight both the model sensitivity to cloud parameterization and the effects of cloud feedbacks in the Eta model. Of course, if we only consider clear sky conditions, it would be easier to identify the links between soil moisture and the surface radiation budget, namely, net radiation at the surface increases with increased soil moisture. Furthermore, wet soil results in a relatively high evaporative fraction (Ef) (by increasing the surface latent heat flux and decreasing the surface sensible

heat flux) and lower surface temperature. Both of them together imply limited sensible heat transfer, and therefore limited entrainment at the top of the BL. The net result is a shallower boundary layer, as suggested by a lower LCL. Essentially, this BL-precipitation link is based on relationships between BL condition—depth of LCL and the probability of precipitation as a lower LCL favors convective precipitation. If the above hypothesis is accurate, we expect a positive correlation between soil moisture and precipitation.

The positive relationship between soil moisture and precipitation has important implications. When soil moisture acts as a positive feedback on climate, it acts to delay and prolong the effect of meteorological drought, and to enhance the severity and persistence of floods (Eltahir 1998, Hong and Kalnay 2000). The climate of summertime precipitation heavily depends upon the soil moisture availability (Findell and Eltahir 1999). Oglesby and Erickson (1989) performed numerical sensitivity experiments and their results demonstrate the important role of soil moisture in prolonging and/or amplifying North American summertime drought. Studies investigating the influences of soil moisture anomalies on monsoon systems (Small 2001) have drawn similar conclusions.

4.4 Seasonal Variations of Soil Moisture Linkages to Surface Terms

From the physical mechanism point of view, since both surface and atmospheric controls are involved in land-atmosphere interaction (Findell and Eltahir, 2003), a considerable effort has been devoted to firstly connecting soil moisture with surface radiation fluxes, and then to connecting cloud fields, boundary layer

conditions, surface energy fluxes, and finally to precipitation processes. The manifestation of the links between cloud, radiation, and boundary conditions can be proposed as the framework to understand land surface-atmosphere interactions. In addition, here we emphasize different strengths in paths linking soil moisture to precipitation among all basins.

Figures 4.2-4.3 present seasonal variations of correlations between soil moisture and some surface energy and other variables for the Mississippi subbasins, the Columbia basin, the Colorado basin and two other regions in Mexico. (Since the other region, Central Mexico, shows the similar results as the Core Monsoon region, it is not shown in the following figures.) These basins illustrate that correlations vary seasonally and regionally. Although they show less clear seasonal variations in lower latitude regions than the northern basins, the linear correlations are significant during the summer months, surpassing the 95% significance level. There is much evidence that linkages are less relevant in winter, because winter-like rainfall regime is dominated by large-scale circulations (Dirmeyer, 2003). These results in that the soil moisture-precipitation interaction is primarily a summertime feature, as clearly consistent with the previous studies. For instance, in an observational study of Findell and Eltahir (1997) it is demonstrated that during summer there are statistically significant lag correlations between soil moisture anomalies and subsequent rainfall anomalies over the state of Illinois.

For this reason, land surface-atmosphere processes during summer (June-September) are inspected further to identify the geographical regions where the land surface-atmosphere interactions are most or least relevant to the water cycle.

4.5 Summer Soil Moisture Linkages to Surface Terms

4.5.1 Surface Radiation Processes

We first present the scatterplots of area-averaged radiation terms versus soil moisture for each basin (Figures 4.4 and 4.5). In order to avoid crowding the figures, we chose Arkansas/Red (dry and warm climate) and Ohio (wet and warm climate) in the Mississippi basin, the Columbia basin (wet and cold), the Colorado basin and the Core monsoon (semiarid and warm). In order to remove the effect of the seasonal variations of these surface variables, we use anomalies by subtracting first the mean annual cycle. Therefore, the data used for analysis here are deviations of monthly mean values from the long-term mean for that month. On a given plot, the abscissa represents the total soil moisture content of the surface layer in mm, and the ordinate represents either surface or atmospheric variables. Different marks represent different basins. In the same basin, each point in the plot represents a monthly anomaly from one of the 96 months (JJAS x 24years). "Best-fit" lines from linear regression for each basin are displayed on each plot.

The soil moisture conditions affect both the shortwave (SW) and the longwave (LW) radiation budget. Firstly, the rough correspondence between soil moisture and surface radiation variables can be observed in all basins: in Figures 4.4-4.5 a and b, both net shortwave radiation and net longwave radiation clearly decrease with increased soil moisture. Again, the close correspondence between soil moisture with longwave radiation and temperature shows that they are physically consistent with each other. The net radiation is given by the sum of net SW and LW radiation.

Both terms tend to cancel each other so that the net radiation is essentially flat and more scattered. Note we use the reversed sign of the net longwave radiation. As soil moisture increases, surface temperature decreases (Figures 4.4d and 4.5d), resulting in the **decrease** of net **outgoing** longwave radiation (the "LW feedback" associated with increasing soil moisture) in Figures 4.4 and 4.5b. In other words, less energy is lost from the surface, which implies a positive contribution to the surface radiation budget such as the Arkansas/Red basin in Figures 4.4c and the Columbia and Colorado basins in Figure 4.5c.

In the two Mississippi subbasins, short wave radiation decreases with increased soil moisture (Figure 4.4a). However, in the eastern half of the Mississippi basin the links are less clear. A similar situation also can be seen in the Columbia basin (Figure 4.5a). In the case of Arkansas/Red subbasin, the "LW" feedback exceeds the "SW" feedback, which implies there is more decreased longwave radiation than shortwave radiation, so it yields a slight increase of the net radiation with soil moisture (Figure 4.4c), implying that there is more energy available at the surface to evaporate surface water. The Arkansas/Red subbasin qualitatively shows a good example of the soil moisture-NetRad relationship proposed by Eltahir (1998) does exist in the basin: that is, NetRad is higher when the soil is relatively wet. In the wetter eastern part, the Ohio and Upper Mississippi basins, the scatter patterns have smaller slopes, implying that there is not enough energy to respond to changes in soil moisture.

In the areas over Mexico, negative correlation between soil moisture and net radiation is found (Figure 4.5c), which is distinctly different from the other basins.

The core monsoon region is strongly affected by cloud effects. Less shortwave radiation reaches the surface due to the strong development and wide spread existence of low thick clouds. In this special case, an increase in soil moisture mainly tends to increase cloud albedo and thereby reduce net radiation. As a result, net radiation declines as soil moisture increases. Therefore, surface net radiation is dominantly affected by low cloud radiation effects, which implies the "SW" feedback exceeds the "LW" feedback. Significant positive correlations with net radiation do not exist when significant cloud effects are considered over those regions. Obviously this basin does not support the previous soil moisture-NetRad relationship as stated by Eltahir (1998), but still shows that increased soil moisture could increase precipitation by following the second path as we stated in the previous Section 4.3. Small and Kurc (2003) have noted that in such a semiarid area, the surface radiation budget is tightly coupled to soil moisture through the surface temperature.

This analysis from NARR does not fully support Eltahir's hypothesis (1998): wet soil yields higher net radiation, and therefore total energy transfer from the land surface to the atmosphere, but is closer to Betts and Ball's studies (1998) which only suggest that net radiation may (but not necessarily) increase when soil is wet.

4.5.2 Surface Energy Processes

Many distinct features of the surface energy processes related to soil moisture support the concept of this positive feedback as proposed by previous studies (Betts, 1996; Eltahir, 1998). We found that the partition of the surface available energy into latent heat flux (LHF) and sensible heat flux (SHF), which controls the surface

Bowen Ratio (BR = SHF/LHF), largely depends on the surface soil moisture conditions. Their relationships are depicted separately for the Mississippi subbasins and the western basins in Figures 4.6-4.7. In all basins, inverse correlations can be seen between soil moisture and sensible heat flux (Figures 4.6a and 4.7a) and the Bowen ratio, while soil moisture has a positive correlation with latent heat flux (Figures 4.6c and 4.7c) and evaporative fraction (Ef = LHF/(LHF+SHF)). The main effect of the soil moisture is clearly evident in terms of the sensible and latent heat fluxes. In all cases, Ef (Figures 4.6e and 4.7e) increases significantly with increasing water content, showing stronger correlation than for the radiation fields. However, the relations have different strength in wet-soil and dry-soil basins.

The influence of soil moisture on surface energy processes is greater in the western part of the Mississippi basin compared to the eastern part, because soil moisture-induced fluctuations in latent heat and sensible heat (i.e. evaporative fraction or Bowen Ratio) are relatively large. The differences are important: there is a small slope of the regression, showing a flatter pattern in wet basins (SM ≥500mm), such as the Upper Mississippi, Ohio, and Columbia basins, indicating that surface energy fluxes do not vary much with soil moisture over wet areas; in the rest of the relatively dry basins (SM<500mm), it is expected that surface fluxes do vary significantly with soil moisture and their slopes are much larger. This suggests that a significant difference exists among these basins. Therefore, the response of surface energy fluxes to soil moisture variations is greater in drier basins than in other regions. The lack of sensitivity at the higher soil moisture values is most likely a result of evaporation reaching the potential evaporation rate (this will be discussed in Chapter

5).

4.5.3 The Boundary Layer

Soil moisture also has a pronounced impact on the depth of the boundary layer (BL) that is important for precipitation processes. We extend the ideas of Section 4.3 for the BL, and continue to explore the relationships between cloud fields and boundary layer conditions with soil moisture. This will establish that the SW and LW feedbacks are tightly correlated to land-surface interactions through linkages of soil moisture and boundary layer processes as Section 4.3 described. Betts et al. (1995, 1998, and 2004) have shown that the BL is closely linked to soil moisture, or to the availability of water vapor for evaporation, especially where the clouds modify the SW and LW radiative flux at the surface. How the Atmospheric Boundary Layer depends on soil moisture is shown in Figure 4.6-4.7. Generally, low cloud cover (Figures 4.6d and 4.7d) increases and the lifting condensation level (Figures 4.6b and 4.7b) falls as soil moisture increases, allowing near-linear dependence on soil moisture. The explanation is that as evaporation increases with soil moisture in summer, generally humidity and cloud cover increase, leading to the decrease of the lifting condensation level (LCL). This will increase the precipitation potential, thus tending to produce more summer precipitation (Figure 4.6f, 4.7f). This suggests that during summer, boundary layer processes are very sensitive to feedbacks from soil moisture. Over the eastern half of the Mississippi and the Columbia basins low cloud cover shows poor dependence on the soil moisture.

Figures 4.6-4.7 also show the dependence of precipitation on soil moisture. The increased soil moisture, through radiative, thermodynamic, and moisture-supply processes, leads to conditions that favor increased precipitation. As we will show later, although the soil moisture has a positive correlation with latent heat, evaporative fraction and low cloud cover but negative correlation with sensible heat, Bowen ratio, LCL and surface temperature, the precipitation scatter point distribution for each basin is rather different.

NARR provides a clear picture of how soil moisture variations relate to the surface radiation balance, surface energy balance, cloud fields, BL conditions and precipitation over North American basins. It is thus instructive to compare the magnitude of the correlation between soil moisture and those variables for all basins. These relationships are summarized in Table 4.2. All the correlations are remarkably high, and significant at the 95% level; most are significant at the 99% level as well [the significance levels are 0.20 and 0.2612 respectively]. Therefore, most correlations are robust above the significance level, with exception of the net radiation for some basins. The basins with higher correlation between soil moisture and precipitation are also most likely to show higher correlations with the other variables, and vice versa. In addition, scatter around the fitted line in all scatterplots is smaller for those basins (not shown). In these figures, larger slopes of the linear fit, which are commonly used to show the higher sensitivity of relationships, also correspond to higher correlation coefficients.

Table 4.2 Correlations between monthly anomaly area-averaged soil moisture and surface variables over the North American basins during summer months JJAS 1979-2002. Correlations marked in bold are significant at the 95% confidence level.

	Prr	LHF	SHF	EF	LCDC	LCL
Core Monsoon	**0.86**	**0.95**	**-0.96**	**0.96**	**0.78**	**-0.82**
Rio Grande	**0.85**	**0.97**	**-0.95**	**0.98**	**0.76**	**-0.85**
Central Mexico	**0.84**	**0.91**	**-0.98**	**0.97**	**0.80**	**-0.91**
Colorado	**0.73**	**0.91**	**-0.78**	**0.92**	**0.69**	**-0.80**
Arkansas-Red	**0.78**	**0.88**	**-0.93**	**0.92**	**0.56**	**-0.86**
Missouri	**0.75**	**0.87**	**-0.91**	**0.91**	**0.67**	**-0.89**
Upper Mississippi	**0.62**	**0.75**	**-0.87**	**0.85**	**0.40**	**-0.85**
Ohio	**0.50**	**0.48**	**-0.85**	**0.79**	**0.40**	**-0.80**
Columbia	**0.58**	**0.67**	**-0.84**	**0.83**	**0.52**	**-0.82**

(Continued)

	NetRad	SW	LW	Ts
Core Monsoon	-0.20	**-0.76**	**-0.89**	**-0.79**
Rio Grande	**0.50**	**-0.72**	**-0.86**	**-0.83**
Central Mexico	0.14	**-0.73**	**-0.90**	**-0.92**
Colorado	**0.84**	**-0.61**	**-0.84**	**-0.35**
Arkansas-Red	**0.44**	**-0.53**	**-0.81**	**-0.87**
Missouri	**0.58**	**-0.65**	**-0.89**	**-0.76**
Upper Mississippi	0.18	**-0.45**	**-0.77**	**-0.57**
Ohio	-0.09	**-0.42**	**-0.63**	**-0.46**
Columbia	**0.48**	**-0.54**	**-0.80**	**-0.61**

4.6 Direct Relationships between Soil Moisture and Precipitation

Soil moisture affecting precipitation involves many physical processes. From the previous sections, we have known that soil moisture conditions affect the surface energy balance by altering the partitioning of latent heat and sensible heat fluxes, thus modifying the boundary layer properties, such as low cloud cover and the depth of the lifting condensation level. Several important links between soil moisture and other variables were shown at the monthly timescales (Table 4.2). Most links also can be seen on seasonal timescale. There are indications that the statistical relationship

appears to be physically plausible as we relate them to Betts' hypothesis (1996): On monthly to seasonal time scale, the NARR exhibits a distinct positive correlation between soil moisture and precipitation. Indeed, the precipitation gives a good response to the surface soil layer in some regions. We will discuss this further through the analysis of the geographical distribution of soil moisture-precipitation correlations.

4.6.1 Geographical Distributions

Figure 4.8a presents the map of temporal correlation between soil moisture and precipitation anomalies. In this case, the monthly correlations are performed for the summer months from June to September and averaged together. A positive correlation of precipitation with soil moisture is apparent almost everywhere over North America, with large values of correlation coefficients exceeding 0.6 over much of Mexico and most part of the central Great Plains, where the soil is not so wet. The maximum correlations are higher than 0.8. The high positive correlations imply strong interactions between the land surface and the atmosphere. It is encouraging to see that the structure of the field is similar to that reported in Koster et al. (2004) from modeling simulations. We need to recognize that our results depend on the physical parameterizations in NARR. The land-atmosphere interactions are represented through many parameterized physical processes and thereby their strength tends to be different from model to model (Koster et al., 2002, 2004), so that they may produce different degrees of strength in the interactions.

Figures 4.8b-d show the correlations between basin-averaged precipitation and the field of soil moisture. In Figure 4.8b, based on Arkansas/Red precipitation, significant correlations cover the entire basin and surrounding areas. As distance from the basin increases, values decay sharply. This might indicate that the linkage between soil moisture and precipitation in the Arkansas/Red is mainly affected by the local surface wetness condition. Similar to the Arkansas/Red basin, precipitation in the Core Monsoon region is well correlated only with its own soil moisture and surrounding areas (Figure 4.8c). Different from the Figures 4.8 b-c, Figure 4.8d shows that the correlation in the Ohio basin is largely reduced, reflecting the lesser relevance of soil moisture to precipitation.

Next, we examine the slope of the linear fit established on the relationships of precipitation with soil moisture. Figure 4.9 corroborates that the regions with stronger land-atmosphere interactions are the ones with higher sensitivity (larger values of slope). Together with Figure 4.8, they emphasize that land-atmosphere interactions are local phenomena. This kind of forcing is usually regional and seasonal dependent.

4.6.2 Basin-Dependent Features

In relation to the inquiry as to where the interactions are strongest or weakest, we introduce Figure 4.10 to illustrate the various degrees of strength of land-atmosphere interactions. The correlation of precipitation and temperature with soil moisture is often taken to be as a measure of Land Surface-Atmosphere (LSA) interactions. Our diagnostic study cannot determine cause-effect relationships, but the results in Figure 4.10 imply that summer precipitation could be a direct influence of

soil moisture. From our correlation analysis we grouped basins by their different strength of LSA interactions. With the support of Figure 4.10, the different kinds of characteristics of each region will be highlighted. In an effort to relate the strength to basin climate background, we use the summer mean rather than anomalous values (although results are similar). The summer-mean estimates also remove the seasonal variations, and they are employed instead of the monthly values to avoid cluttering in the plots (although there are 24 points, one point for each summer, the significance was discussed earlier from the monthly values). Results of the distinct degrees of interaction are summarized:

- **Strong interaction regions**

The monsoon-affected regions, the Colorado basin, as well as the western half of the Mississippi basin in Figure 4.10a-b can be identified as strong interaction regions. Note that those basins have generally drier soil and warmer temperature with respect to the other basins during the summer. Compared to other basins, the influence of soil moisture on precipitation and surface temperature is likely greater as the influence of their soil moisture-induced fluctuations is relatively large. Both precipitation and temperature over these basins show high sensitivity to soil moisture, because over these areas, the evaporation process is an important forcing for the evolution of precipitation. This indicates that soil moisture there may enhance precipitation prediction skill during summer. Summertime precipitation induced by positive soil moisture-rainfall feedback in Mexico regions is also consistent with previous studies (Small, 2003). According to Small, wet soil in the NAMS region

enhances summer precipitation in that area — thus, a positive soil moisture-rainfall feedback exists.

To gain a better understanding of which factors or variables might have indirect impact on soil moisture and precipitation positive feedbacks, especially with respect to their strength in a given region, we trace the pathways as presented in Figure 4.1 for the Core Monsoon region, as a case of strong interactions. We calculate correlations between adjacent pairs and label them in corresponding linking line. We distinguish positive correlation (red line) and negative correlation (blue line). Shown in Figure 4.11, most pairs of components show rather high correlations (above 0.7), except for the net radiation links associated with cloud feedbacks. This suggests that each component is closely related to the other adjacent one in most paths, thus implying strong links between land surface and atmosphere.

- **Weak interaction regions**

The eastern part of the Mississippi basin in Figure 4.10 c-d depicts weak strength of such interactions. Precipitation in the eastern part of Mississippi basins shows less correspondence with overall weaker correlations. The reason is straightforward: in wet and intermediate warm climates with plentiful soil water, evaporation is controlled not only by soil moisture but also by net radiation. In other words, evaporation is determined by the potential evaporation which is related with temperature (energy availability) and soil wetness (water availability).

The basins characterized as “water abundant” plus “energy limited” are prone to weaker land surface–atmosphere interactions, and here moisture advective

processes are likely to dominate and act to weaken these interactions. These are regions that are frequently saturated. Under such conditions, i.e. not so cold and not so warm, the wet soil has little impact on evaporation, latent heat flux, and thereby on the precipitation processes. The results mean that land surface forcing tends to be weak and less relevant to precipitation processes.

As the counterpart of Figure 4.11, Figure 4.12 for the Ohio basin shows a different scenario, although with the same sign of correlations in each pair, most values are rather small (below 0.5). In particular, correlations between soil moisture and evaporation (or latent heat flux), cloud cover, and surface temperature are small, implying that the linkage of soil moisture to precipitation breaks down at the starting point. Hence, this figure vividly shows the Ohio as a basin with weak connection between the land surface and atmosphere.

- **Undefined regions**

The Columbia basin almost has no clear linkages, as shown in Figure 4.10e-f. We found in such regions with a cool summer (Figure 4.10f), that summer precipitation is in fact insensitive to soil moisture. The reason is not clear yet, as there is a broad range of possibilities. First, this basin is near the coastal areas so that it is more likely to be influenced by the oceans, which can break down any relationship between land surface and atmosphere. Second, precipitation processes are mostly controlled by atmospheric moisture transport, consequently, land surface tends to be less relevant to precipitation processes (Findell et al., 2003). Third, the winter snow effect and spring high runoff are other important factors to affect summer

precipitation (Gutzler, 2000). Lastly, as a prominent feature in the western United States, the complex topography adds other impacts on the precipitation processes (Adam et al., 2003). They are potential factors that likely contribute to the lowest correlations.

Through the analysis of multiyear soil moisture-precipitation interactions basin by basin, we can now say that during the summer months (June, July, August and September) positive relationships between soil moisture and precipitation are most likely in most of the North American basins, although with different degrees in the strength of the interactions. Figure 4.13 summarizes the above results by grouping the regions which are identified as strong, weak, and no clear linkage regions. This map illustrates that the land surface effects tend to play different roles in different regions.

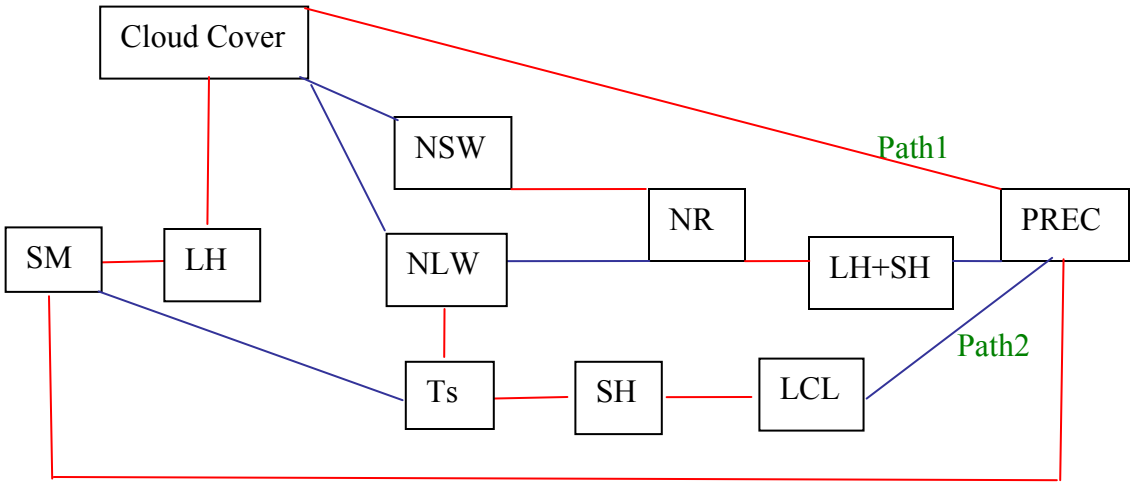

Figure 4.1 A schematic depiction of the relationship between soil moisture and precipitation. The links between the boxes indicate processes that establish the land surface-atmosphere interactions. Positive correlations (red line) and negative correlations (blue line) are distinguished showing how each component is related to its adjacent ones. Soil moisture can affect precipitation through two pathways. Path1 is going through this precipitation recycling process (e.g. via the water balance equation). Path2 is going through surface energy processes.

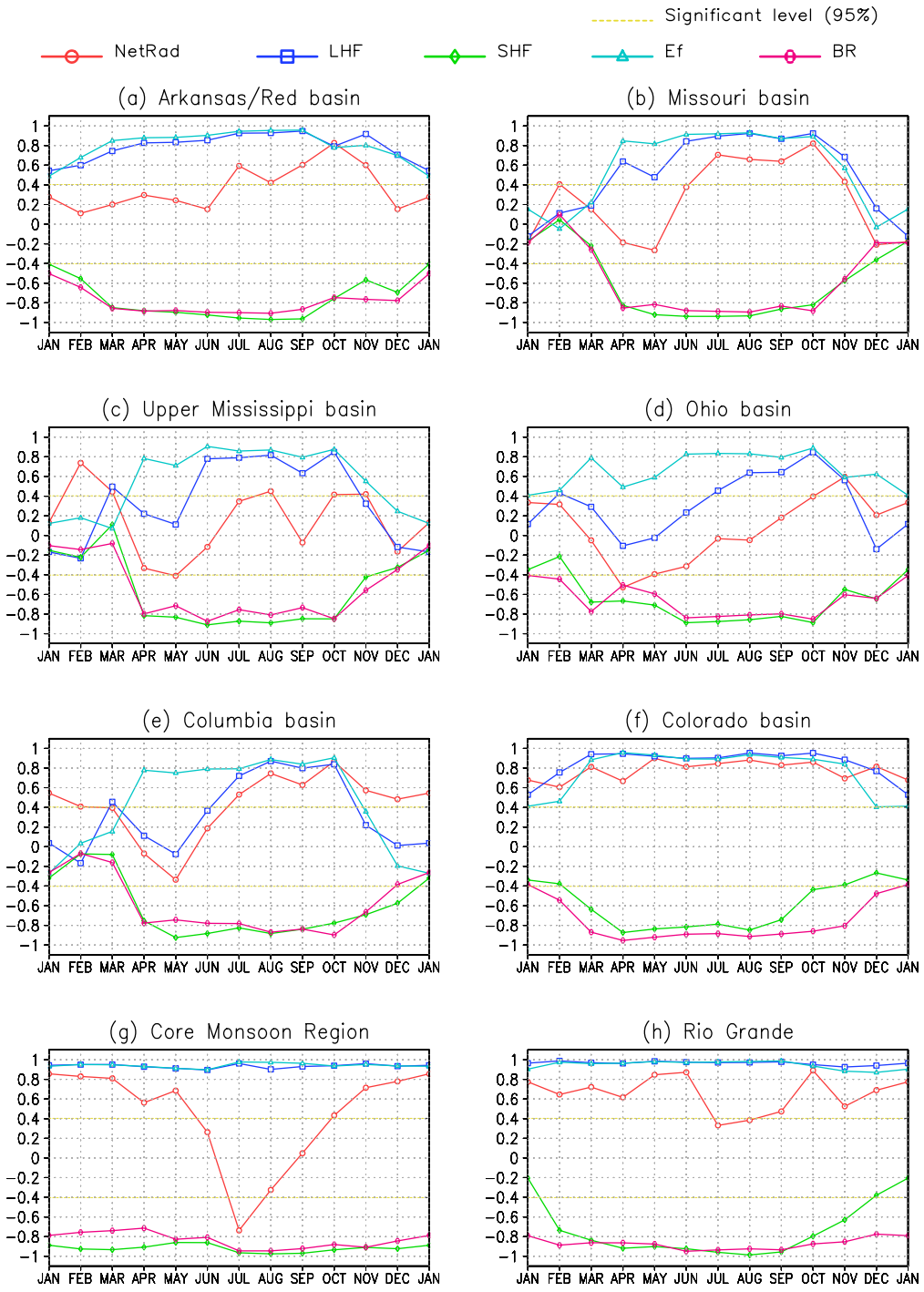

Figure 4.2 Seasonal variation of correlations between soil moisture and surface energy variables for (a)-(d) Mississippi subbasins, (e) Columbia basin, (f) Colorado basin, (g) Core Monsoon regions, and (h) Rio Grande.

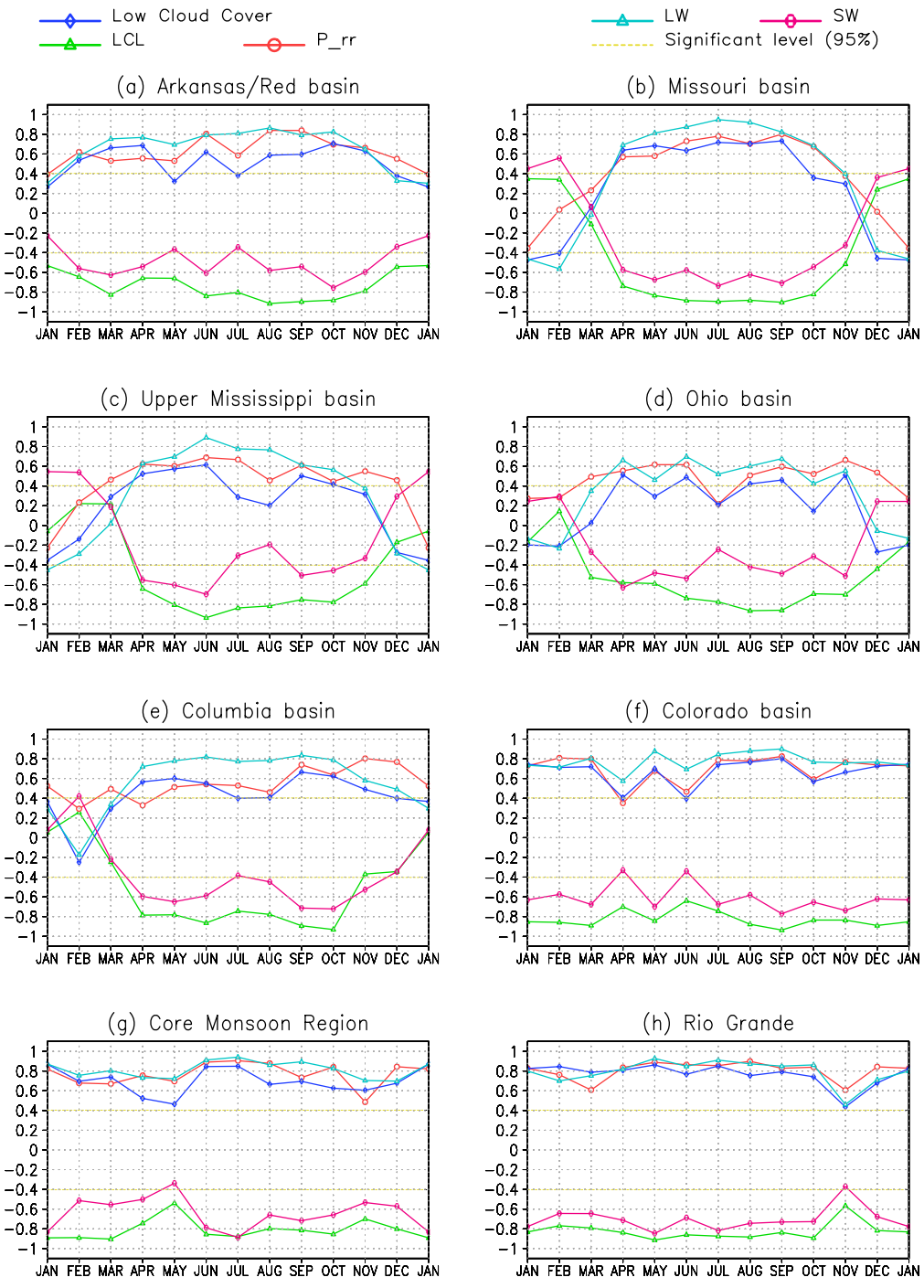

Figure 4.3 Same as Figure 4.2 but for seasonal variation of correlations between soil moisture and some surface and atmospheric variables.

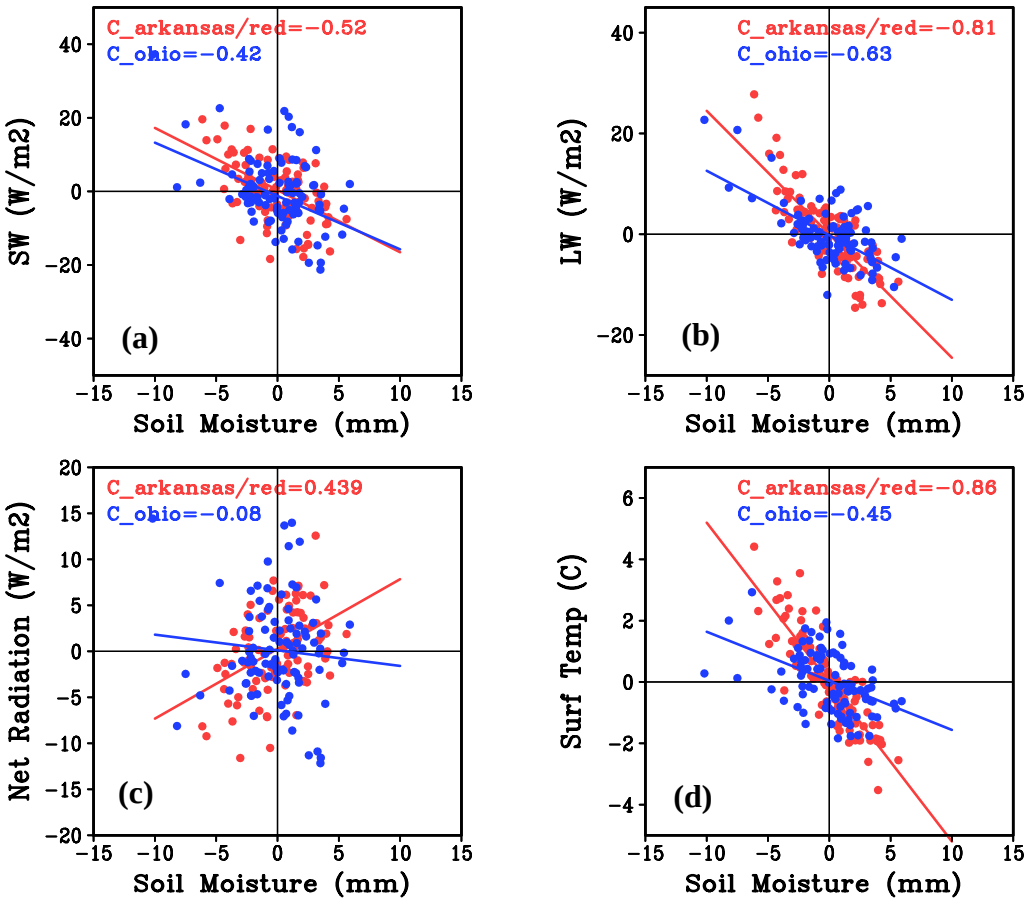

Figure 4.4 Scatterplots of summer (JJAS) 1979-2002 area-averaged monthly anomalies of soil moisture versus monthly anomalies of: (a) shortwave radiation; (b) longwave radiation; (c) net radiation; and (d) surface temperature for Arkansas/Red basin (red) and Ohio basin (blue), respectively.

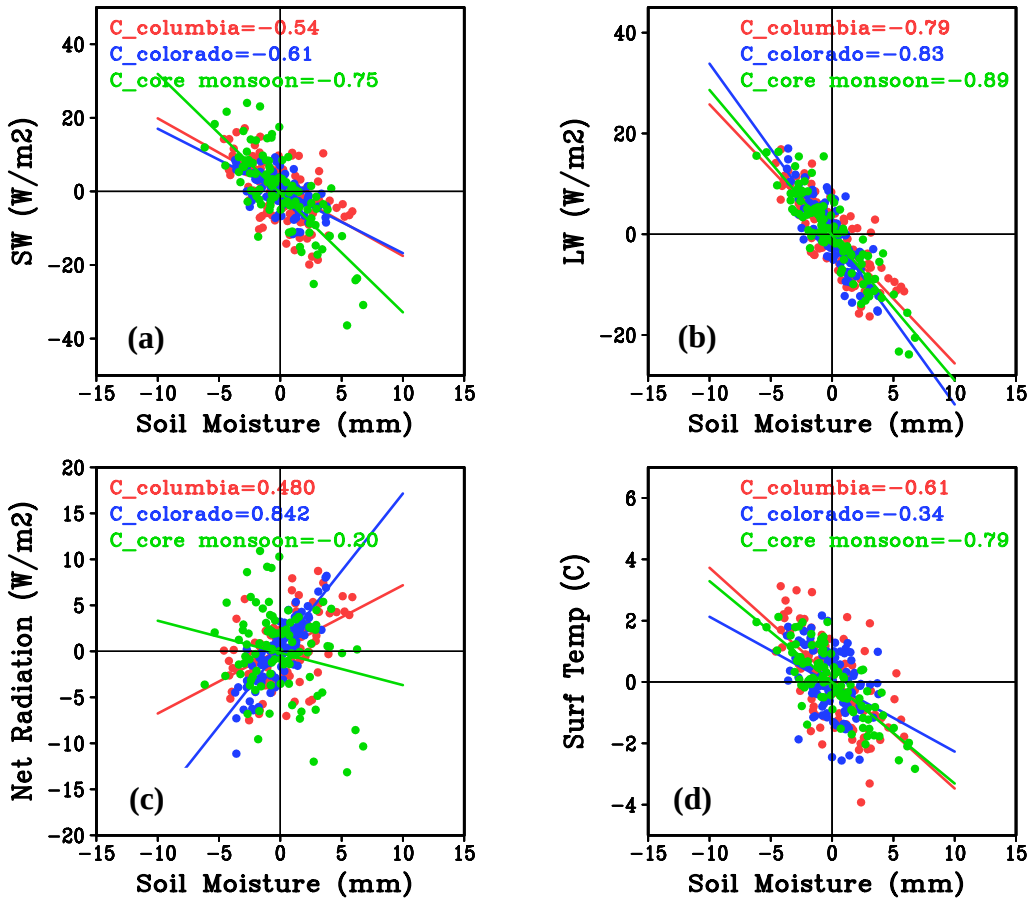

Figure 4.5 Scatterplots of summer (JJAS) 1979-2002 area-averaged monthly anomalies of soil moisture versus monthly anomalies of: (a) shortwave radiation; (b) longwave radiation; (c) net radiation; and (d) surface temperature for Columbia basin (red), Colorado basin (blue) and Core Monsoon region (green), respectively.

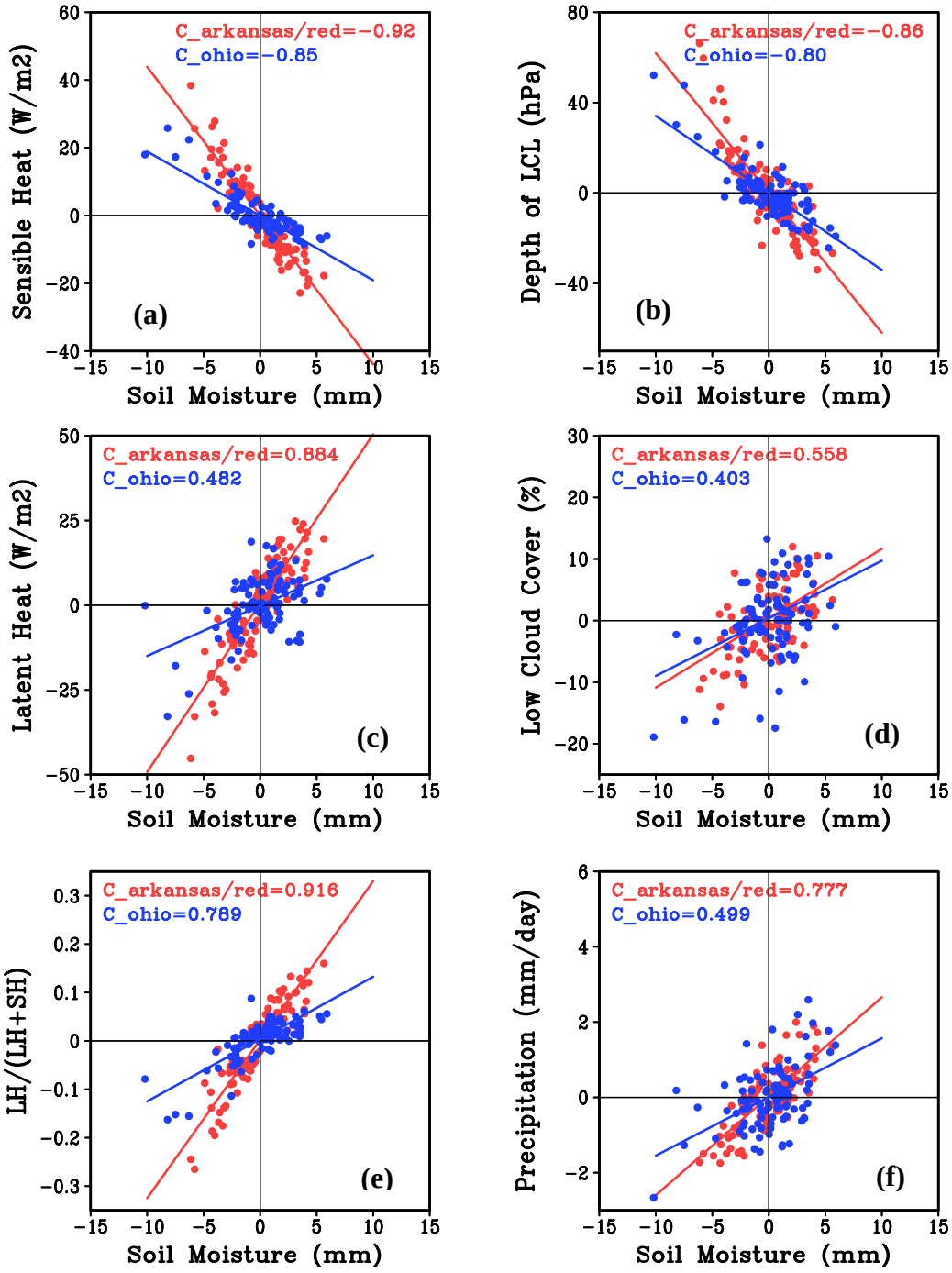

Figure 4.6 Scatterplots of summer (JJAS) 1979-2002 area-averaged monthly anomalies of soil moisture versus monthly anomalies of: (a) sensible heat flux; (b) the depth of LCL; (c) latent heat flux; (d) low cloud cover; (e) evaporative ratio; and (f) precipitation for Arkansas/Red basin (red) and Ohio basin (blue), respectively.

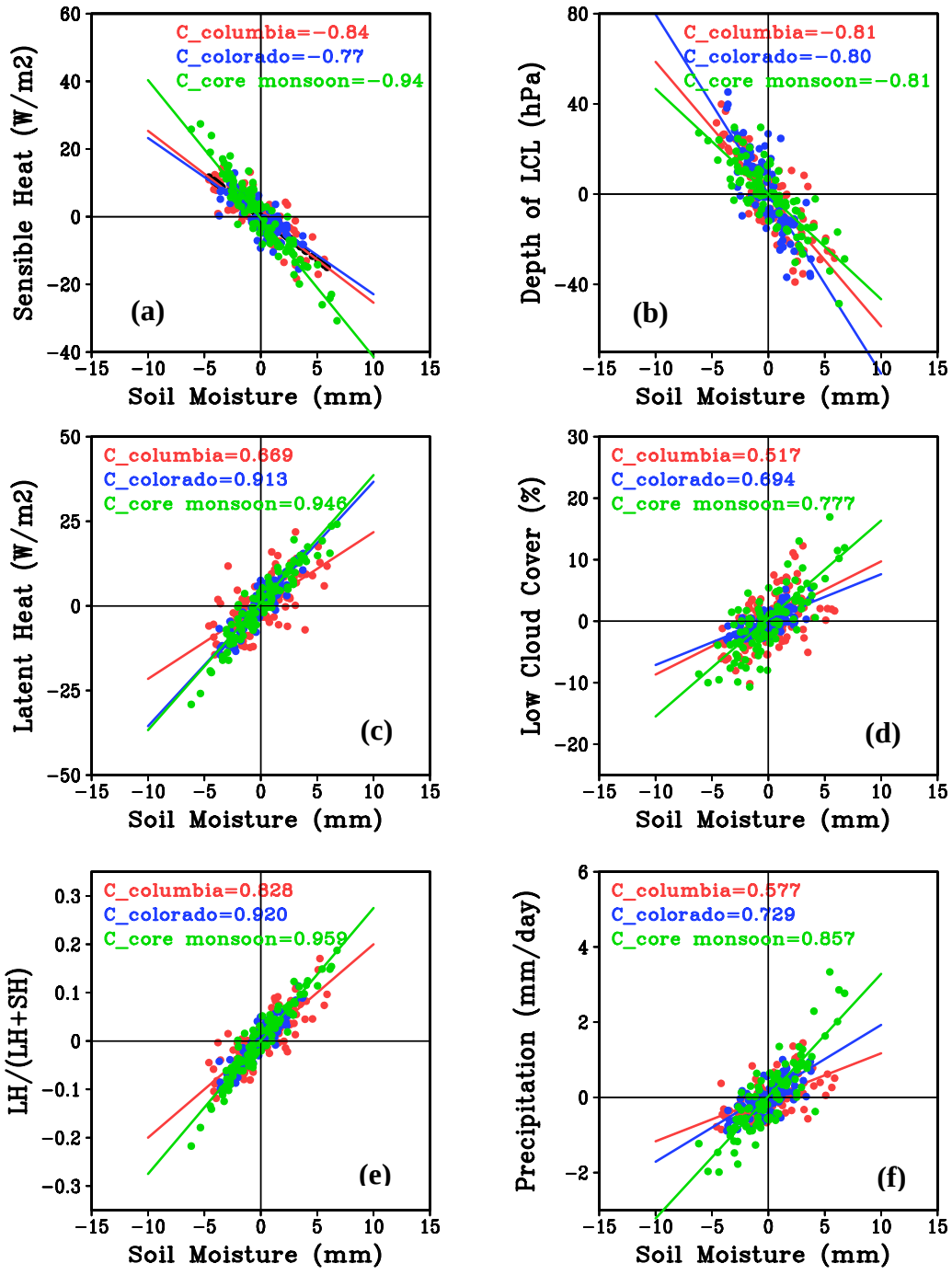

Figure 4.7 Scatterplots of summer (JJAS) 1979-2002 area-averaged monthly anomalies of soil moisture versus monthly anomalies of: (a) sensible heat flux; (b) the depth of LCL; (c) latent heat flux; (d) low cloud cover; (e) evaporative ratio; and (f) precipitation for Columbia basin (red), Colorado basin (blue) and Core Monsoon region (green), respectively.

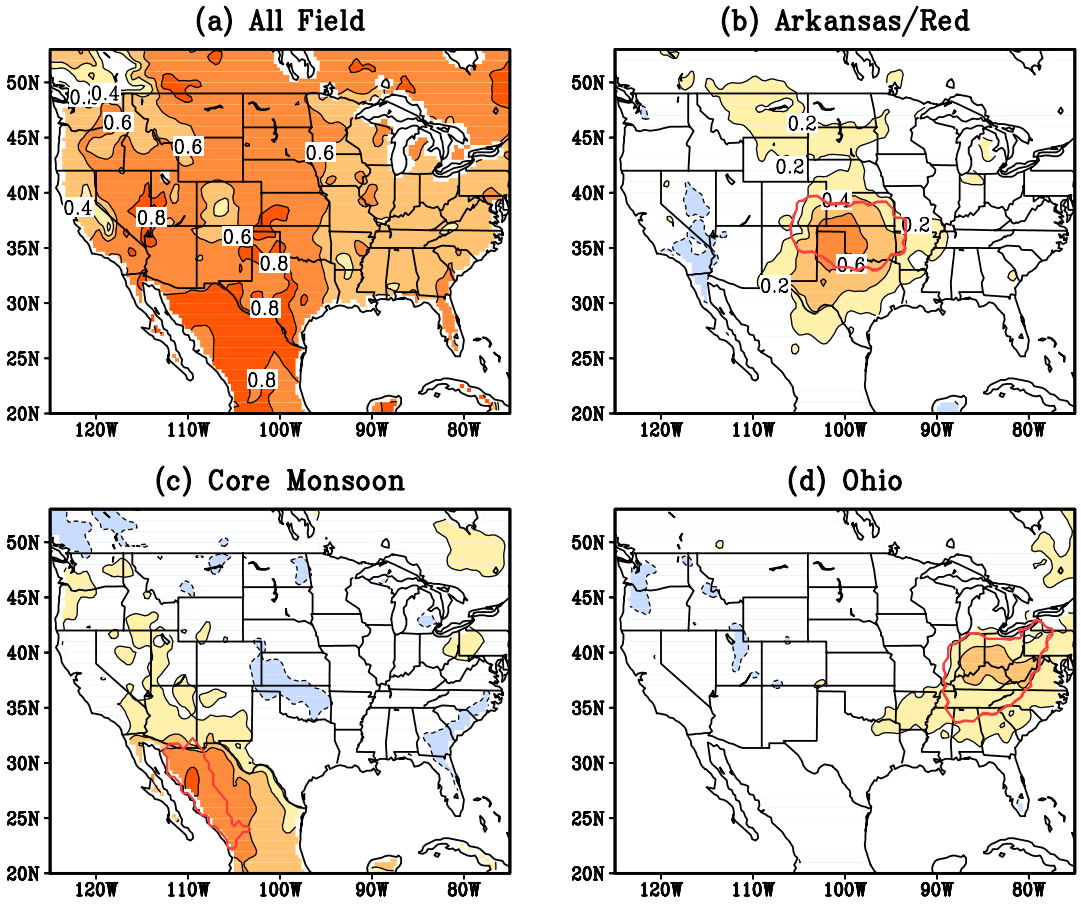

Figure 4.8 Point-to-point correlations between soil moisture and: (a) precipitation, (b) Arkansas/Red basin area-averaged precipitation, (c) Core Monsoon region area-averaged precipitation and (d) Ohio basin area-averaged precipitation. The correlation coefficients (r) are statistically significant at 95% confidence level if r>0.4.

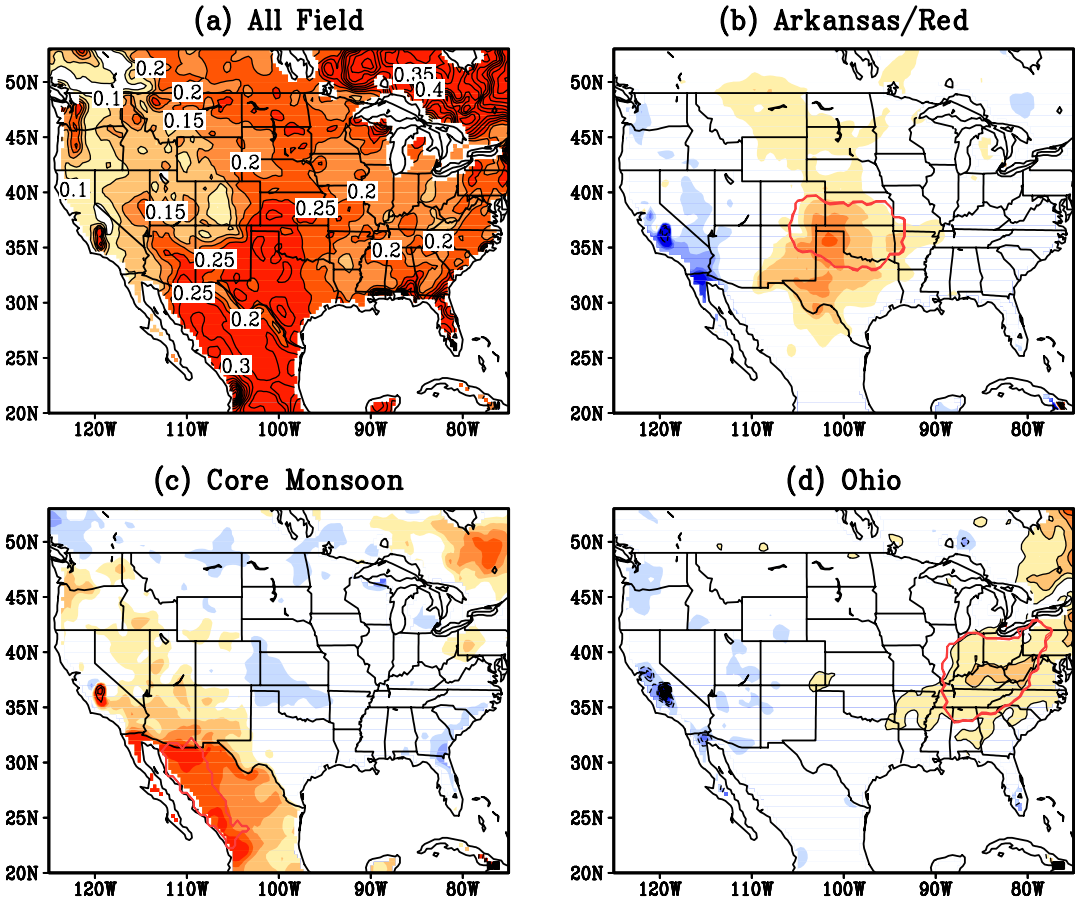

Figure 4.9 The slope of the linear fit for point-to-point relationships between soil moisture and: (a) precipitation, (b) Arkansas/Red basin area-averaged precipitation, (c) Core Monsoon region area-averaged precipitation, and (d) Ohio basin area-averaged precipitation.

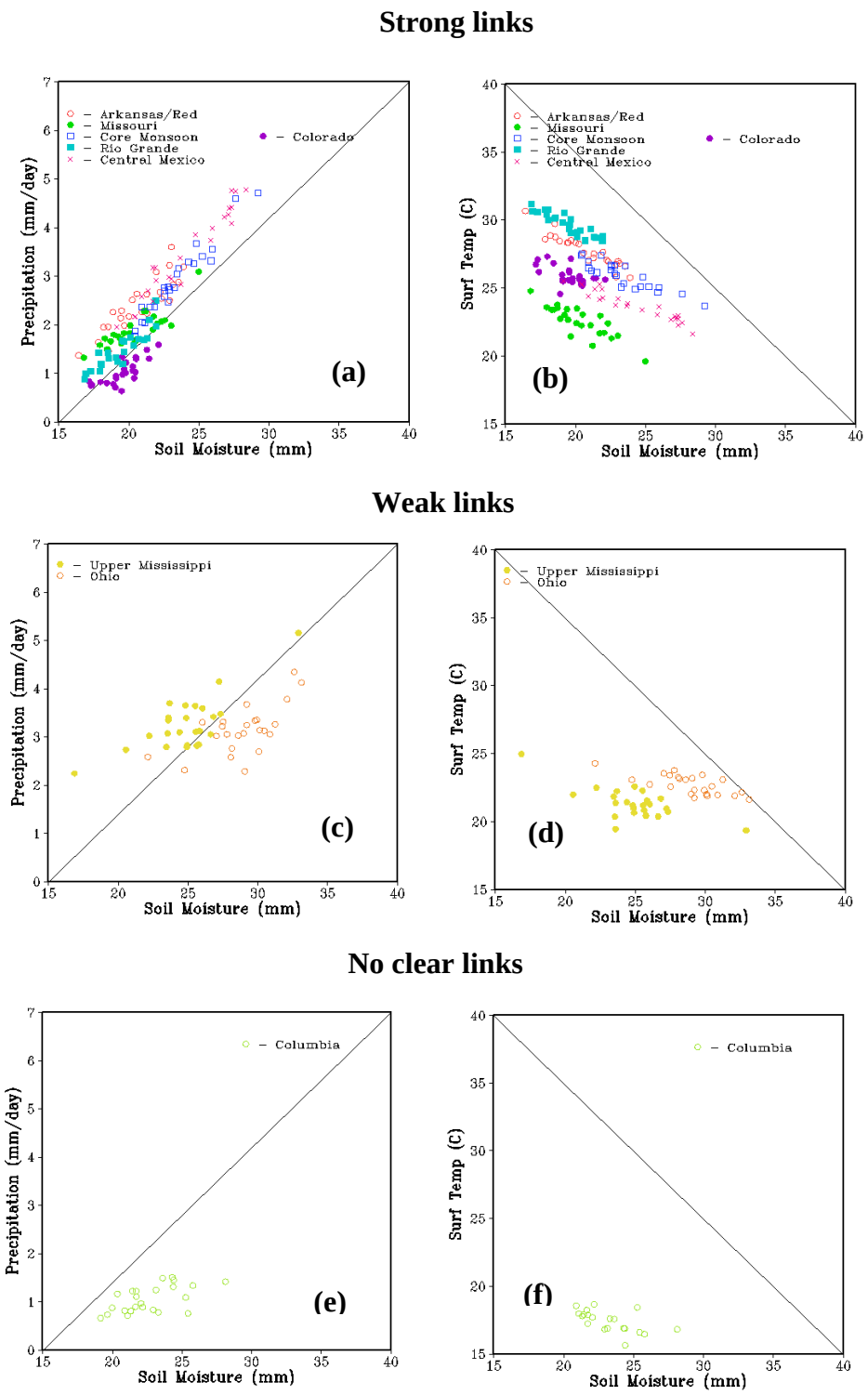

Figure 4.10 Scatterplots of 1979 -2002 mean summer (JJAS) area-averaged precipitation (on the left) and surface temperature (on the right) versus soil moisture content, showing three groups of regions according to the strength of land surface – atmosphere interactions: (upper) Strong links; (middle) Weak links; (bottom) Undefined links.

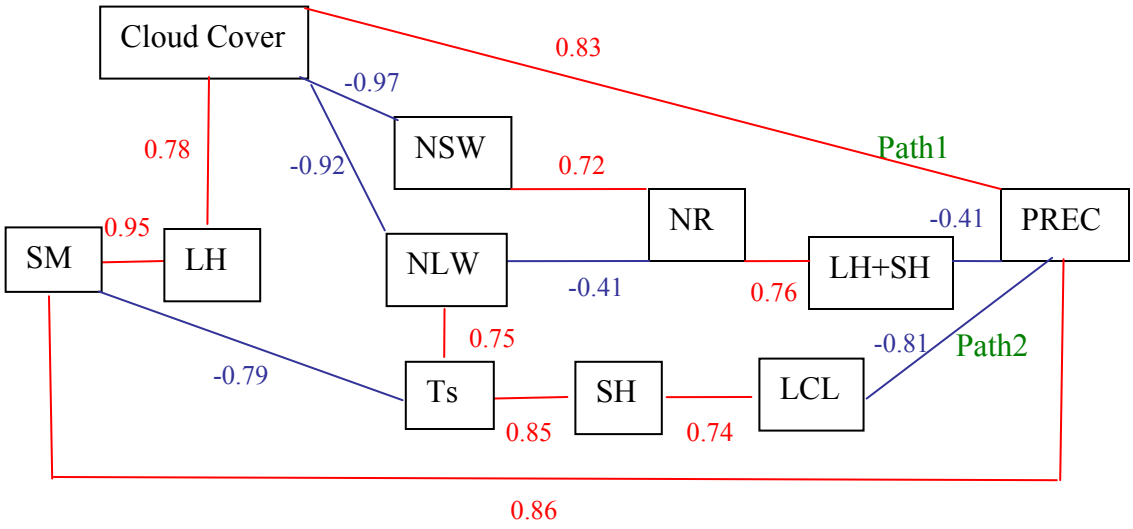

Figure 4.11 A schematic depiction of the relationship between soil moisture and precipitation. The links between the boxes indicate processes that establish the land surface-atmosphere interactions. Positive correlations (red line) and negative correlations (blue line) are distinguished showing how each component is related to its adjacent ones. Soil moisture can affect precipitation through two pathways. Path1 is going through this precipitation recycling process (e.g. via the water balance equation). Path2 is going through surface energy processes. The values are exemplified by the **Core Monsoon** region showing correlation coefficients between two adjacent variables. The correlation coefficients (r) are statistically significant at 95% confidence level if r>0.2.

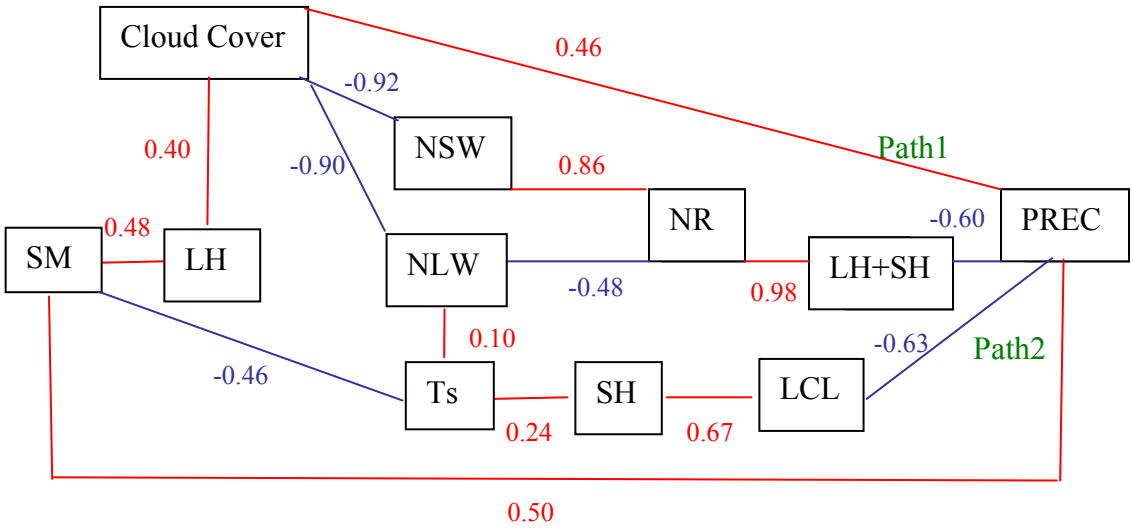

Figure 4.12 Same as Figure 4.11 but for the **Ohio** Basin.

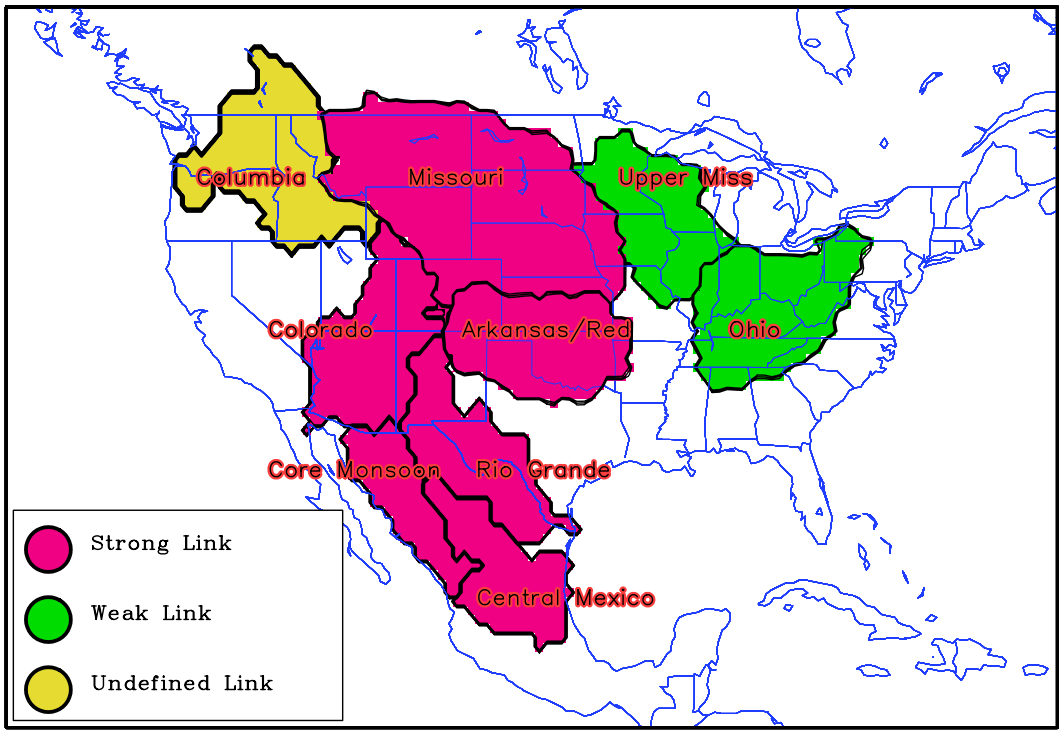

Figure 4.13 Qualitative representation of the land surface-atmosphere interaction regions within North America based on the correlations between soil moisture and surface water and energy variables for the nine regions with 24 year (1979-2002) NARR data.

CHAPTER 5: SOIL MOISTURE MEMORY

5.1 Introduction

Interest in land surface-atmosphere interactions brings to the forefront an emphasis on seasonal precipitation prediction. The results from the diagnosed land surface-atmosphere interactions at regional scales derived from the NARR dataset in the last chapter demonstrate the feasibility of relating those interactions to the role of soil moisture memory on the hydrological cycle, and therefore to assess the predictability of the hydrologic system at basin scales. In the previous chapter, it was found there is a good correlation between soil moisture and land surface energy processes during summer in the western part of the Mississippi basin and Monsoon-affected regions. Similar strong relations were found in the relationship of soil moisture and precipitation processes in the same regions.

To further understand the influence of the variability of soil moisture on the variability of the atmosphere, one should also be familiar with the variability of soil moisture itself. The emphasis of this chapter is on understanding more detailed soil moisture memory processes which can improve the predictability of precipitation. For this, it is necessary to identify how soil moisture memory relates to the predictability of the hydrologic cycle, and thus further assessments and strategies are needed.

The main focus of this chapter is the explicit study of the temporal and spatial distribution of soil moisture memory processes. In this framework, we will show that the soil moisture anomaly persistence has regional and soil depth dependences. In

such sense, Koster and Suarez (2001) provide guidance by determining an accurate measure of soil moisture memory based on the estimates of July NSIPP global products. In the current investigation, we will focus on North American basins on different time scales.

Finally, persistence of soil moisture anomalies can be expected to induce persistence in precipitation anomalies. We then address the importance of soil moisture anomalies on the predictability of the summer precipitation. In some conditions, the skillful prediction of soil moisture may be translated into a skillful prediction of precipitation. Therefore, we will investigate the regions where and when the change in soil moisture can alter precipitation.

5.2 Seasonal and Spatial Variations of Soil Moisture Profile

NARR has four unevenly spaced soil layers for a total soil depth of 2 m as shown in Figure 5.1. The first layer defines the bare soil evaporation, while the second and third layers correspond to the root region. The soil moisture profiles contain notable temporal and spatial variations. The variability of soil moisture serves as an indication of coupling to the atmosphere on various time scales, and thus can be used to identify how well land surface processes are represented in numerical models.

Figure 5.2 describes the amplitude change and phase shifting of the seasonal cycle of soil moisture with depth. The seasonal cycle of soil moisture is pronounced due to the impact of evapotranspiration (ET), which is highest in summer months because of the warmest temperatures, highest solar radiation, and peak greenness. The soil moisture is near maximum during spring months, thus indicating that winter and

early spring precipitation (while evaporation is low) is generally sufficient to fully recharge the soil moisture over given regions. The drying of soil during the summer can be intensified by high air temperatures and low humidity, and thus high evaporation. It can be seen that fluctuations in soil moisture propagate from the surface down to the deep soil. The topmost two layers show closer annual cycles in amplitude and phase, while the third layer is the driest with much smaller values. In general, the seasonal change is quite small below the root zone (100 cm) except in the Ohio basin. A time shift can also be noticed from the soil surface to the bottom, with the dates of maximum and minimum values of soil water being delayed by about 1-2 months. The amplitude change and phase shifting effect could be substantially dependent on vegetation and soil types, vegetation densities, root structure, topography, etc.

Generally, the soil is drying during warmer portions of the year when evaporation tends to exceed rainfall (typically late spring and early summer) and wetting during the colder portions of the year (autumn and winter) except for the North American Monsoon (NAM) regions (Figures 5.2g-h), where soil conditions are strongly connected to summer monsoon rainfall. The NAM regions have a different soil moisture seasonal cycle which is characterized by wet summers and dry winters. The soil in the NAM regions is typically dry in May and June, prior to the onset of the North American monsoon. In July through September, the soil in the NAM regions is repeatedly wetted and dried. In northern parts in the winter, including the western mountain areas and the northern half of the Mississippi basin, soils are mostly frozen.

The study of the phase and amplitude variability of soil wetness with depth hence provides a basis for further investigation of the layered soil moisture memory and its relation to summertime precipitation. The soil moisture variability presented here is highly dependent on the model's ability to estimate the real climate system correctly. In the case of NARR, the reliability of the soil moisture estimate depends on the accuracy of both the atmospheric observed forcing data provided by EDAS, but also on the land surface model physics (Mitchell, 2004).

5.3 Variations of Soil Moisture Memory

The persistence of soil moisture depends on the regions where we study. It also depends on climatological characteristics such as the seasonal amount and the nature of precipitation. We will characterize such soil moisture memory in terms of its time scale, with spatial, vertical and seasonal variations of one-month-lagged and multi-month-lagged autocorrelation coefficients.

As discussed more fully in the study of Delworth and Manabe (1989), the persistence of monthly soil moisture may be viewed as the red-noise response of the soil layer to the time series of monthly mean precipitation, which resembles white noise (lag-one autocorrelations near zero). In other words, the soil layer acts as an integrator of the time series of rainfall, producing a time series of soil moisture which is similar to red noise (lag-one autocorrelation significantly greater than zero).

If we consider that the time series of soil moisture is similar to the red noise of a first-order Markov process (Delworth and Manabe 1988), its temporal

autocorrelations can be translated into e-folding times. For a red-noise process (Jones, 1975), the autocorrelation function $r(t)$ is exponential, that is:

$$r(t)=\exp(-t/\tau),$$

where $r(t)$ is the autocorrelation at lag t and τ is the e-folding time of anomalies in the absence of forcing. As shown in Figure 5.3, one-month-lag autocorrelation values of 0.2, 0.4, 0.6, and 0.8 correspond to e-folding times of 0.6, 1.1, 2.0, and 4.5 months, respectively, implying that larger r is relevant to longer time scale τ. The limitations of the idealized Markovian framework are noteworthy, as questioned in a study by Koster and Suarez (2001); that is, it neglects (1) seasonal variation in the statistics of the meteorological forcing (precipitation and radiation) and (2) persistence in the meteorological forcing. Nevertheless, since it captures the basic feature of soil moisture as a red-noise process responding to the "white" atmospheric forcing, it can be used as an important parameter to measure soil moisture memory.

5.3.1 Spatial and Vertical Variations

One measure of the temporal variability of monthly mean soil moisture is the one-month-lagged autocorrelation coefficient. For each grid point and layer, the anomaly time series of soil moisture was correlated with itself, but lagged one month. An anomaly is defined as the deviation of the monthly mean from its long-term mean for that month. The autocorrelation fields at four layers are plotted in Figure 5.4. For comparison, we also include the precipitation autocorrelation following the same method.

The autocorrelations of soil moisture are generally positive and increasing with soil depth, demonstrating that anomalies of soil moisture persist on monthly time scales. Because the time series of soil moisture is similar to red noise, the first-order Markov process assumption provides a plausible comparison of time scales at different regions and soil depths as displayed in Figure 5.4. The autocorrelations are greater than 0.9 almost everywhere in the deepest soil layer (Figure 5.4d). In addition, the differences between the scales of the upper 10 cm to 100 cm layers are not significantly different. Typically, the seasonal decay time scales increase from approximately 1-4 months at the surface to more than 4 months at 100 cm depth and much longer (over 10 months) at the bottom. These decay time scales vary regionally. For example, for the top 40 cm of soil, smaller values predominate at the western dry areas, and greater values at the eastern wet areas in Mississippi. The general characteristics were consistent with previous studies. A comparison of this figure with the results from Koster et al. (2001) reveals some broad similarities which are very encouraging. Autocorrelations are positive and of comparable magnitude in both cases. It is also important to note that soil moisture has a memory considerably longer than that of precipitation. This is because as stated earlier, the time series of monthly mean precipitation only resemble white noise (a random feature) which results in small values of the coefficients. However, there is a significantly small but clear persistence of precipitation in monsoon-affected regions, with autocorrelation coefficients of 0.2~0.4 which is statistically significant above the 95% level. In such a way, it indirectly indicates that the soil layer acts as an integrator of short-timescale precipitation anomalies, transforming the almost white noise time series of monthly

mean precipitation into the red noise time series of soil moisture (Delworth and Manabe, 1988, 1989).

Another way to view the layered soil moisture persistence is through a profile of autocorrelation coefficients for the four representative basins, two dry and two wet, as displayed in Figure 5.5. The deep soil moisture anomalies exhibit a more powerful, long-lasting effect than do anomalies closer to the surface. Hence, the contribution of soil moisture to atmospheric variability should depend on the depth of the soil moisture. This suggests water stored at the surface has an immediate response to the atmospheric forcing such as precipitation and evaporation, while soil moisture's longer memory may be carried in the deeper soil layers (Dickinson et al. 2003).

5.3.2 Seasonal Variations

The decay time scales of the soil moisture profile vary not only vertically but also seasonally. This is exemplified in Figure 5.6, where it is shown that soil moisture memory varies vertically and horizontally during the year (the one-month-lagged autocorrelation coefficients at each soil layer for each month are displayed). Figure 5.6 shows soil moisture autocorrelations as a function of the month. The autocorrelation coefficients increase from approximately 0.2-0.3 (τ~0.6-0.8 months) at the surface to about 0.8 (τ~4.5 months) at 100 cm with the exception of monsoon regions in summer, of which the autocorrelation coefficients below the surface are smaller; for example, they are about 0.6 (τ~2.0months) at 100 cm. The soil moisture below the root zone has a very long time scale and very little change with the season.

The seasonal variations of the persistence of soil moisture are very complex and show somewhat basin-dependent features. While persistence changes with season, the soil moisture memory is not necessarily longer in wintertime and shorter in summertime. In snow affected areas, especially the northern regions where snow accumulation dominates, persistence is smaller in winter than in summer. The largest values during winter are mostly in the southern regions, a result of smaller potential evaporation when insolation is weak, resulting in soil moisture autocorrelations larger than 0.8. In the Columbia basin and the northern portion of the Mississippi basin, the decay time is longer during the summer months than during the winter for all layers, but the opposite is true in the North American Monsoon regions and other dry regions. It is indicated again that the time scales of soil moisture memory are longer (shorter) in wet (dry) regions during summer, but the opposite, with shorter (longer) memory in wet (dry) regions, during winter. For example, in the wet eastern half of the Mississippi basin and the Columbia basin, the time scales are longer in summer and shorter in winter, with the opposite pattern in the semiarid North America Monsoon Regions. These results may be interpreted in terms of the surface water balance as we will discuss in Section 5.4.

5.3.3 Multi-Month-Lagged Autocorrelation

In Figure 5.7, we show the correlations between the August soil moisture anomaly and that of the preceding months. We focus on results for August only, as results for the neighboring summer months June, July and September are similar. This figure shows the persistence of NARR soil moisture anomalies from the preceding

months into August. The relevant soil moisture memory processes can be represented by autocorrelations above 0.404 (to be significant); this occurs over the eastern half of the Mississippi and the western US basins, where the lag can be 2-4 months long. In the western half of the Mississippi basin and the Mexico Monsoon regions, by contrast, it is less than 2 months.

The comparatively long-term memory is useful for the soil moisture predictability studies, and thus these results for each basin will be further studied.

5.3.4 Connections between Different Layers of Soil Moisture

It is important to keep in mind that soil moisture in all layers is interrelated. Persistence can be translated in the vertical (not shown). The straightforward interpretation of this result is that the soil moisture variations are just simply transported by gravity effect (infiltration process) from the upper layers to the deeper layers and by evaporative effect (Evapotranspiration processes) from the deeper layers to the upper layers. The deeper layer is sometimes responsible for providing the upper layer with moisture in times of water stress.

5.4 Mechanisms behind Soil Moisture Memory

We have examined the variations of soil moisture memory, and will continue to investigate their physical interpretations. To this end, we will examine how the time scales of the soil moisture profile depend on 1) the ratio of precipitation to potential evaporation (**P/PET**), 2) the ratio of evaporation to potential evaporation (**ET/PET**, evaporation ratio). This section examines how the precipitation,

evaporation, and runoff combine to affect the layered soil moisture memory at different geographical locations with different climate regimes. It is desirable to understand how the persistence of soil moisture depends on those combined effects.

We start with soil moisture changes in time, according to the surface soil water balance equation

$$\frac{dW}{dt} = P - ET - R \tag{5.1}$$

that is, the changes in time of total soil water $\boldsymbol{W}$ balance the precipitation into the ground $\boldsymbol{P}$, minus the sum of evaporation from the ground $\boldsymbol{ET}$, and subsurface runoff $\boldsymbol{R}$. The atmospheric forcings are responsible for the amount of water available to the soil through precipitation (rainfall or snowmelt), and for the removal of water from the soil through evaporation. Interactions of the three right-side forcing terms $\boldsymbol{P}$, $\boldsymbol{ET}$, and $\boldsymbol{R}$ with the left-side term $\boldsymbol{W}$ will affect the decay time scales of soil moisture profile and, so, influence any seasonal predictions that relate to such memory. In other words, the temporal structure and vertical profile of soil moisture depends on the temporal variability of precipitation, evaporation and runoff. Seasonal variations in soil moisture persistence could stem from seasonal changes in those forcing terms.

Much effort has been dedicated to investigating the mechanisms controlling soil moisture memory. For example, Koster and Suarez (2001) indicate that the autocorrelation of soil moisture – that is, soil moisture memory, is mainly controlled by four distinct factors: (i) seasonality in the statistics of the atmospheric forcing, such as precipitation and net radiation; (ii) the effect of ET in removing soil moisture and hence its memory; (iii) the similar removal effect by runoff; and (iv) persistence in atmospheric forcing, perhaps as triggered by land-atmosphere feedbacks. We will

further examine these mechanisms responsible for such variations in the soil moisture memory.

We assume that water and energy relative availability in terms of the above two ratios contributes to such a soil moisture memory. Either potential evaporation or solar radiation (Delworth and Manabe 1989) reflects the energy supply and water demand (evaporative demand). Conversely, evaporation stands for water supply and energy demand. These two features are strongly related.

The purpose of inspecting the seasonal cycle of precipitation, evaporation, potential evaporation, and the two related ratios (Figure 5.8) is to investigate how those quantities control the soil moisture time scales. Most quantities have strong seasonal cycles, and thus soil moisture memory usually differ. In general, the temporal variability of NARR computed soil moisture is strongly influenced by potential evaporation and runoff. Soil moisture memory can be reduced not only by potential evaporation but also by runoff. The ratio of **P** to **PET** determines which mechanism is dominant. On one hand, for seasons and locations where the ratio of **P** to **PET** is less than one, such as drier regions with large potential evaporation values (like Figures 5.8 a and c), a result of the large net radiative flux, but with limited water supply (small **ET**) at the surface, allow soil moisture anomalies to be rapidly damped. Potential evaporation thus determines the decay time scales of soil moisture as they are inversely correlated. The time scales of soil moisture variability are thus quite short. Variations in potential evaporation, resulting from differing mean values of soil wetness, temperature and net radiation at the surface, account for some of this dependence. Furthermore, since **ET** has a pronounced maximum in summer and a

pronounced minimum in winter, soil moisture will be more persistent in winter than in summer over the relatively dry areas. Otherwise, for seasons and locations where this ratio is greater than one (usually wet regions), frequent runoff, dictated by the hydrologic balance, is the mechanism by which the decay time scales of soil moisture are substantially shortened (Figures 5.8 b and d). We discuss these two ratios and their different roles in affecting soil memory in summer and winter seasons, as soil memory has remarkably distinct features in the wet and dry regions.

5.4.1 Summer Season

In summer when the ratio of **P/PET** usually less than one, **ET** acts as a dominant role controlling the soil moisture persistence. We use the ratio of actual evaporation to potential **(ET/PET)** as a measure of water/energy supply ability.

During summer, the degree of persistence of soil moisture anomalies depends on how rapidly anomalies are removed from the soil layer by evaporation; the persistence of soil moisture is primarily controlled by not only net radiation (energy supply) in terms of potential evaporation, which is highly temperature dependent, but by the variability of soil wetness (water supply) in terms of evaporation as well. That is, the smaller (larger) the potential evaporation and larger (smaller) evaporation, the more slowly (rapidly) anomalies of soil moisture dissipate, and the larger (smaller) the autocorrelations of soil moisture. This can be seen by comparing Figure 5.4(a) with Figure 5.9, a map of the difference between potential evaporation (**PET**) and evaporation (**ET**) for JJAS: during summer, wetter regions have larger evaporation ratios, implying abundant water but insufficient energy supply, and thus tend to keep

soil wet and sustain longer memory. Such memory is quite short over drier regions which have smaller evaporation ratios, because there is plentiful energy but limited water supply and soil moisture stored during spring is quickly removed. In summary, the summer soil moisture memory pattern is much similar to the distribution of the difference between potential evaporation and evaporation. Therefore, this difference between **PET** and evaporation **ET** is of interest, because it indicates the water and energy relative availability to remove or enhance soil moisture memory.

a. Dry Regions

As shown in Figure 5.6a and c, the time scale of the soil moisture memory computed as one-month-lagged autocorrelation showed that over the monsoon region and western part of the Mississippi river basin the persistence is lower than that in wetter regions.

In such regions with drier soil conditions, there are large differences between values of **PET** and **ET**. There is ample energy for the removal of moisture from the surface by evaporation but limited water supply from the surface. The consequence is frequent loss of water from the surface, and thus the persistence of soil wetness is low.

Over the monsoon areas, the soil moisture evolution is quite different from the other dry regions since it is mostly determined by precipitation. More interestingly, Figure 5.8c shows the onset of monsoonal precipitation starts abruptly in June-July. As we discussed in Chapter 4, in the semiarid environments, where the connection between the land surface and the atmosphere is believed to be strong, the soil

moisture time scale appears to depend largely on the time scales for land-atmosphere interactions through **ET** (or availability of water to be evaporated). This relationship does hold and persists into the later monsoon season. Soil moisture-precipitation feedback tends to promote long soil moisture memory in monsoon-affected areas, which contributes to seasonal prediction predictability.

b. Wet Regions

Figures 5.6 b and d show the time scales of soil moisture memory are longer in the Ohio and Columbia basins during summer. This indicates the soil moisture memory was very high over regions that have wet soil conditions. Physically, soil moisture excesses are dissipated more slowly wet areas especially at higher latitudes when the energy available for evaporation is relatively insufficient. This favors longer memory, although there is sufficient water (as measured by evaporation) from the surface. In conclusion, under wet conditions, the time scales of soil moisture appear to be controlled by energy-limited (or water abundant) conditions; and more specifically such dependence is seen for values of small differences between **PET** and **ET** (Figure 5.9).

5.4.2 Winter Season

Soil Moisture memory can be reduced not only by evaporation but also by runoff. Some processes other than evaporation may play an important role in determining soil moisture decay time scales. The analysis of Delworth and Manabe (1989) indicated longer time scales for colder seasons and climates. According to

their studies, one exception, however, is the minimum in autocorrelation over the northern basins during winter until early spring. This feature is caused by frequent saturation of the soil layer from snowmelt. The freezing and melting processes have a major role in soil moisture memory for those northern regions. Energy used to melt snow decreases the evaporation rate, thereby lengthening memory in regions where snow cover is frequent. The runoff process also removes moisture from the soil, and its effect on the temporal variability of soil moisture is considerable and thus should be taken into account.

Soil moisture memory is regulated by potential evaporation and precipitation. It should be emphasized that the values of **P** and **PET** are the primary determinants of the characteristics of the soil moisture temporal variability. Their difference is an indicative of the shortened soil moisture decay time scales due to evaporation or runoff. Runoff is a residual term as a result of values of **P/PET** greater than one, and occurs only because of the requirement of a surface hydrologic balance. Such a process may have contributions to the less persistent anomalies of soil moisture.

a. Dry Regions

Figures 5.6 a and c show again that the time scales of soil moisture memory are longer in dry regions during winter than during summer. The largest values of autocorrelation coefficients in winter are mostly in the southern dry regions, a result of smaller potential evaporation in winter when insolation is weak, resulting in soil moisture autocorrelations larger than 0.8. In winter, small potential evaporation values, a result of the small net radiative flux at the surface, allow only a very slow

dissipation of soil moisture anomalies. Time scales of soil moisture variability are thus quite long. Typically, in dry regions, the ratio of **P** to **PET** is less than one all year around. These results demonstrate that the evaporation mechanism is still the primary control on the time scales of soil moisture variability over these dry regions in winter.

b. Wet Regions

In mountains and higher latitudes, there is a maximum of persistence in the summer months. This may be attributed to wet soil conditions present in these regions. Nevertheless, during the winter seasonality of snow accumulation and melt as well as freezing and melting of soil water reduces the soil moisture memory. This explains the small autocorrelation values in regions of frequent runoff, especially occurring during winter until early spring. A different type of variability is observed when the ratio of **P** to **PET** is greater than 1. Under these conditions, the maintenance of a hydrologic balance at the ground surface results in frequent saturation and runoff. A consequence of this is that decay time scales of soil moisture are shortened from what they would be if evaporation were the only mechanism removing moisture from the surface. In such regions, decay time scales can be quite short, even where potential evaporation values are very small in the annual cycle.

It is indicated again that the time scales of soil moisture memory are shorter in wet regions during winter. It should be noted that for winter, soil moisture decay time scales can still be very short despite the influence of the weak evaporative process

owing to the very small net radiation values in winter. Increment of these times by potential evaporation still leaves soil moisture decay time scales quite short.

The analysis of NARR on soil moisture persistence indicates that the mechanisms controlling soil moisture time scales may be more complex. For example, interpreting the soil moisture time scales in northern basins is more complex because of the lagged memory introduced by snowfall and its later melting, while our analysis considers only liquid soil water. The shorter time scale in spring appears to be connected with snow-melt or soil water phase change. These contributions cannot be quantified at present. Further study would be necessary to determine the exact effects upon the soil moisture time scale caused by the minimum potential evaporation and wintertime water frozen and melt processes.

Our major findings are:

1) The influence of potential evaporation on soil moisture memory can be seen in the summer or whenever it exceeds precipitation; otherwise soil moisture memory is dominated by runoff. The ratio of precipitation to potential evaporation (Liu and Avissar 1999 a, b) is a critical element to determine whether potential evaporation or runoff affects soil moisture memory.

2) Under wet conditions, the time scales of soil moisture appear to be controlled by limited energy supply conditions (or temperature-dependent climatic demand).

3) However, for drier conditions, the time scales appear to be controlled by water-limited conditions or to be largely dependent on the time scales for land-atmosphere interactions through ET (or availability of water to be evaporated). Strong

soil moisture-precipitation feedback tends to promote long soil moisture memory in many areas of Mexico, which may contribute to seasonal predictability. These inferences are supported by the seasonal cycle of precipitation, evaporation, and potential evaporation as discussed in the previous part of this section.

Our analysis here is not fully consistent with that of Delworth and Manabe (1988) and Yeh et al. (1984). They show a latitude-dependence of soil memory that is partially different from our results. Their studies only consider the energy availability and use less sophisticated model physical parameterizations as well. Our results show more complicated features of soil memory and suggest that soil moisture memory depends both on water and energy availability rather than only control of energy supply ability in the forms of potential evaporation. These conclusions are significant for assessing the regional predictability and expectations for climate prediction.

5.5 Connections between Warm-Season Precipitation and Prior Soil Moisture

As the typical time-scale length of soil moisture is 2-4 months in the North American continent, is there any connection between prior soil moisture and subsequent precipitation? How do prior soil moisture variations modulate the subsequent precipitation variability? To explore such questions, we will examine the relationships between precipitation and soil moisture in different temporal phases. In conjunction with soil moisture memory, this will allow us to further evaluate the predictability of summer precipitation.

Correlation analysis was applied to obtain the relationships between soil moisture and precipitation with different time lags in summer months (JJAS):

simultaneous correlation ($SM1_{(t)}$ Vs. $P_{(t)}$), soil moisture lagged precipitation by one month ($SM1_{(t)}$ Vs. $P_{(t-1)}$), and precipitation lagged soil moisture by one month ($SM1_{(t-1)}$ Vs. $P_{(t)}$) at a given month t. The anomaly time series of precipitation and soil moisture were constructed as defined in section 5.3 by subtracting the annual cycle from the 24-year monthly means. Since we have 96 months of anomalies (24 years with four summer months (JJAS) pear year), the correlation coefficient for the 95% (99%) confidence level is 0.2006 (0.262). The contours in Figure 5.10 a-b range from 0.2 to 0.8, and therefore all contours plotted are above the 95% confidence level. Large correlation coefficients above 0.6 of SM1(t)-P(t) occur in the Midwest, extending to the southwestern US and Mexico. With precipitation preceding soil moisture by one month, one can infer from Figure 5.10b, that precipitation affects soil moisture, and displays higher correlations than when soil moisture precedes precipitation (Figure 5.10c). This can be explained as water stored at the surface has an immediate response to atmospheric forcing such as precipitation and evaporation. Soil moisture would directly increase in response to a rainfall event. From Figure 5.10c, few areas except the monsoon regions in Mexico reach the significant level, implying a limited effect of soil moisture on precipitation. Interestingly, Figure 5.10a and Figure 5.9 show some similarities in distribution and relative magnitudes, reflecting the influence of soil moisture on the precipitation is greater in regions where the values of difference between **PET** and **ET** are larger.

To further investigate the vertical dependence of the correlations of SM(t)-P(t), we show the vertical profiles of the correlations in JJAS for four basins in Figure 5.11. The overall correlation coefficients decrease with depth and with smaller values

at wet basins than those at dry basins: towards the surface, soil moisture shows relatively strong connections with precipitation at the Arkansas/Red basin and the Core Monsoon region, but such connections are weak at the Ohio and Columbia basins. Significant correlations are mostly confined to the top 40 cm of soil. The values appear to be in the range of 0.4-0.8. In the deeper layers of 100-200 cm, the correlations become even smaller. The soil moisture below the rooting zone has a long time scale and is poorly correlated with precipitation.

5.6 Predictability and Uncertainty of the Regional Hydrologic Cycle

Precipitation is a key driver in the hydrologic cycle. Accuracy in precipitation estimation largely determines the realistic description of the cycle. More importantly, the presence of strong soil moisture-precipitation interactions in conjunction with the persistence of soil moisture anomalies provides additional elements for seasonal forecasting of the regional hydrologic cycle. An evaluation of predictability of summer precipitation anomalies in response to soil moisture anomalies could be assessed from the analysis that follows.

In this section, we propose a complete framework to evaluate how the North American land-atmosphere interactions contribute to the predictability of the precipitation and thereby to the regional hydrologic cycle. Why the land surface contributes more to predictability in some regions than in others is shown in Figure 5.12. We use the simultaneous correlation between precipitation (P_t) and soil moisture ($SM1_t$) to represent the strength of land-atmosphere interactions, a one-month-lagged autocorrelation of soil moisture ($SM1_t$ Vs. $SM1_{t-1}$) to measure the strength of soil

moisture memory, meaning that the previous month soil moisture condition persists well into that month, and the lag correlation with precipitation (P_t) lagging soil moisture by one month ($SM1_{t-1}$) to imply the predictability of precipitation. Here the subscript "t" refers to the predicted month with unknown precipitation, while "t-1" refers to the previous month with known soil moisture. Climatologically, if given the month "t", and given the possibility that we know that there is a strong positive correlation between P_t and $SM1_t$, and the autocorrelation of SM1 anomaly is high as well, then we can expect that previous month precipitation anomaly will also persist into that month. This is the logic behind our prediction strategy, serving as a straightforward and practical way to utilize the land surface conditions to qualitatively forecast precipitation.

Such qualitative evaluation of the summer precipitation predictability is explored by bar graphs such as those shown in Figure 5.12. The first two bars in each basin represent the precipitation and soil moisture interactions, and soil moisture memory, respectively. Their lengths can be compared directly to determine the relative importance of the land surface effects. The first correlation bar addresses the question to what extent precipitation anomalies are related to contemporaneous soil moisture anomalies. The second autocorrelation bar addresses the question to what extent soil moisture anomalies can be predicted in the first place. The third bar represents the predictability which is represented by the value of lag correlation between precipitation and the preceding month soil moisture. It addresses the question to what extent precipitation anomalies are guided by soil moisture

anomalies. If the third bar is shorter under 0.2, the precipitation is not strongly affected by the soil moisture, and there is no clear contribution from the land surface.

Each basin in the Figure 5.12 corresponds to three values of coefficients. Relatively high correlations imply that strong land surface-atmosphere interactions and good soil moisture memory should lead to high predictability of the hydrologic cycle. In other words, a study of Figure 5.12 should elucidate the contributions of such interactions and help us to quantify their relative importance. This representation is advantageous because by establishing the relative strengths, it may allow an indirect evaluation of predictability.

Figure 5.12 helps distinguish regions that have good memory or strong interactions. If both effects of soil moisture work efficiently, they can create extremely wet/dry conditions. For example, the plentiful moisture available for evaporation in the eastern Mississippi is relevant to low-level moisture advection from the Gulf of Mexico. The summer Great Plains LLJ constantly supplies water to keep that region wet (good memory), while precipitation itself is more sensitive to atmospheric moisture advection than to soil moisture. In the drier environments, the connection between the land surface and the atmosphere is believed to be strong. The strong interactions tend to promote long soil moisture memory, which contributes to seasonal precipitation predictability.

The surprising feature is the noticeably opposite pattern of interactions and memories. Through analysis of Figure 5.12, we can now say that predictability in the Columbia basin and the eastern Mississippi basin is reduced by the weak land surface-atmosphere interactions, in contrast to the low predictability in the western

Mississippi basin and Colorado basin, which have low soil moisture memory. Since strong interactions promote soil moisture memory in the Monsoon affected regions, the predictability is largely enhanced and reaches near or above significant levels. Again, the predictability depends on both factors, and neither of them can lead to high predictability if acting alone.

In general, wet basins tend to be weak in interactions, but good in memory; dry basins like Arkansas/Red are usually associated with strong interactions, but poor in memory (Figure5.12). In both cases, low precipitation predictability can be expected. The above results give an indication of the difficulty in the precipitation prediction. Furthermore, the predictability results shown here for some basins are not extremely statistically significant. Most of the correlations (less than 0.2) cannot hold statistical significance at the 95% confidence level.

Using the Core Monsoon region as an example of a region with strong land surface-atmosphere interactions but low soil moisture memory, Figure 5.13 supports this possibility to predict precipitation by showing that variability in the soil layer increases the persistence of precipitation, although the precipitation persistence is short (about one month). Thus, foreknowledge of land surface moisture states does imply a potential increase in precipitation predictability. However, we couldn't find a direct connection of spring soil wetness condition with the summer climate from this figure, since we found there is a lagged relationship between soil moisture and precipitation only for short time scales. To get a better practical application of the land surface condition for summertime precipitation prediction, it is necessary to do monthly-based analysis.

We further test the summer months (JJAS) month by month. The bar graphs in Figures 5.14-5.15, showing the three kinds of correlation coefficients as in Figure 5.12, assess the predictability of precipitation month by month. From these relationships, the summer precipitation expectations could be inferred, thus giving a sense of the added predictability. It is clear that, if dry soil in one month tends to be followed by dry soil in the next one, then lack of precipitation is expected in the second month.

Results for the Mississippi subbasins are presented in Figure 5.14. Similar analyses for the western basins are presented in Figure 5.15. In both figures, for any basin, the month that has high predictability (implied from the third correlation bar reaching the significance level) may occur only if strong interactions and good soil memory are found. This is quantified as both the first two correlation bars exceeding 0.6. According to the criteria, we do find that some dry regions have high precipitation predictability from soil moisture condition in some particular months, such as Arkansas/Red in September, and Mexico's regions in late summer, e.g. July, August, and September. No predictability from soil moisture can be expected in the wet basins, including the Ohio and Columbia basins.

When the wet season occurs in summer, such as in the Core Monsoon region, strong interactions could promote soil moisture memory and thus precipitation predictability. In Figure 5.15, from the increasing trend in autocorrelation of soil moisture month by month, we attribute strong interactions in the Mexico regions to the increased soil moisture memory in their wet season, and therefore the predictability can be enhanced as reflected by the correlation reaching the significant

level. The situation was very different from the other basins. When the dry season occurs in summer like in the Missouri (Figure 5.14) and Colorado basins (Figure 5.15), although strong in interactions, it is still unable to enhance soil memory, the combined effects of the both factors result in low predictability.

Overall, how well the land-atmosphere interactions and soil moisture memory are captured depends on how well the Eta model's land surface model (Noah) can represent the soil component correctly. Provided that the strength of the estimated soil moisture-precipitation relationship and soil moisture variations are approximately correct from NARR, some far-reaching conclusions about seasonal forecasting can be drawn:

1) Our results provide strong support for a hypothesis, namely, that the predictability of local effects is lowered severely in regions that have either weak land-atmosphere interaction or poor soil moisture memory.

2) Given that the predictability of summer precipitation may depend on the strength of land-atmosphere interactions and soil moisture memory, it is important to consider its regional dependence: high predictability is observed in regions of Mexico; no clear predictability could be found in the Mississippi river basin, Columbia and Colorado basins.

3) The basin (usually dry) that has strong interactions tends to have poor soil moisture memory, and the basin (usually wet) that has good soil memory tends to have weak land surface-atmosphere interactions. The opposite pattern introduces the difficulty and uncertainty in precipitation prediction inferred from land surface state

alone. Summer precipitation prediction should take other contributions into account to clear its uncertainty.

4) In the real world and modeling system, this knowledge depends on the ability to forecast the land soil moisture state.

Especially at present, statistical seasonal climate prediction is still more skilful than the predictions of numerical models (Anderson et al., 1999). If our calculations are indeed applicable to nature, the implication for summer precipitation prediction is pronounced. Observations (foreknowledge) of soil moisture are therefore necessary for the precipitation predictions.

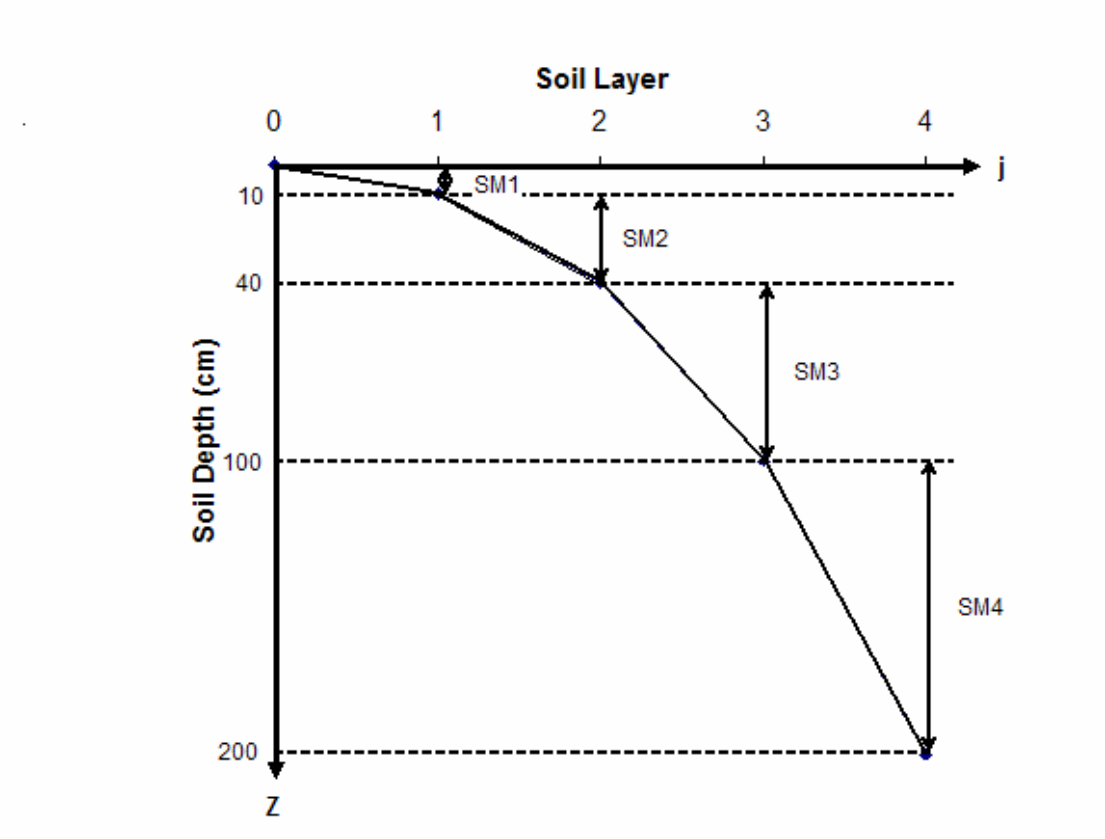

Figure 5.1 The discretization of soil column in NARR: SMj, j=1,4 represents soil moisture content for each layer j, respectively.

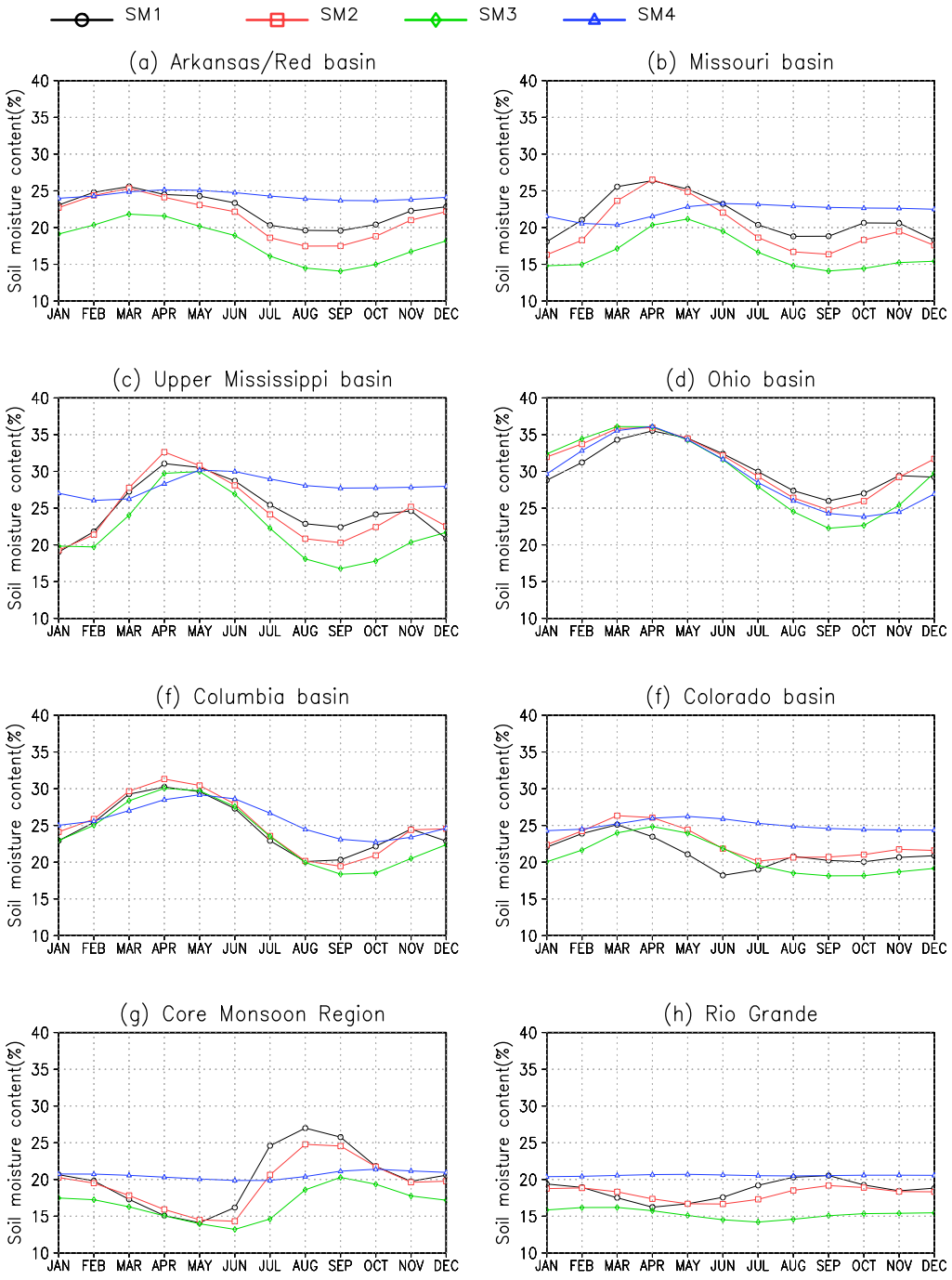

Figure 5.2 Mean annual cycle of monthly volumetric soil moisture at the four soil layers, area-averaged over each basin for the period 1979-2002. Units are percentages of volume of liquid water per volume of soil.

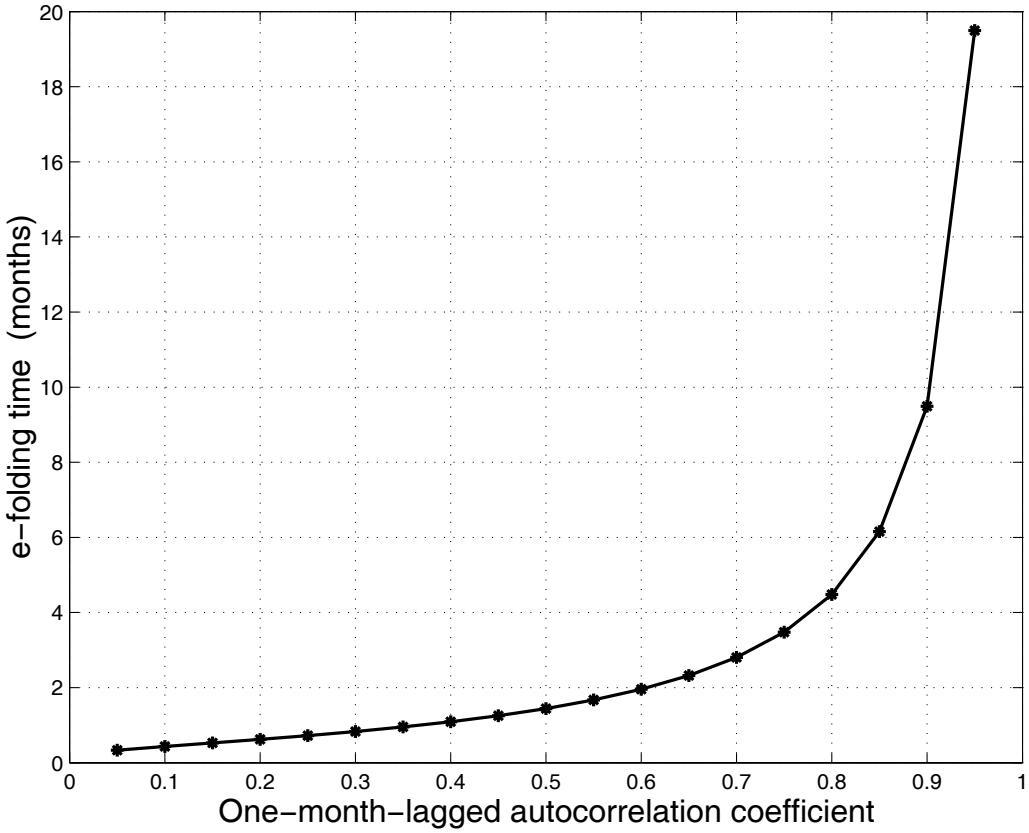

Figure 5.3 Relation between one-month-lagged autocorrelation and the e-folding time of soil moisture anomaly assuming that the time series of soil moisture is similar to the red noise of a first–order Markov process (Delworth and Manabe 1988).

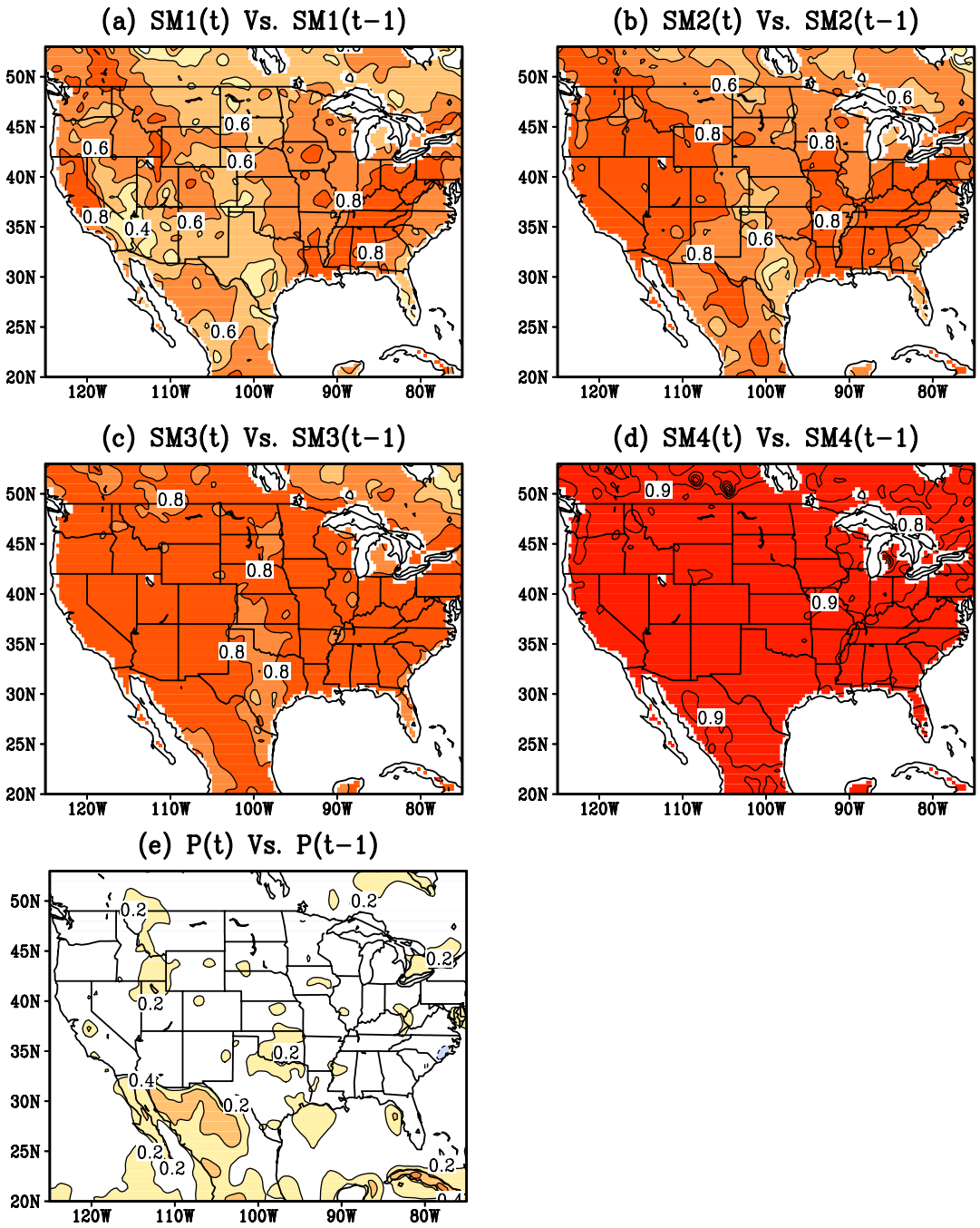

Figure 5.4 One-month-lagged autocorrelations of soil moisture for (a) top 0-10cm of soil layer, (b) 10-40cm of soil layer, (c) 40-100cm of soil layer, (d) 100-200cm of soil layer, and (e) precipitation in JJAS. The anomaly time series used to compute the lag autocorrelation coefficients of soil moisture or precipitation at each grid point and layer are constructed by the monthly value of June, July, August and September, respectively, with the climatological mean for the month removed.

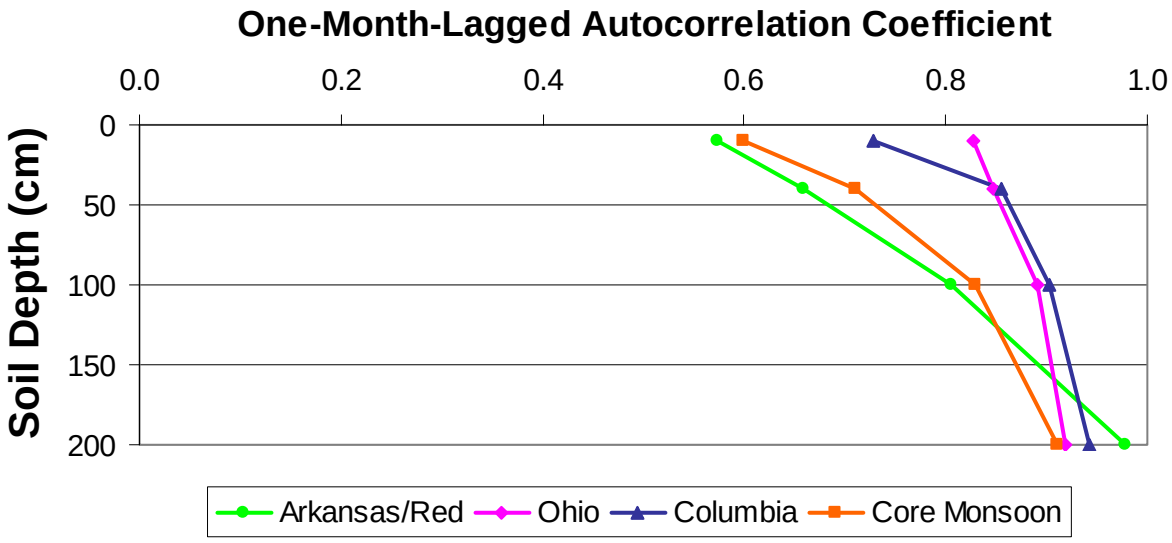

Figure 5.5 The one-month-lagged autocorrelation coefficients of soil moisture as a function of depth for four representative regions in North America for JJAS 1979-2002.

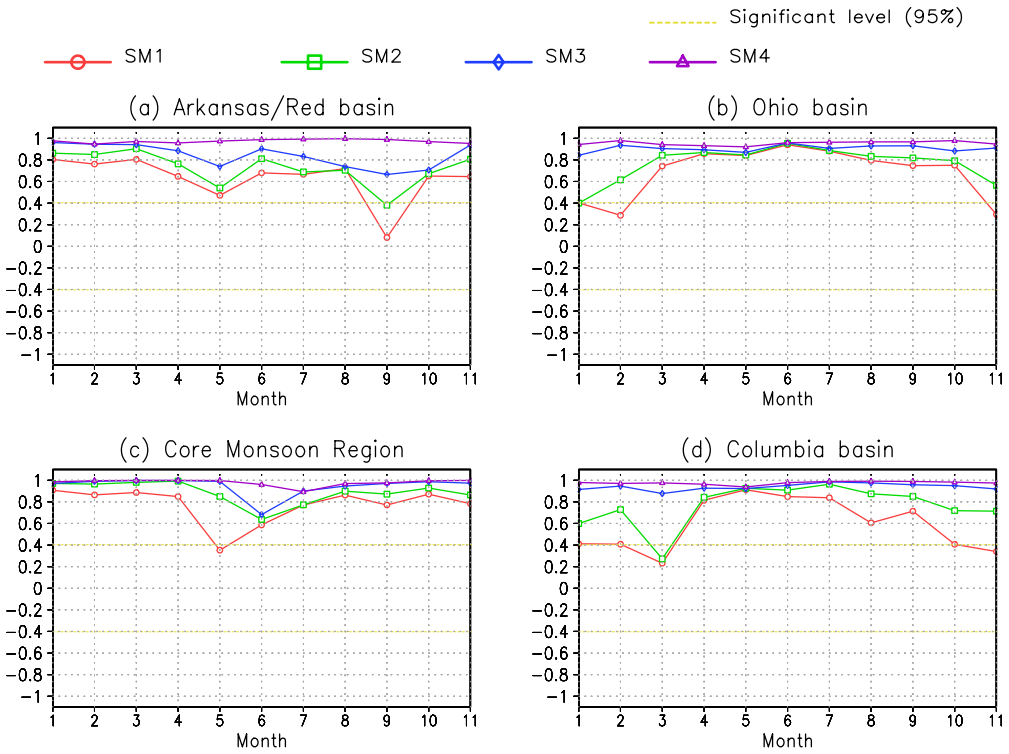

Figure 5.6 One-month-lagged autocorrelation values calculated on basin-averaged soil moisture pairs of months in the year (e.g., a value for January denotes the correlation between anomalies in January and anomalies in February for all 24-year data).

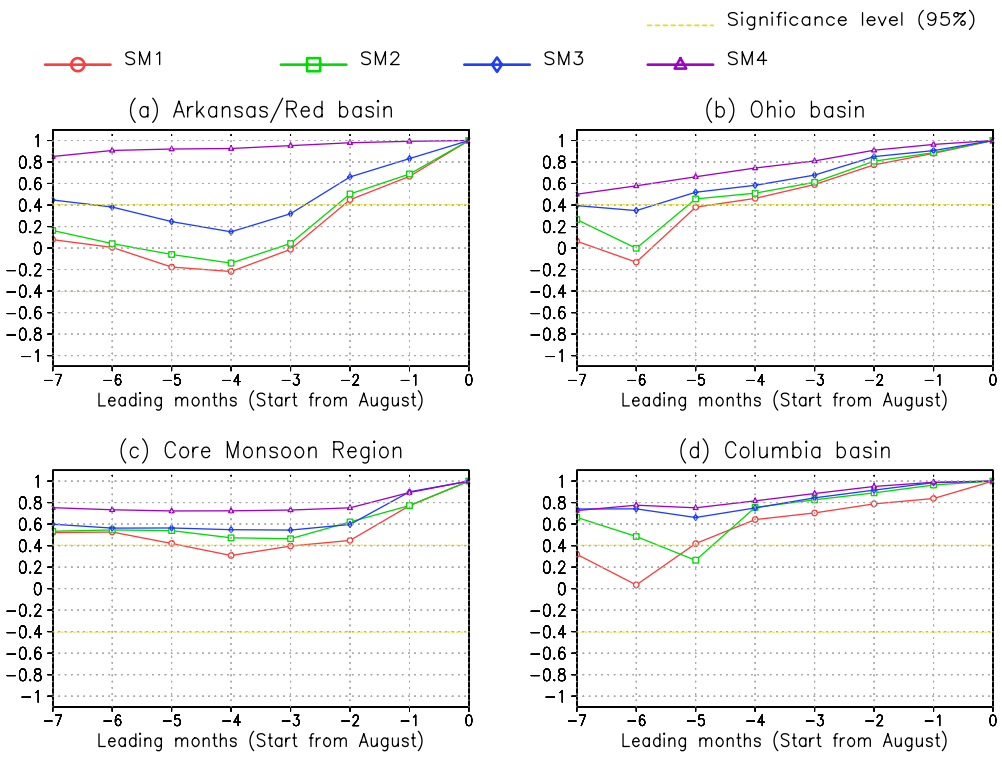

Figure 5.7 Persistence curve of soil moisture (mm) within each layer: SM1 (0-10cm, red line); SM2 (10-40cm, green line); SM3 (40-100cm, blue line); SM4 (100-200cm, purple line). Persistence is estimated from the anomaly correlation between August and preceding months.

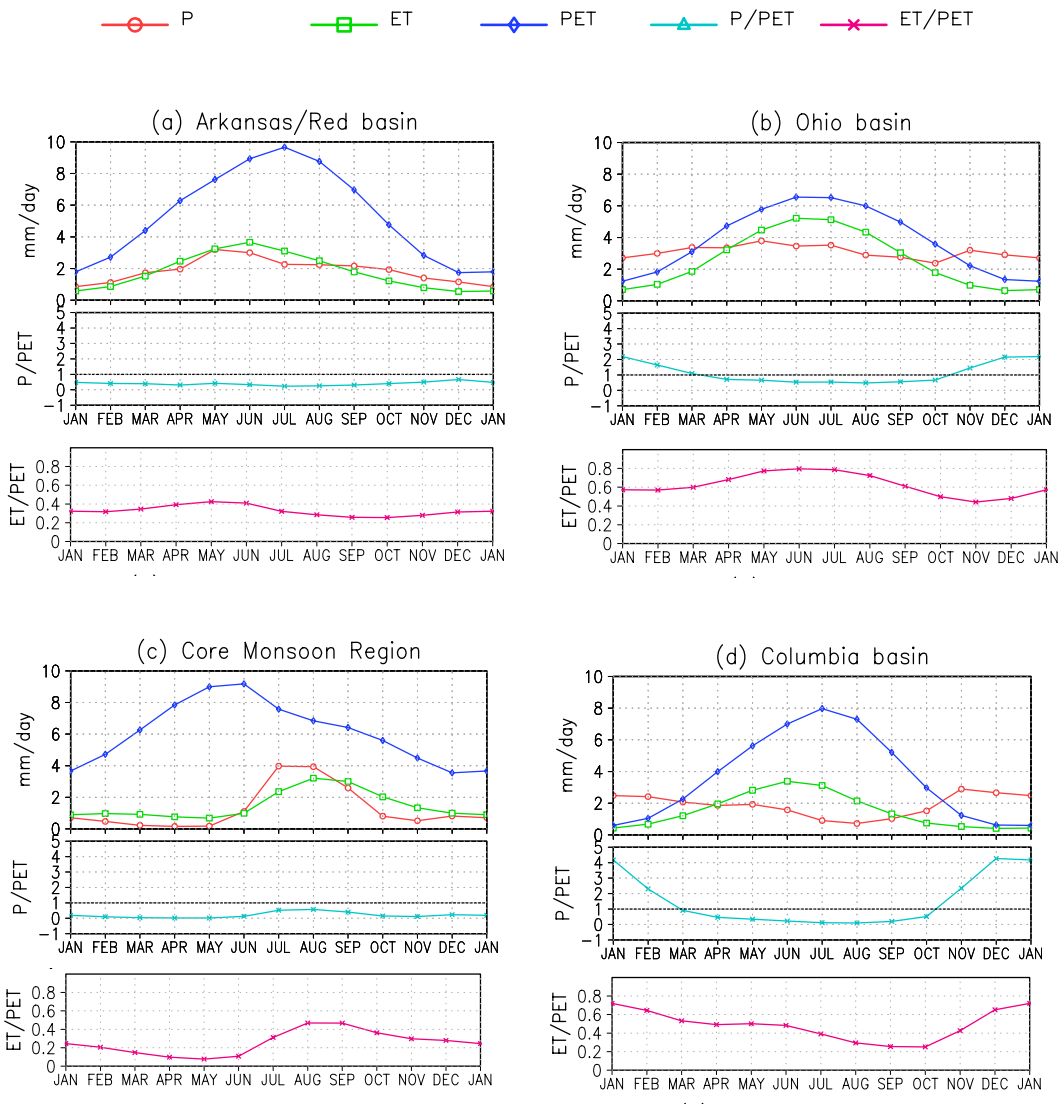

Figure 5.8 Mean annual cycle of monthly precipitation (P), evapotranspiration (ET), potential evaporation (PET), the ratio of P/PET and the ratio of ET/PET, area-averaged over each basin for the period 1979-2002. Units are mm day^{-1}.

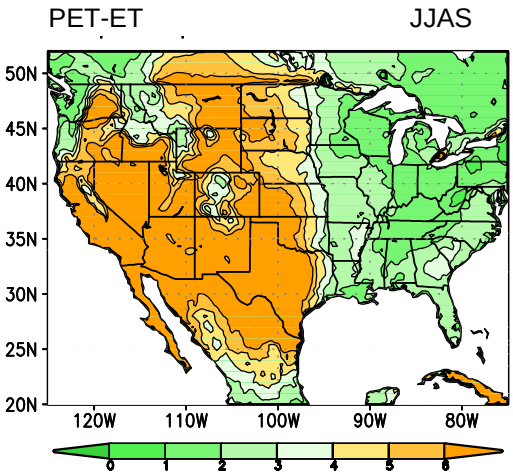

Figure 5.9 1979-2002 summer mean field of the difference between potential evaporation and evaporation. Units are mm day^{-1}.

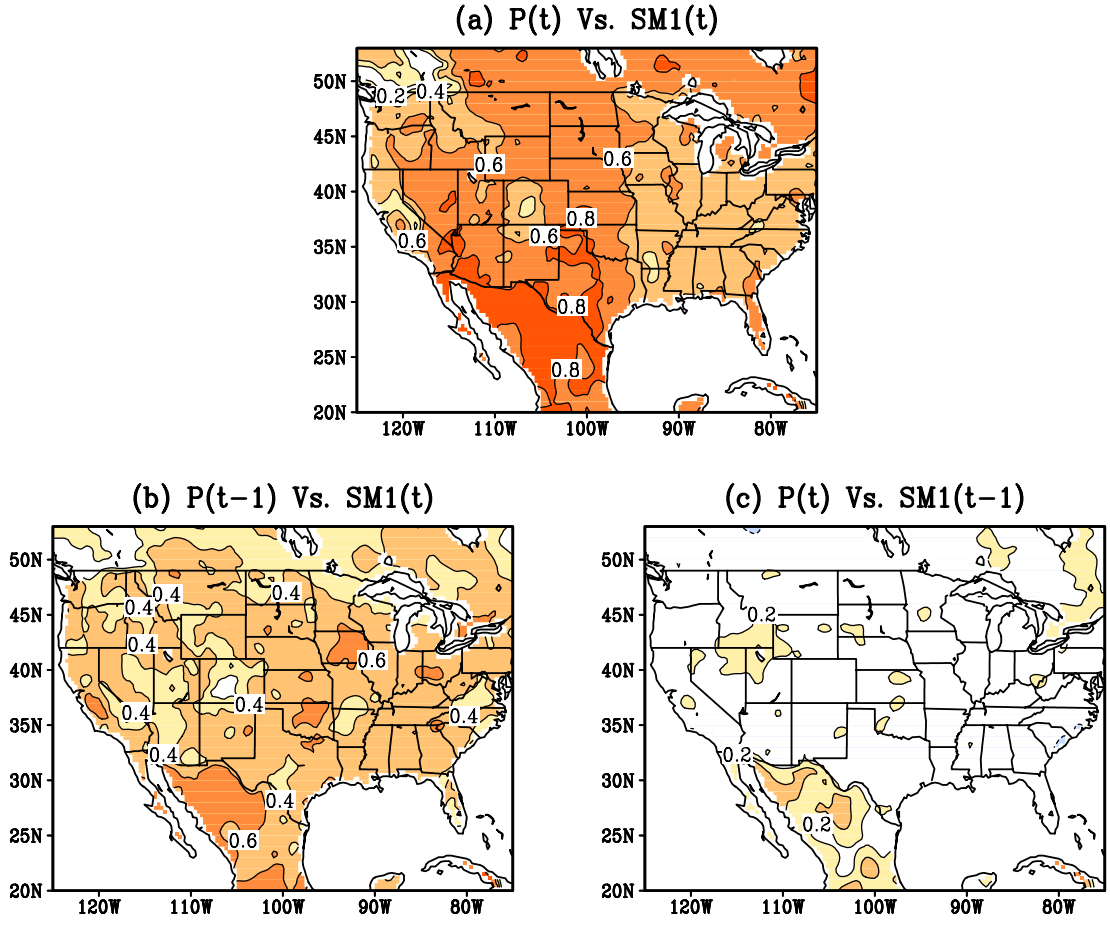

Figure 5.10 Maps of JJAS 1979-2002 for (a) simultaneous correlation coefficients of soil moisture versus precipitation, (b) lag correlation coefficient of precipitation versus one-month-lagged soil moisture, and (c) lag correlation coefficient of soil moisture versus one-month-lagged precipitation.

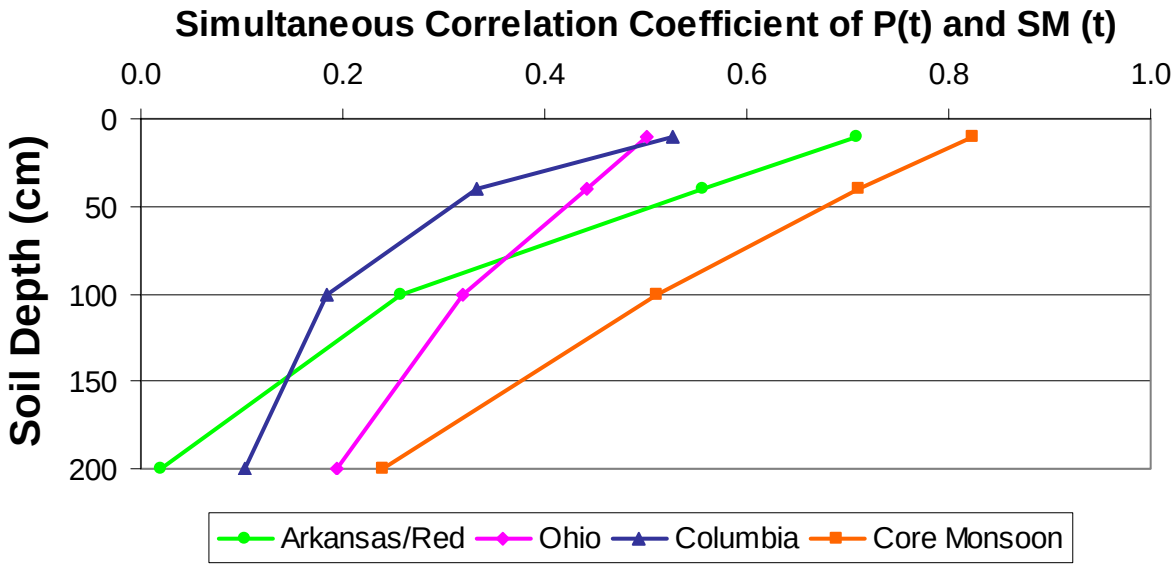

Figure 5.11 The simultaneous correlation coefficient between soil moisture and precipitation as a function of depth for four representative regions in North America for JJAS 1979-2002.

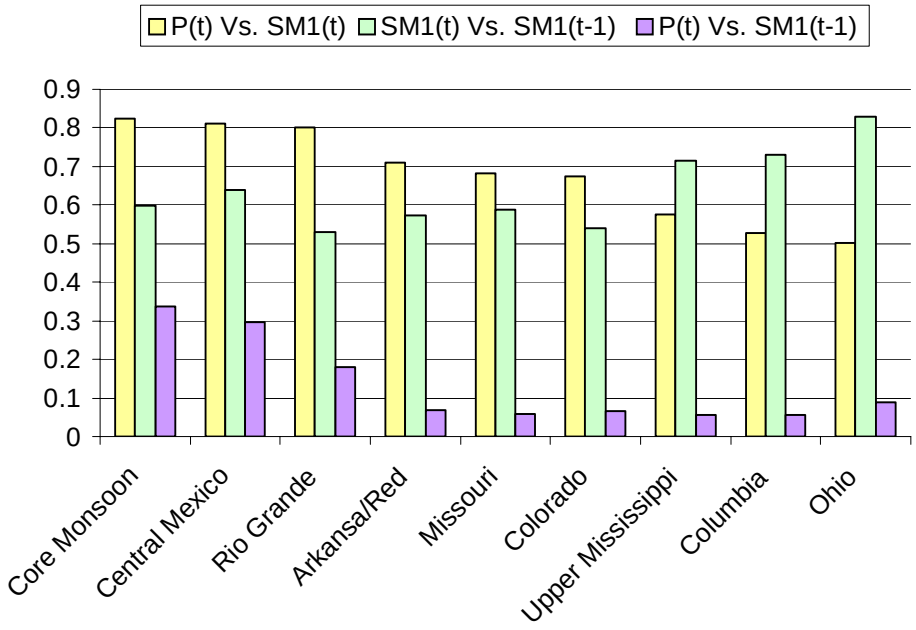

Figure 5.12 Bar graph showing for summer (JJAS) for each basin: simultaneous correlation coefficients of soil moisture (SM1(t)) versus precipitation (P(t)) (yellow bar); one-month-lagged autocorrelation coefficients of soil moisture (green bar); correlation coefficients of soil moisture (SM1(t-1)) versus one-month-lagged precipitation (P(t)) (purple bar). Results presented here are to assess the predictability of summer precipitation through a comparison of these three coefficients. Values greater than 0.2006 (0.2616) are above the 95% (99%) confidence level.

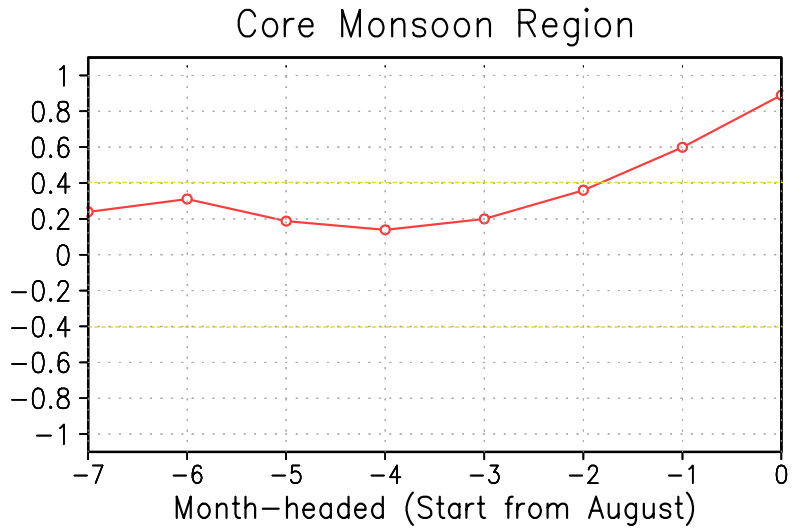

Figure 5.13 Correlation between August precipitation and soil moisture of the prior months for the Core Monsoon region.

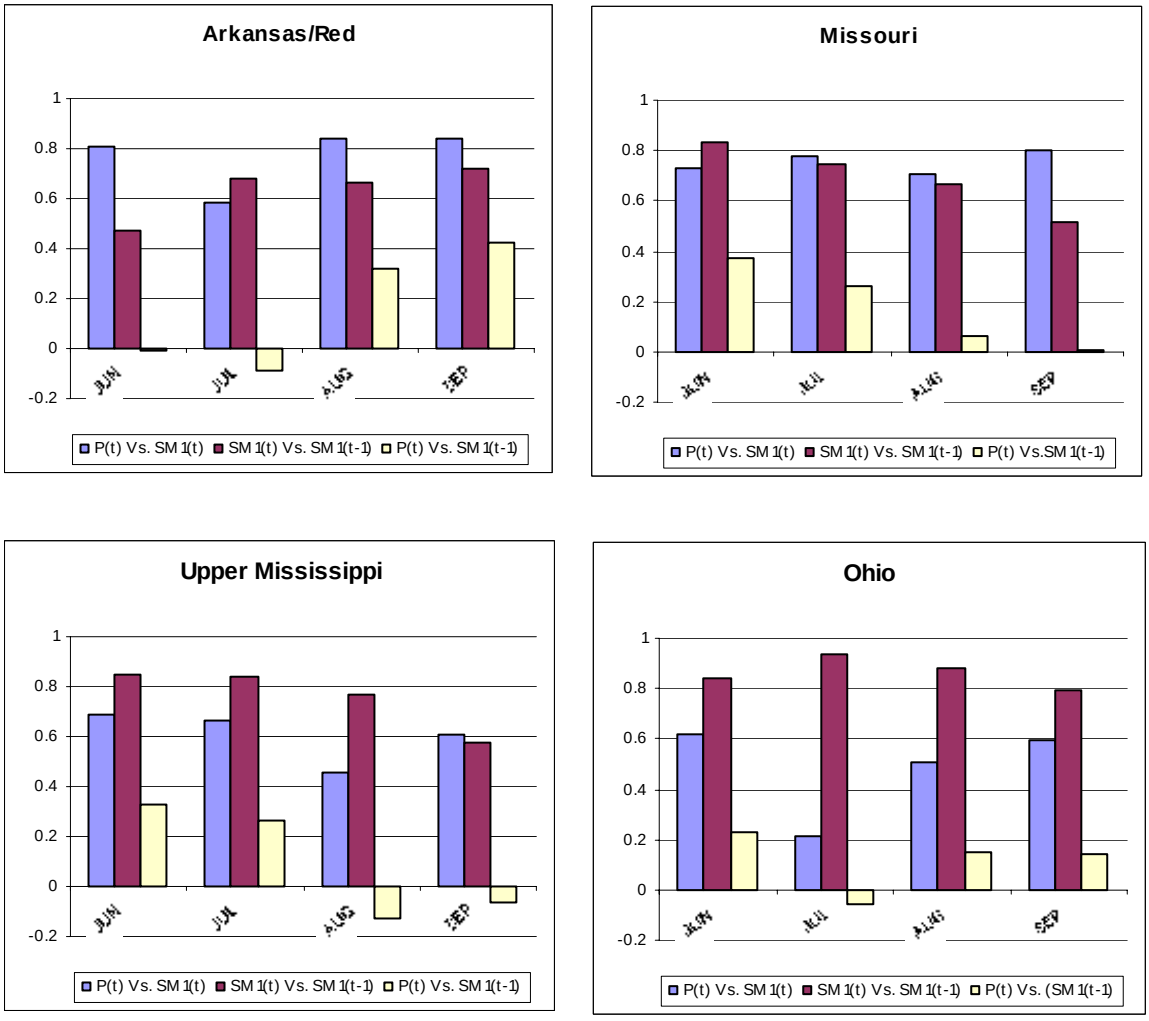

Figure 5.14 Bar graph showing for month by month for summer (JJAS) for the Mississippi subbasins: simultaneous correlation coefficients of soil moisture (SM1(t)) versus precipitation (P(t)) (blue bar); one-month-lagged autocorrelation coefficients of soil moisture (red bar); correlation coefficients of soil moisture (SM1(t-1)) versus on-month-lagged precipitation (P(t)) (yellow bar). Values greater than 0.404 (0.515) are above the 95% (99%) confidence level.

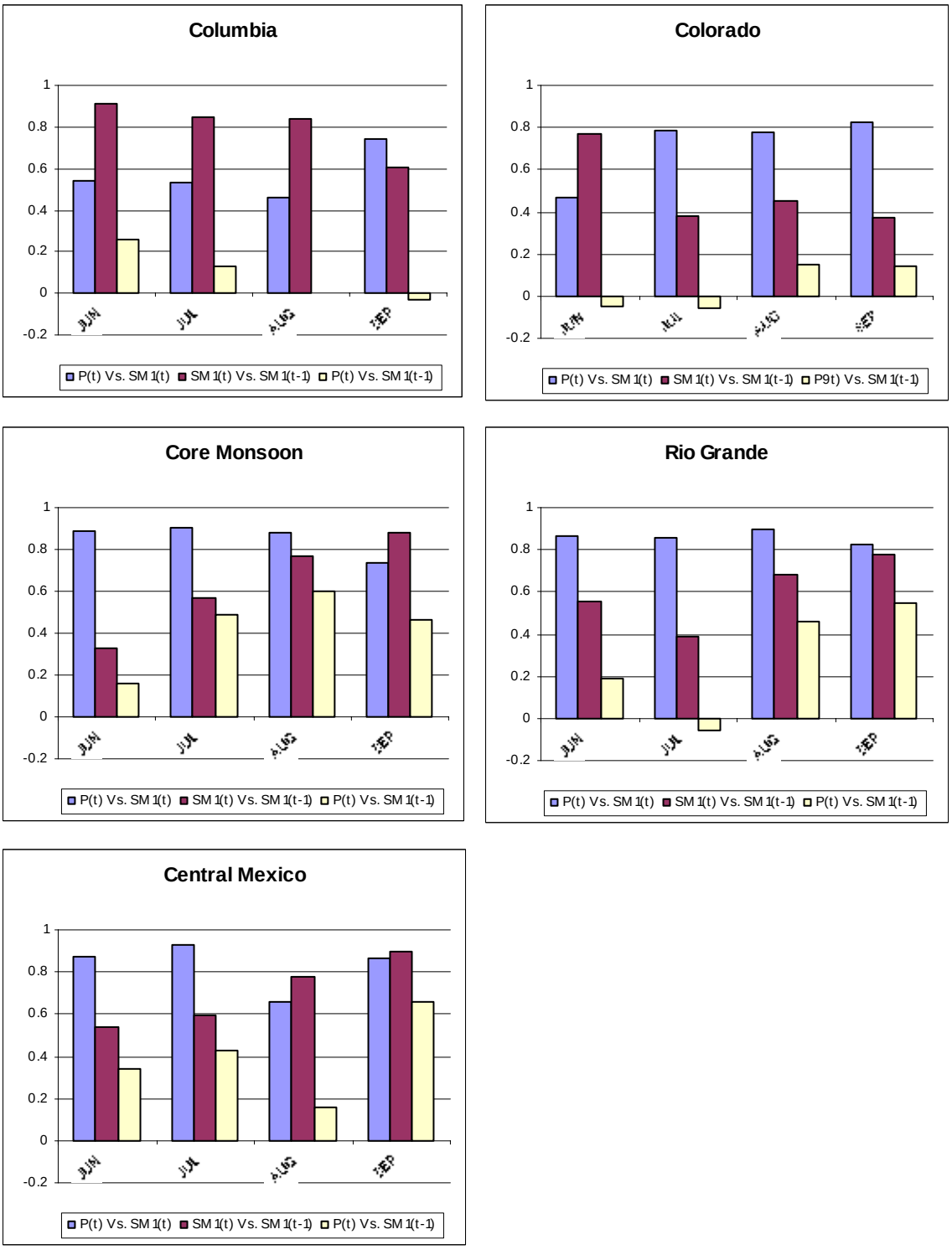

Figure 5.15 Same as Figure 5.14 but for the western basins.

CHAPTER 6: CONCLUSIONS

6.1 Main Results

Our goal was to investigate the regional aspects of the land surface-atmosphere interactions that together with soil moisture memory mechanisms are expected to help determine the predictability of the hydrologic cycle of the North American basins. The present research aimed to explore three basic questions:

1. What are the local mechanisms that enhance or weaken atmospheric anomalies and soil moisture persistence?
2. Where are land surface-atmosphere interactions or soil moisture persistence strongest or weakest?
3. How much hydro-climate predictability (for each basin and season) can be expected from land surface-atmosphere interactions and soil moisture memory?

The hypothesis being proposed here is that: areas which have strong interactions and high soil moisture memory will have great contribution to the predictability of water cycle; areas which have weak or no clear interactions or low soil moisture memory can be associated with high uncertainty and less predictability.

To this end, an accurate representation of land surface water and energy processes is crucial for a successful application of precipitation prediction to real forecast systems. In Chapter 2 and Chapter 3, we have studied the reliability of Eta model-based NARR data to describe the regional surface water and energy budgets.

Since the Eta/EDAS operational forecast system is the origin of the NARR system, Chapter 2 focuses on the operational Eta model's successes, improvements and problems to produce reliable estimates of the hydrologic cycle of basins over the United States. Further investigated in Chapter 3, NARR, with its assimilation of observed precipitation with the PRISM correction and frozen model configuration, helps identify better the structure and intensity of surface hydrologic cycles over the North American basins. We believe that the effort to produce a long period of Eta regional reanalysis has allowed a much improved description of the surface water and energy budgets.

During recent years the Eta/EDAS operational forecast system has been subject to changes and upgrades that positively affected its performance. We discuss these effects on the surface hydrologic cycle by analyzing the period June 1995-May 2003. Characterizing all aspects of the hydrologic cycle accurately from observations and model products over complex terrain involves many challenges. Prior to the model assessment, three gauge-based precipitation analyses that are potential sources of model validation are appraised. Substantial uncertainties remain in the quality of the gridded observed precipitation analyses. For example, a fairly large disparity between the gridded precipitation analyses is found in the long term area-averages over the Columbia basin (~23% difference) and over the Colorado basin (~12% difference). These basins are chosen because they reflect one of the most complex regions that are very demanding for model simulations. The model precipitation, on the other hand, falls within the range of observations, thus giving confidence that no substantial errors are being added.

The basin-averaged Eta model precipitation forecasts correlate well with the observations at monthly timescales and, after 1999, show a small bias. The noticeable reduction is observed in the magnitude of the bias and root mean square error. The origin of the model biases depends on the basin that is considered. The Eta model positive bias in the early period over the Columbia basin was due to a poor representation of the large scale precipitation during winter; the negative bias over the Colorado basin was due to the poor representation of the convective precipitation during summer. Both biases were largely reduced after 1999/2000. Nevertheless, the Eta model water balance residual continued to decrease in recent years, likely from improvements in Eta/Noah physics yielding smaller increments from the daily snowpack update. The results presented here suggest that continued improvements have been achieved along the years, best exemplified in such basic terms like the forecast of precipitation and the reduction of the water balance residual term, confirming that at least similar (or better) quality can be found in studies based on NCEP's recently completed Eta model-based North American Regional Reanalysis as we evaluated in Chapter 3. Similar behavior and good representation have been found for the whole period covered by NARR.

Next in Chapter 3, the longer-term period (1979-1999) in common between the VIC and NARR encourages us to completely assess their surface water terms. In the absence of observations, the NARR land surface hydrological variables were compared with the VIC model variables generated from uncoupled VIC simulations driven by observation-based surface forcing.

The mean annual hydrologic fields of the NARR and VIC models bear encouraging resemblance in shape, location and scale at regional-to-large scales, but local discrepancies exist, mostly related to topography. In both the Colorado and Columbia basins, the NARR and VIC models agree reasonably well during the snow accumulation phase; but in spring the NARR melts snow comparatively too fast. As a result, the NARR spring runoff and soil moisture peaks occur about two months earlier than those of VIC. In addition, the NARR runoff, when compared to VIC's, is too low. The amplitudes of the mean annual cycle of evaporation of the two models are similar, but again, associated with the phase shift in soil moisture, the NARR also has an early peak of evaporation.

Larger residuals in the NARR monthly water balance occur during periods and in regions of substantial snowpack. As expected, the surface water balance in the NARR closed at about the same level as the Eta/EDAS operational forecast products in the latter years.

The difficulties in estimating the hydrologic cycle in regions like the Columbia basin arise from the complex terrain and sparsely sampled observational data. Model parameterizations, which despite great efforts still cannot handle properly these regions of complex orography and physiography, further add to the uncertainties. Such uncertainties highlight the critical need for an improved ability to determine the accuracy of model surface hydrology parameterizations with respect to the real climate system.

The ultimate goal of the work is to identify the regions where components of the hydrologic cycle have higher predictability due to land surface processes. In

Chapters 4 and 5, we evaluate the predictability of warm season precipitation that may be associated with the slowly varying soil moisture. Much of the discussion in this dissertation focuses on the impact of the soil moisture anomalies on the variability and predictability of the precipitation from the monthly to seasonal time scale. Our analysis of the interaction component (Chapter 4) and soil moisture memory component (Chapter 5) provides guidelines on variability of the hydrologic system, thus contributing to its predictability. We thus investigated the land surface state's influence on the variability and predictability of precipitation. Our research should establish a basis that can be applied in practice within the seasonal forecast system.

To achieve this goal, we first studied the possible relationships between soil moisture and precipitation by relating soil moisture to surface radiation and energy processes, and to near-surface boundary layer processes that are important for precipitation processes.

We first outlined pathways through which soil moisture at the land surface and precipitation from the atmosphere mutually influence one another at the regional scales. From there, we identified and grouped the North American basins as shown in Figure 4.12, based on the strength of the relations, to diagnose the reliability of physical mechanisms behind these pathways linking soil moisture to precipitation. Overall, the classification of regions by their relationships between soil moisture and precipitation, as carried out in this study, provides more understanding on the nature of the local coupling of land surface and atmosphere, and its impact on the duration of anomalies. The final steps in this work are investigations of all aspects of the rainfall-

soil moisture linkage and the likelihood of the soil moisture introduced persistence in precipitation. An effective and simple analysis procedure obtained reliable evaluation of precipitation predictability, and identified which regions of the land surface have significant contribution to the predictability. The statistics resulting from this approach support and give confidence to previous model-based studies. The main findings of this study are summarized as follows:

1) Based on the physical hypothesis (Fig. 4.1), we have analyzed the links and directions in the coupled land-atmospheric anomalies in monthly data from NCEP's Regional Reanalysis. The geographic distribution of correlations of soil moisture versus precipitation indicates that soil moisture tends to affect precipitation more in water-limited regions than in water-abundant regions. In other words, soil moisture has more significant and positive contributions to the variability of precipitation in dry regions than that in wet regions. Similar results in the regions of strong coupling between soil moisture and precipitation (Hot Spots) were found from the experiments of a dozen climate-modeling groups (Koster et al., 2004).

2) The strength of the land-atmosphere interactions from NARR estimations shows substantial variations with geography and season. The interactions were found to be stronger in the warm season than in the cold season in most of the North American basins. This can be attributed to the relative availability of water and energy for evaporation at seasonal and basin scales.

3) We found, remarkably, meteorologically dry (defined by Bowen Ratios

rather than soil moisture) regions tend to have strong land surface-atmosphere interactions, especially in the monsoon regions. The potential for interactions is weakened severely in regions that have excessive wetness – with not enough energy to evaporate them out, as a result, these regions lose the great potential for predictability. The land surface effect on precipitation variability is limited, which is constrained by water and energy relative availability.

4) The physical mechanisms controlling soil moisture memory respond to the ratios of precipitation to potential evaporation (**P/PET**) and evaporation to potential evaporation (**P/PET**): firstly, when the ratio of **P/PET** is less than one, **ET** acts as a dominant role in controlling the soil moisture persistence; otherwise, runoff plays dominant role. Secondly, during the summer, a larger ratio of **ET/PET** is most likely associated with lower memory, and vice versa. Because the ratio represents relative availability of water and energy, a large value implies enough energy, but limited water supply, causing soil moisture to be easily evaporated, thus losing memory.

5) Soil moisture persistence and the contribution of soil moisture to atmospheric variability depend on the depth of the soil moisture: the former one increases with depth, but the latter one decreases.

6) Strong interactions promoting soil moisture memory may manifest in important ways in some monsoon regions. Land surface interacting closely with the atmosphere can further lengthen the soil moisture time scales (e.g. Koster et al., 2000; Dickinson, 2000). As described in the Core Monsoon

region as a particular case in Section 5.4, positive feedback mechanisms are likely responsible for the lengthened time scale of soil moisture.

7) Our results suggest that the persistence of summer soil moisture anomalies in North America is on the order of 2-4 months. The concurrent relationship between soil moisture and precipitation and future precipitation prediction might need to take into account the soil moisture introduced persistence and the strength of the land surface-atmosphere interactions.

8) The results from diagnosed land surface-atmosphere interactions at regional scales derived from NARR dataset suggest that the statistical link between soil moisture and precipitation during summer is physically consistent and statistically significant, and demonstrates the feasibility of applying the concept of land surface effects for predictability studies.

9) The analysis has demonstrated that precipitation predictability is sensitive to land surface effects. High predictability was found in the Mexico monsoon regions. Our results suggest that the soil moisture conditions in monsoon regions in Mexico can indeed be employed to improve summer precipitation prediction associated with the local surface effects.

Although models are a powerful tool for understanding the coupling of physical processes (Betts and Viterbo, 2005), one also should keep in mind the present study is in some sense model-dependent, despite the amount of observations ingested. The estimation of some land surface processes and other physical processes,

and the description of the land surface water and energy budgets, are yet to be determined. For example, both the current study and the work of Betts and Viterbo (2005) suggest that cloud effects are one of the greatest uncertainties in land surface models, and also are an important determinant of the surface radiation responses to the land surface. In particular, the effect of cloud feedbacks on the surface energy budget remains a subject for future research. In this sense, independent measures such as satellite observations can be extremely important to reduce any model-dependent results.

Some uncertainties exist in the results found here, as these results can be sensitive to the data used, particularly the runoff data. The land surface model used in the reanalysis is driven by observed precipitation, and the atmosphere and land are not fully coupled; for example, possible vegetation feedbacks are not included. Still, it is not totally clear what impacts this would have on the conclusions drawn above. Further studies using other data can be very useful in narrowing down these uncertainties.

In addition, the opposite tendency between land atmosphere interaction and soil moisture persistence represents a challenge in predictability studies. Our research emphasizes improved predictability based on an enhanced understanding of regional land surface processes, but unraveling the source of summer precipitation prediction requires consideration of the interactions between the atmosphere, land, and ocean altogether.

6.2 Future Directions

Our analysis has revealed a highly physically and statistically consistent picture. However, the extent to which all of these results apply to the real world depends on the accuracy of the reanalysis and the underlying model. The conclusions obtained from the present study should be thoroughly compared with independent observations. The fact that NARR has employed such a vast amount of observations has not left much as independent, though. Such a comparison is essential for establishing the credibility of the present study.

Attention should be paid to several difficulties in the study, primarily due to the limitations such as 1) a lack of observational data with appropriate temporal and spatial resolution, 2) the model dependence of computational estimates, 3) inability to isolate the contributions of land surface effects from others. Future studies will be a combination of simulations and observations analysis directed toward addressing the following issues:

Firstly, satellite observations and field observation campaigns in progress are expected to counter the first limitation in the future.

Secondly, to counter the second limitation, retrospective LDAS data sets may be an attractive choice for further investigation by employing a similar approach presented here. The results from different datasets highlight the confidence level of the computations and narrow down the uncertainties due to the model dependent feature.

Thirdly, to counter the third limitation, ensembles of Eta model seasonal simulations are planned to be employed for sensitivity experiments. The ensemble members are designed to have different initial land and atmospheric states. In case or

regions where no feedbacks are found, the analysis will focus on how this relates to the degree of uncertainty of the water cycle. The relationship between regions of well-defined land surface-hydrologic cycle interactions and the dispersion of the ensemble members will be examined. Similarly, the relationship (or lack of) between regions of weak land influences and the dispersion of the ensemble members will be inspected. Future work in this area will help in discerning the various contributions from the land surface in regulation of precipitation variability.

Finally, this approach and future work are expected to contribute to the understanding of warm season predictability arising from the land surface influences, and thus provide robust and stable results that capture natural precipitation phenomena in a consistent manner.

REFERENCES

Adam, J. C., and D. L. Lettenmaier, 2003: Adjustment of global gridded precipitation for systematic bias, *J. Geophys. Res*., **108**, (D9), 1-14.

Barlow, M., S. Nigam, and E. H. Berbery, 1998: Evolution of the North American monsoon system. *J. Climate*, **11**, 2238-2257.

Beljaars, A. C. M., P. Viterbo, M.J. Miller, and A. K. Betts, 1996: The anomalous rainfall over the United States during July 1993: Sensitivity to land surface parameterization and soil moisture anomalies. *Mon. Wea. Rev*., **124,** 362-383.

Berbery, E. H., 2001: Mesoscale moisture analysis of the North American monsoon. *J. Climate*, **14**, 121-137.

___, and E. M. Rasmusson, 1999: Mississippi moisture budgets on regional scales. *Mon. Wea. Rev.*, **127**, 2654-2673

___, K. E. Mitchell, S. Benjamin, T. Smirnova, H. Ritchie, R. Hogue, and E. Radeva, 1999: Assessment of land surface energy budgets from regional and global models. *J. Geophys. Res.,* **104**, D16, 19,329-19,348.

___, Y. Luo, K. E. Mitchell, and A. K. Betts, 2003: Eta model-estimated land surface processes and the hydrologic cycle of the Mississippi basin. *J. Geophys. Res*. **108**, D22, 8852, doi:10.1029/2002JD003192.

Betts, A.K., J. H. Ball, A. C. M. Beljaars, M. J. Miller, and P. A. Viterbo, 1996: The land surface-atmosphere interaction: A review based on observational and modeling perspectives. *J. Geophys. Res.,* **101**, 7209-7225.

___, F. Chen, K. E. Mitchell, and Z. I. Janjić, 1997: Assessment of the land surface and boundary layer models in the two operational versions of the NCEP Eta model using FIFE data. *Mon. Wea. Rev.*, **125**, 2896-2916.

___, P. Viterbo, A. Beljaars, H.-L. Pan, S.-H. Hong, M. Goulden and S. Wofsy, 1998: Evaluation of the land-surface interaction in the ECMWF and NCEP/NCAR Reanalysis models over grassland (FIFE) and Boreal forest (BOREAS). *J. Geophys. Res*., **103**, 23079-23085.

___, J. H. Ball, and P. Viterbo, 1999: Basin-scale surface water and energy budgets for the Mississippi from ECMWF reanalysis. *J. Geophys. Res*., **104**, 19,293-19,306.

___, and P. Viterbo, 2000: Hydrological budgets and surface energy balance of seven subbasins of the Mackenzie River from the ECMWF model. *J. Hydromet*., **1**, 47-60.

___, and P. Viterbo, 2005: Land-surface, boundary layer, and cloud-field coupling over the southwestern Amazon in ERA-40. *J. Geophys. Res.*, **110**, D14108, doi:10.1029/2004JD005702.

Black, T. L., 1994: The new NMC Mesoscale Eta model: Description and forecast examples. *Wea. Forecasting*, **9**, 265-278.

Brubaker, K.L., D. Entekhabi, and P.S. Eagleson, 1993: Estimation of continental precipitation recycling. *J. Climate,* **6**, 1077-1089.

Chen F., K. Mitchell and J. Schaake, 1996: Modeling of land surface evaporation by four schemes and comparison with FIFE observations, *J. Geophys. Res*., **101***(D3)*, 7251-7268.

___, Z. Janjić, and K. Mitchell, 1997: Impact of atmospheric surface-layer parameterizations in the new land-surface scheme of the NCEP mesoscale Eta model. *Boundary-Layer Meteo,* **85**, 391-421.

Christensen, N. S., A. W. Wood, N. Voisin, D. P. Lettenmaier, and R. N. Palmer, 2004: Effects of Climate Change on the Hydrology and Water Resources of the Colorado River Basin. *Climatic Change*, **62**, 337-363.

Coughlan, M. and R. Avissar, 1996: The global energy and water cycle experiment (GEWEX) continental-scale international project (GCIP): An overview. *J. Geophys. Res*., **101**, D3, 7139-7147.

Daly, C., R. P. Neilson, and D. L. Phillips, 1994: A statistical-topographic model for mapping climatological precipitation over mountainous terrain. *J. Appl. Meteor*., **33**, 140-158.

Delworth, T., and S. Manabe, 1988: The influence of potential evaporation on the variabilities of simulated soil wetness and climate. *J. Climate*, **1**, 523-547.

Delworth, T., and S. Manabe, 1989: The influence of soil wetness on near-surface atmospheric variability. *J. Climate*, **2**(12), 1447-1462.

Dickinson, R.E., G. Wang, X. Zeng, and Q.-C. Zeng, 2003: How does the partitioning of evapotranspiration and runoff between different processes affect the variability and predictability of soil moisture and precipitation? *Adv. in Atmos. Sci.,* **20**(3), 475-478.

Dirmeyer, P. A., 2003: The role of land surface background state in climate predictability. *J. Hydromet.*, **4**, 599- 610.

Douglas, A. V., and P. J. Englehart, 1996: Variability of the summer monsoon in Mexico and relationships with drought in the United States. *Proceedings of the Twenty-First Annual Climate Diagnostics Workshop*. Available from the Climate Prediction Center, Washington D.C., 20233.

Ek, M. B., K. E. Mitchell, Y. Lin, P. Grunmann, E. Rogers, G. Gayno, V. Koren, and J. D. Tarpley, 2003: Implementation of Noah land surface model advances in the National Centers for Environmental Prediction operational mesoscale Eta model. *J. Geophys. Res*., 108(D22), 8851, doi:10.1029/2002JD003296.

Eltahir, E. A. B., 1998: A soil moisture-rainfall feedback mechanism. 1. Theory and observations. *Water Res. Res.*, **34**, 765-776.

Entekhabi, D. 1995: Recent advances in land-atmosphere interaction research. *Rev. Geophys*., supplement, 995-1003.

Entekhabi, D., I. Rodriguez-Iturbe, and R. L. Bras, 1992: Variability in large-scale water balance with land surface-atmosphere interaction. *J. Climate*, **5**, 798-813.

Findell, K. L., and E. A. B. Eltahir, 1997: An analysis of the soil moisture-rainfall feedback, based on direct observations from Illinois. *Water Resources Res.*, **33**, 725-735.

___, and __, 1999: Analysis of the pathways relating soil moisture and subsequent rainfall in Illinois. *J. Geophys. Res.,* **104**, 31565-31574.

___, and __, 2003: Atmospheric controls on soil moisture-boundary layer interactions; Part I: framework development. *J. Hydromet.*, **4**, 552-569.

Gochis, D. J., W. J. Shuttleworth, and Z.-L Yang, 2003: Hydrometeorological response of the modeled North American monsoon to convective precipitation. *J. Hydromet*., **4**, 235-250.

Groisman, P. Y., and D. R. Legates, 1994: The accuracy of United States precipitation data. *Bull. Amer. Meteor. Soc*., **75**, 215-227.

Gutzler D. S., 2000: Covariability of spring snowpack and summer rainfall across the southwest United States. *J. Climate*, **13**, 4018-4027.

Higgins, Y. Yao, X. L. Wang, 1997: Influence of the North American monsoon system on the U.S. Summer precipitation regime. *J. Climate*, **10**, 2600-2622.

___, W. Shi, E. Yarosh and R. Joyce, 2000: Improved United States precipitation quality control system and analysis. *NCEP/Climate Prediction Center ATLAS* No. 7. U. S. Department of Commerce, National Oceanic and Atmospheric Administration. Available online from http://www.cpc.ncep.noaa.gov/products/precip/realtime/hist_us.html.

Hong, S.-Y., and E. Kalnay, 2000: Origin and maintenance of the Oklahoma-Texas drought of 1998. *Nature*, 842-845.

Hong, S.-Y., and Eugenia Kalnay, 2002: The 1998 Oklahoma-Texas Drought: Mechanistic Experiments with NCEP Global and Regional Models. *J. Climate*, **15**, 945-963.

Huang, J., H. M. van den Dool, and K. P. Georgakakos, 1996: Analysis of model-calculated soil moisture over the United States (1931-1993) and applications to long -range temperature forecasts. *J. Climate*, **9**, 1350-1362.

Jones, R. H., 1975: Estimating the variance of time averages. *J. Appl. Meteor.*, **14**, 159-163.

Kalnay, E., and Coauthors, 1996: The NCEP/NCAR 40-Year Reanalysis Project. *Bull. Amer. Meteor. Soc.*, **77**, 437-471.

Kim, J., and J.-E. Lee, 2003: A multiyear regional climate hindcast for the western United States using the mesoscale atmospheric simulation model. *J. Hydrometeorology*, **4**, 878-890.

Koren, V., J. Schaake, K. Mitchell, Q. Duan, F. Chen, and J. Baker, 1999: A parameterization of snowpack and frozen ground intended for NCEP weather and climate models. *J. Geophys. Res.,* **104**, 19569-19585.

Koster R. D., and M. J. Suarez, 2001: Soil moisture memory in climate models. *J. Hydromet,* **2**, 558- 570.

___, and ___, 2003: Impacts of land surface initialization on seasonal precipitation prediction and temperature prediction. *J. Hydromet*., **4**, 408-423.

___, ___, and M. Heiser, 2000: Variance and predictability of precipitation at seasonal-to-interannual timescales. *J. Hydromet*., **1**, 26-46.

___, and P. C. Milly, 1997: The interplay between transpiration and run-off formulations in land-surface schemes used with atmospheric models, *J. Climate*, **10**, 1578– 1591.

___, and coauthors, 2002: Comparing the degree of land-atmosphere interaction in four atmospheric General Circulation Models. *J. Hydromet.*, **3**, 363-375.

___, P. A. Dirmeyer, Z. Guo and the GLACE team, 2004: Regions of strong coupling between soil moisture and precipitation. *Science*, **305**, 1138-1140.

Leung, L. R., and S. J. Ghan, 1998: Parameterizing subgrid orographic precipitation and surface cover in climate models. *Mon. Wea. Rev*., **126**, 3271-3291.

___, Y. Qian, J. Han, and J. O. Roads, 2003: Intercomparison of global reanalyses and regional simulations of cold season water budgets in the western United States. *J. Hydrometeorology*, **4**, 1067-1087.

___, Y. Qian, and X. Bian, 2003: Hydroclimate of the western United States based on observations and regional climate simulation of 1981-2000. Part I: Seasonal statistics. *J. Climate*, **16**, 1892-1911.

Liang, X., D. P. Lettenmaier, E. F. Wood, and S. J. Burges, 1994: A Simple Hydrologically Based Model of Land and Energy Fluxes for General Circulation Models. *J. Geophys. Res.*, *99(D7)*, **14**, 415-14,428.

___, E. F. Wood, and D. P. Lettenmaier, 1996: Surface soil moisture parameterization of the VIC-2L model: Evaluation and modifications. *Global and Planetary Change*, **13**, 195-206.

Liu, Y., and R. Avissar, 1999a: A study of persistence in the land– atmosphere system using a general circulation model and observations. *J. Climate.,* **12**, 2139–2153.

___, and ___, 1999b: A study of persistence in the land–atmosphere system with a fourth-order analytical model. *J. Climate.,* **12**, 2154–2168.

Lohmann, D., and coauthors, 2004: Streamflow and water balance intercomparisons of four land surface models in the North American Land Data Assimilation System project, *J. Geophys. Res*., **109**, D07S91, doi:10.1029/2003JD003517.

Luo, Y., E. H. Berbery, E. Kalnay, P. Shafran, F. Mesinger, G. DiMego, and K. Mitchell, 2002: The mesoscale nature of the water and energy budgets. Part 2: Evaluation of the regional reanalysis. *Mississippi River Climate and Hydrology Conference*, New Orleans, May 13-18, 2002.

Luo, Y., E. H. Berbery, and K. Mitchell, 2005: The operational Eta model precipitation and surface hydrologic cycle of the Columbia and Colorado basins. *J. Hydromet.*, **6**, 341-370.

Maurer, E. P., G. M. O'Donnell, D. P. Lettenmaier, and J. O. Roads, 2001: Evaluation of the Land Surface Water Budget in NCEP/NCAR and NCEP/DOE Reanalyses using an Off-line Hydrologic Model. *J. Geophys. Res.* **106***(D16)*, 17,841-17,862.

___, A.W. Wood, J. C. Adam, D. P. Lettenmaier, and B. Nijssen, 2002: A long-term hydrologically-based data set of land surface fluxes and states for the conterminous United States, *J. Climate,* **15***,* 3237-3251.

Mesinger, F., G. DiMego, E. Kalnay, P. Shafran, E. H. Berbery, and coauthors, 2002: NCEP regional reanalyses. *Symposium on observations, data assimilation and probabilistic prediction. AMS Annual Meeting.* January 2002.

Mitchell, K. E., and coauthors, 2002: Reducing near-surface cool/moist biases over snowpack and early spring wet soils in NCEP Eta model forecasts via land surface model upgrades. *Proceedings of the 16th Conference on Hydrology, American Meteorological Society*, Orlando, FL, 2002.

___, and coauthors, 2004: The multi-institution North American Land Data Assimilation System (NLDAS): Utilizing multiple GCIP products and partners

in a continental distributed hydrological modeling system. *J. Geophys. Res*., **109,** D07S90, doi:10.1029/2003JD003823.

Oglesby, R. J., and D. J. Erickson III, 1989: Soil moisture and the persistence of North American drought. *J. Climate,* **2**, 1362-1380.

Pan, H.-L., and L. Mahrt, 1987: Interaction between soil hydrology and boundary-layer development. *Boundary-Layer Meteor*., **38**, 185-202.

Pan, M., and coauthors, 2003: Snow process modeling in the North American Land Data Assimilation System (NLDAS): 2. Evaluation of model simulated snow water equivalent, *J. Geophys. Res.*, ***108****(D22), 8850, doi:10.1029/2003JD003994.*

Payne, J. T., A. W. Wood, A. F. Hamlet, R. N. Palmer, and D. P. Lettenmaier, 2004: Mitigating the effects of climate change on the water resources of the Columbia River basin, *Climatic Change*, **62**, 233-256.

Pulwarty, R. S., and K. T. Redmond, 1997: Climate and salmon restoration in the Columbia River Basin: The role and usability of seasonal forecasts. *Bull. Amer. Meteor. Soc*, **78**, 381-397.

Roads, J. O., S. C. Chen, A. K. Guetter, and K. P. Georgakakos, 1994: Large-scale aspects of the United States hydrologic cycle. *Bull. Amer. Meteor. Soc*.,**75**, 1589-1610.

___, and coauthors, 2003: GCIP water and energy budget synthesis (WEBS). *J. Geophys. Res.*, **108**(D16), 8609, doi:10.1029/2002JD002583.

Robock, A., and coauthors, 2003: Evaluation of the North American Land Data Assimilation System over the southern Great Plains during the warm season. *J. Geophys. Res*., **108**(D22), 8846, doi:10.1029/2002JD003245, 2003.

Rogers, E., T. L. Black, D. G. Deaven and G. J. DiMego, 1996: Changes to the operational early Eta analysis/forecast system at the National Centers for Environmental Prediction. *Wea. Forecasting*, **11**, 391-413.

___, D. Parrish, and G. DiMego, 1999: Changes to the NCEP Operational Eta Analysis. NWS/NOAA Tech. Proc. Bull., 454. [Available on line at http://www.nws.noaa.gov/ om/tpb/454.html].

___, T. L. Black, W. Collins, G. Manikin, F. Mesinger, D. Parrish, and G. DiMego, 2001a: Changes to the NCEP Meso Eta analysis and forecast system: Assimilation of satellite radiances and increase in resolution. NWS/NOAA Tech. Proc. Bull., 473.

[Available on line at http://www.nws.noaa.gov/om/tpb/inddraft.htm].

___, M. Ek, Y. Lin, K. Mitchell, D. Parrish, and G. DiMego, 2001b: Changes to the NCEP Meso Eta analysis and forecast system: Assimilation of observed precipitation, upgrades to land-surface physics, modified 3DVAR analysis. NWS/NOAA Tech. Proc. Bull., 479. [Available on line at http://www.nws.noaa.gov/om/tpb/inddraft.htm].

___, M. Ek, Y. Lin, K. Mitchell, D. Parrish, and G. DiMego, 2002: Changes to the NCEP Meso Eta analysis and forecast system: Assimilation of observed precipitation, upgrades to land-surface physics, modified 3DVAR analysis. *NWS/NOAA Tech. Proc. Bull.,* 479.

[Available online at http://www.nws.noaa.gov/om/tpb/inddraft.htm].

Schaake, J. C., and coauthors, 2004: An intercomparison of soil moisture fields in the North American Land Data Assimilation System (NLDAS), *J. Geophys. Res.,* **109**, D01S90, doi:10.1029/2002JD003309.

Schlosser, C. A., and coauthors, 2000: Simulations of a Boreal Grassland Hydrology at Valdai, Russia: PILPS Phase 2(d). *Mon. Wea. Rev.,* **128**, 301–321.

Sheffield, J., and coathors, 2003: Snow process modeling in the North American Land Data Assimilation System (NLDAS): 1. Evaluation of model-simulated snow cover extent, *J. Geophys. Res.*, ***108***(D22), 8849, doi:10.1029/2002JD003274.

Shepard, D. S., 1984: Computer mapping: The SYMAP interpolation algorithm. In Spatial Statistics and Models, pp 133-145. G. L. Gaile and C. J.Willmott, eds. Reidel Publishing Company, Norwell, Mass.

Shukla, J., and Y. Mintz, 1982: The influence of land surface evapotranspiration on Earth's climate. *Science*, **215**, 1948-1501.

Shukla, J., J. Anderson, D. Baumhefner, C. Brankovic, Y. Chang, E. Kalnay, L. Marx, T. Palmer, D. Paolino, J. Ploshay, S. Schubert, D. Straus, M. Suarez, J. Tribbia, 2000: Dynamical Seasonal Prediction. *Bull. Amer. Meteor. Soc*., **81**, 2593-2606.

Small, E. E. and S.A. Kurc, 2003: Tight coupling between soil moisture between soil moisture and the surface radiation budget in semiarid environments: Implications for land-atmosphere interactions. *Water Resources Res.*, **39**, 10, 1278, doi:10.1029/2002WR001297.

Small, E. E., 2001: The influence of soil moisture anomalies on variability of the North American monsoon system. *Geophys. Res. Lett.*, **28**, 139-142.

Xie P., and P. A. Arkin, 1997: Global Precipitation: A 17-year monthly analysis based on gauge observations, satellite estimates and numerical model outputs. *Bull. Amer. Meteor. Soc*., **78**, 2539-2558.

Yeh, T. C., R. T. Wetherald, and S. Manabe, 1984: The effect of soil moisture on the short-term climate and hydrology change — a numerical experiment. *Mon. Wea. Rev.*, **112**, 474-490.

___, R. T. Wetherald, and S. Manabe, 1983: A model study of the short-term climatic and hydrologic effects of sudden snow removal. *Mon. Wea. Rev.*, **111**, 1013-1024.